AA   LC   SIMS

FTIR   TAS-MS   XRS

XRF   HPLC   GC   UE

NMR   ICP-MS   CP-AES

XPS   SFC/SFE   MS

IC   CZE   NIR   SIE

TLC   UV-VIS   AMS

FFF   RIMS   ESR

C.H. Lochmüller
Editor-in-Chief

Contents

Lead Analysis: Past and Present

Alanah Fitch

Department of Chemistry, Loyola University Chicago, 6525 N. Sheridan Road, Chicago, Illinois 60626

[The suspected material] is to be acted on with dilute nitric acid, and the resulting liquid filtered. If the addition of dilute sulphuric acid to the filtered liquid produce a white, if chromate of postash a yellow, and , lastly, if sulphuretted hydrogen a black precipitate, the presence of lead is fully determined.

Mitchell, 1848 A.D.: An Early Analytical Text

Take two to three pounds of the juice of the Lunaria, add a solution of lead, alum, salpetre, sal ammoniac, silver-litharge, quick-silver sublimate, vinegar and ginger, then distil and calcinate. This powder is then thickened with a silver solution into paste. One part in a hundred of this paste, heated on a copper plate, could theoretically turn tin, lead, or quicksilver into silver at a ratio of one to a hundred parts.

Raymond Lully, 1235 A.D.

TABLE OF CONTENTS

I. SELECTING A METHOD FOR LEAD ANALYSIS

The measurement of lead is based on similar chemistry to that which made lead so useful to humanity. There are many insoluble salts of lead, leading to the earliest known methods for determination of lead: precipitation-based reactions. Because of its easily accessible redox states of 0, 2^+, and 4^+, lead can be changed from two different cations to a metal. Lead can be electrolytically deposited as the metal or as the metal oxide onto an electrode for subsequent gravimetric (precipitation)-based measurements.

Lead forms alloys of metals and metal sulfides easily. Lead can be reduced from the divalent state to the metal and solubi-

lized in mercury, or even into or on a gold surface for an electrochemical determination known as anodic or cathodic stripping voltammetry. The alloy of PbS with Ag_2S, which can also be considered a precipitation reaction, can be used to develop voltages depending on the lead concentration. Other voltage measurements can be devised based on the chelation of aqueous lead to a non-aqueous carrier in which lead is partially transported into a membrane. The voltage across the membrane will be altered by the extent of lead transport.

The valence shell electron configuration of metallic lead is $s^2d^{10}p^2$. That of the divalent lead is $s^2d^{10}p^0$. The fact that the d orbital is filled makes the divalent cation "silent" to light in the visible region, a surprising fact, because lead is a major component in two of the three primary artist's colors, red and yellow. The color in the pigments lies in a charge transfer band (an internal oxidation/reduction of the oxide compound) as opposed to a perturbation of d electrons from a filled lower state to an unfilled higher energy state. As a result, the most popular method for analysis, colorimetric, is the most difficult to create. Colorimetric methods rely on the charge transfer reaction (PbI_2) or on the chelation of the lead ion in which the chelate undergoes a color change with reaction with lead. The electron promotion occurs within the chelate's valence shell from the highest occupied molecular orbital (HOMO) to its lowest unoccupied molecular orbital (LUMO). Therefore, this method relies on chelation for selectivity, something that is particularly difficult to achieve.

Better success is achieved with manipulating the s and p valence electrons or the inner shell electrons. The 6p/7s,p electronic transitions can be accessed through atomic absorption spectroscopy, atomic emission spectroscopy, or atomic fluorescence. The most commonly used methods are those of atomic absorption spectroscopy using electrothermal gas phase production, and that of atomic emission spectroscopy using a plasma

source for the gas phase production and excitation of the electrons. Internal shell electrons can be probed using X-ray fluorescence methods.

Success is also obtained by probing the electrons within the bonds in vibrational spectroscopies. Traditional infrared techniques have been used to understand the structure of the charge transfer-based pigments. Nondestructive vibrational methods involving reflection of light that are very sensitive and very accurate have been introduced recently for art analysis using Raman spectroscopy.

Manipulation of the lead into the gas phase and separation based on weight (gas diffusion or acceleration) provide a method for isotopic analysis. Although in some senses this is a weight-based measurement, it falls under the general category of spectroscopic analysis, as a spectrum of isotopes is scanned.

Separation-based methods in which a flowing stream of gas or liquid is carried past a stationary support can also be used. The most common method is that of gas chromatography for the determination of the organolead compounds. Liquid-based methods (useful for divalent lead or a chelate of divalent lead) have been reported but are not among the most common or validated methods.

The use of biotechniques (enzyme assays, monoclonal antibody assays) is in its infancy.

The LOD of the instrumental method, its ability to determine species (qualitative analysis), and the destructive, nondestructive nature of the method are matched against regulatory limits for lead (Figure 1) in selecting a method. The regulatory limits have dropped as the LOD has dropped with date of introduction of the method (Table 1).

II. DETERMINATIONS BASED ON SOLUBILITY

The insolubility of lead (Table 2) is important in its historical applications, and in establishing its toxicity as a substitute for calcium. The affinity of lead for oxides is

TABLE 1
Limits of Detection

Acronym	~Dates	Method	LOD ppb = ng/g = μg/L
Gravimetric	1823	Lead sulfide spot tests	
	1823–1920	Lead chromate precipitation	
UV-Vis	1920–1960	Complexation with dithizone	20–500 ppb
EP	<1980	Erythrocyte protoporphyrin fluorescence assay	>250 ppb
ASV	1960–present	Anodic stripping voltammetry	20–50 ppb
FAAS	1960–1970	Flame atomic absorption spectroscopy	20–50 ppb
Hydride AA	1970–80	Hydride generation AA	40 ppb
FAFS	1960	Flame atomic fluorescence spectroscopy	500
ISE		PbS/Ag_2S ion selective membranes	$10^{-5}M$ (2 ppm)
GFAA	1970–1985	Graphite Furnace atomic absorption	50 ppb
GFAA+ preconc.		Graphite furnace AA	0.05 ppb
XRD		X-Ray diffraction	Qualitative
IR		Infrared spectroscopy	Qualitative
XRF		X-Ray fluorescence, house paint	0.9 mg/cm^2
NMR	1970s on	Nuclear magnetic resonance	1%
Raman	1980s	Raman spectroscopy	Qualitative
LEAF	1980s	Laser excited atomic fluorescence	0.2 to 9 ppt
IEC		Ion exchange chromatography	50
ICP-AES	1980s	Inductively coupled plasma atomic emission	20
ICP-MS	1980s	Inductively coupled plasma mass spectroscopy	1–10 ppt
EXAFS	1990s	Extended X-Ray absorption fine structure	Qualitative
LIB-LEAF	1995	Laser induced breakdown/LEAF	0.055 μg/m^3
Optodes	1990	UV-Vis methods coupled to fiber optics	Sub ppt
Immonoassays	2000s	Monoclonal antibodies will be raised to chelates of lead	Sub ppt

based on the unique position of lead as a member of the carbon family. Lead can bind both ionically and covalently with lead as an oxide. Lead oxides are important in the chemistry of batteries.

The reaction of lead with phosphates is also an important solubility system, because of the deposition of lead into bone and tooth material. Phosphate precipitates of lead are used to line plumbing material.

A. Sulfate

The time-honored method determination of lead, prior to the flood of instrumental methods beginning in the 1970s, was a gravi-metric method.[1,2] Two main methods were used:

$$Pb^{2+} + SO_4^{2-} \rightleftarrows PbSO_4 \quad -\log K_{sp} = 7.8 \quad (1)$$

$$Pb^{2+} + CrO_4^{2-} \rightleftarrows PbCrO_4 \quad -\log K_{sp} = 13.75(88°) \quad (2)$$
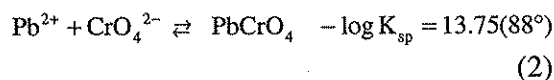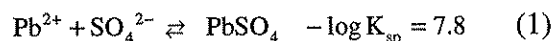
The lead sulfate method is less reliable than the chromate because of its higher solubility which implies that some of the lead in solution may escape precipitation. Furthermore, bismuth, tungsten, niobium, tantalum, and barium co-precipitate in the presence of lead. Barium can be removed by redissolving the
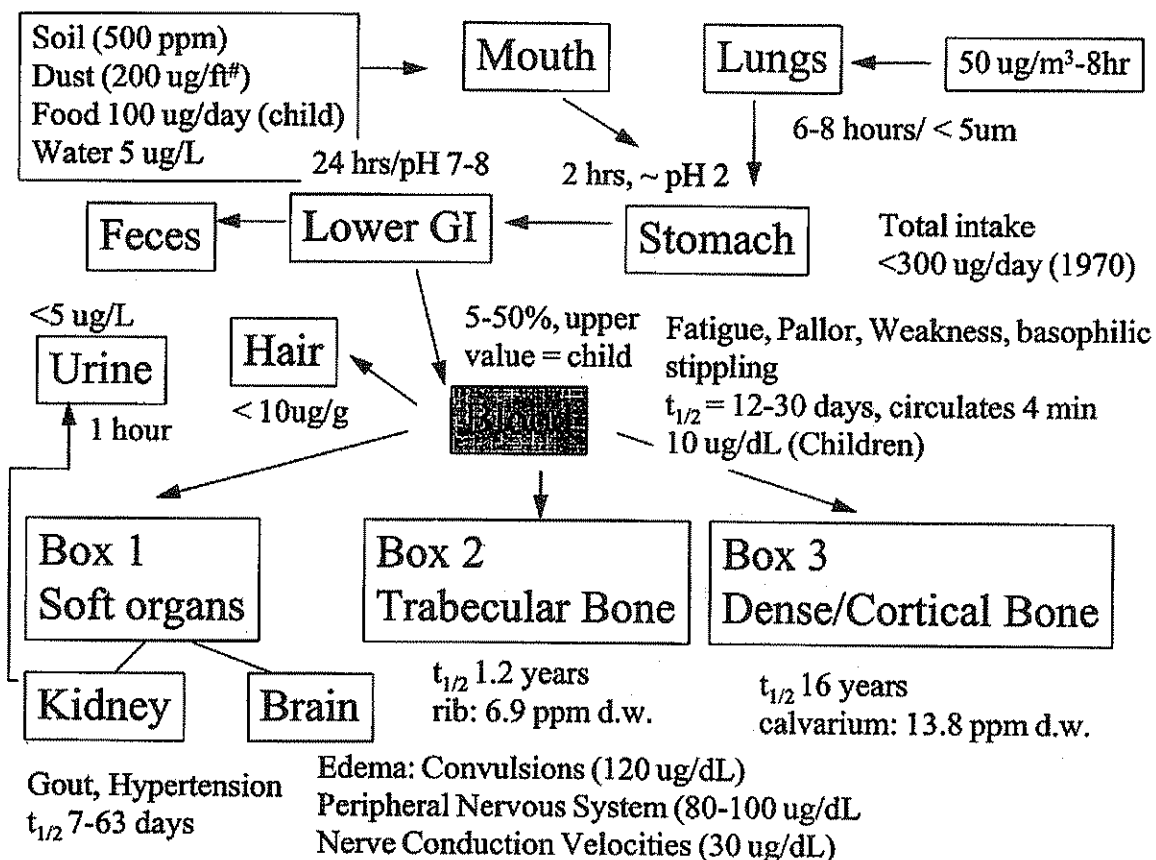
FIGURE 1. Schematic of the pathway of lead into man and the action levels of lead. These numbers determine the limit of detection required in a particular analysis.

TABLE 2
Solubility of Pb^{2+} and Ca^{2+}

Salt	-Log Ksp	
	Pb^{2+}	Ca^{2+}
MCl_2	3.74	−3.08
MSO_4	7.75	4.21(est.)
MCO_3	13.5	8.3
$M(OH)_2$	15.6	5.2
$MCrO_3$	13.75	−0.037 (est.)
MO (yellow)	15.3	3.3
MS	29	5.11 (est.)
$M_3(PO_4)_2$	42.1	28.7
MO_2	Insoluble	Not applicable
Iionic radius	0.175 nm	0.197 nm
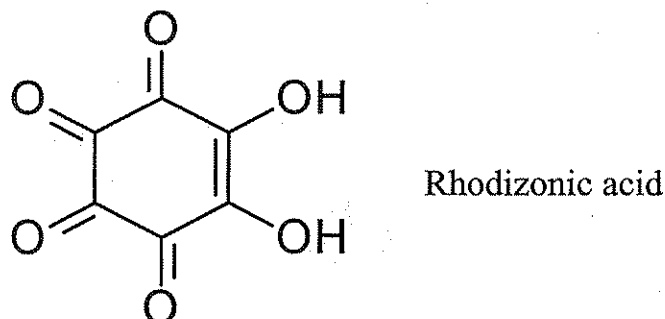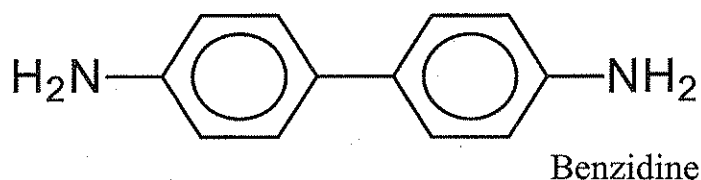
FIGURE 2. Structure of benzidine and rhodizonate used in spot tests for lead.

precipitate in ammonium acetate. Under these conditions, barium is removed but lead remains insoluble. Strontium, calcium, antimony, bismuth, silver, and copper may be partially precipitated.

B. Lead Chromate

Lead chromate is more insoluble than lead sulfate, which increases the reliability of determining the total lead in solution. (The reaction of lead with chromates was one of the principal means of obtaining orange-based pigments in older paints.) Some **selectivity** is also achieved because lead chromate is precipitated from acidic solution where $HCrO_4^-$ is also present. Other metals such as Ag^+, Ba^{2+}, and Bi^{2+} will not precipitate as chromates from acidic conditions. The primary difficulty with the lead chromate method is that the precipitate does not always conform to the $PbCrO_4$ formula, suggesting that reaction 2 does not describe the precipitate well. The variable nature of the precipitate is apparently the result of the precipitation process and the drying conditions.

C. Spot Tests

The binding of lead with sulfur is quite strong due to polarizability effects and has significant implications for its mode of action in biological systems. Accum (1820)[3] describes one of the first methods of lead analysis based on bubbling sulfide gas through suspected water or wine. The dark sulfide precipitate was a measure of the adulteration of the wine. Lead sulfide spot tests have been recommended as a public health education method for battery factory workers.[4]

Several commercial spot tests rely on color development of a lead solid, most likely with either benzidine or rhodizonate as coloring agents. The benzidine (Figure 2) spot test for lead normally involves digestion of the sample in acid. A drop of the digested solution is placed on a filter paper with a drop of a hydroxide. A drop of bromine water (contains alkali hypobromite) is added to the paper. The added base stabilizes the hypobromite that serves to oxidize lead to Pb^{2+}. Ammonia is added to keep the solution basic. Divalent lead combines with oxygen to form PbO_2. A drop of benzidine is added, which reacts with PbO_2 to form a deep blue fleck. This technique can measure approximately 1 μg of lead.

The rhodizonate (Figure 2) spot test is so sensitive to lead that it can develop a color just from the amount of lead that goes into solution with water in contact with the lead

salt. The same general steps for benzidine are followed: digest, add to filter paper with NaOH, add bromine water, then add rhodizonate. A compound of lead-rhodizonate+lead-hydroxide solid ($Pb(C_6O_6)$-$Pb(OH)_2 \cdot H_2O$) is formed, which gives an intensely scarlet color similar to the charge transfer color developed in the red pigment Pb_3O_4. Because of the intensity of the color, very small amounts of lead can be determined. Positive results are obtained on slightly soluble materials such as PbS.

D. Effect of Hydroxides

While lead hydroxide does not give a good quantitative measure of lead, particularly in the presence of competing species, it is an important reaction in all analytical determinations. The manipulation of the test solution for further, instrumental, analysis nearly always requires a pH adjustment to deprotonate a reagent or to prevent lead hydroxide formation.

A metal ion can bind to a ligand, L (Cl⁻, CN⁻, OH⁻, etc.), in sequential steps.

Reaction	Constant	Conc in terms of stepwise and overall formation constants

$$M + L = ML \quad K_1 \qquad [ML] = K_1[M][L] \qquad (3)$$

$$ML + L = ML_2 \quad K_2 \qquad [ML_2] = K_2[ML][L] = K_1K_2[M][L]^2$$
$$= \beta_2[M][L]^2 \qquad (4)$$

$$ML_2 + L = ML_3 \quad K_3 \qquad [ML_3] = K_3[ML_2][L]$$
$$= K_1K_2K_3[M][L]^3 = \beta_3[M][L]^3$$
$$(5)$$

$$ML_{(n-1)} + L = ML_n \quad K_n \qquad [ML_n] = K_n[ML_{(n-1)}][L]$$
$$= K_1K_2 ... K_n[M][L]^n = \beta_n[M][L]^n$$
$$(6)$$

The constants for lead hydroxide are $logK_1 = 7.82$; $Log\beta_2 = 10.88$; $Log\beta_3 = 13.94$; $Log\beta_4 = 16.30$. Each reaction has been solved for the equilibrium concentration of the appropriate species in terms of the sequential or stepwise equilibrium constants, K_i, and in terms of the overall equilibrium constant, β_i. A

Alpha Fraction Plot
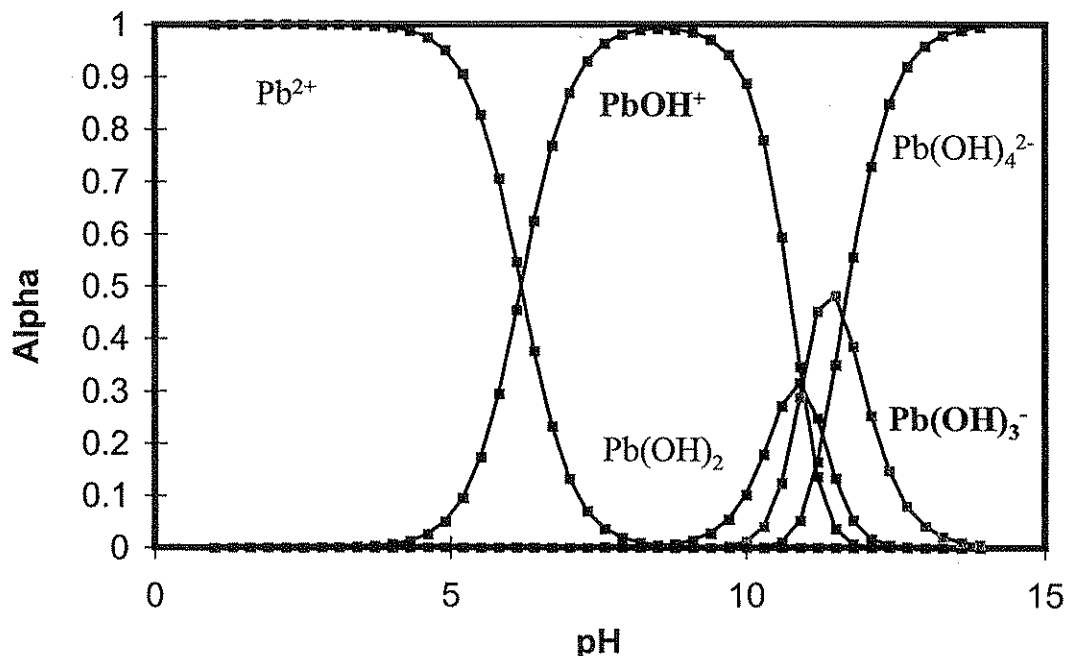
FIGURE 3. Plot of the fraction of lead in various hydroxy forms as a function of pH.

mass balance for all forms of the metal is written as:

$$C_M = [M] + [ML] + [ML_2] + [ML_3] ...+ [ML_n] \tag{7}$$

where C_M is the total metal concentration. Each of the concentration terms can be replaced:

$$C_M = [M] + K_1[M][L] + \beta_2[M][L]^2 + \beta_3[M][L]^3 + ..._n[M][L]^n \tag{8}$$

A denominator "D" is defined as:

$$D = C_M/[M] = 1 + K_1[L] + \beta_2[L]^2 + \beta_3[L]^3 + ...\beta_n[L]^n \tag{9}$$

To calculate the fraction of the total amount of metal in each form "alpha" fractions are defined as:

$$\alpha_0 = [M]/C_M = 1/D \tag{10}$$

$$\alpha_1 = [ML]/C_M = K_1[M][L]/C_M = K_1[L]^2/D \tag{11}$$

$$\alpha_2 = [ML_2]/C_M = \beta_2[M][L]^2/C_M = \beta_2[L]^2/D \tag{12}$$

$$\alpha_3 = [ML_3]/C_M = \beta_3[M][L]^3/C_M = \beta_3[L]^3/D \tag{13}$$

$$\alpha_n = [M\ln]/C_M = \beta_2[M][L]^n/C_M = \beta_n[L]^n/D \tag{14}$$

Figure 3 shows the change in lead ion concentration with pH. The plot indicates that most lead is present as the divalent ion up to a pH of 5 where the monohydroxide species becomes important.

E. Carbonates

While lead carbonates were used extensively in cosmetics and white paints, they are soluble enough that they do not work well in gravimetric analysis.

274

III. TITRATION METHODS OF ANALYSIS

A variety of Lewis acids bind to lead, leading to the formation of soluble lead compounds, such as chlorides and bromides. Lead binds to more complex compounds containing a variety of S-, N-, and O-containing ligands. The sulfur bond, based on the difference in electronegativities of the atoms (0.6), can be very covalent in nature, and therefore likely to result in a "permanent" attachment. The nitrogen bond to lead, predicted from the difference in electronegativities (1.1), is less covalent in nature than sulfur. The difference in electronegativity of lead to oxygen is 1.7, which places it exactly in the middle of an ionic vs. a covalent bond. The result is a strong attachment with the possibility of release, a requirement for a reusuable sensor.

In addition to considerations of potential bond strength, the complexing reagent has a unique interaction with lead based on the potential stereochemical activation of the $6s^2$ configuration of lead.

A. Soluble Complexes: Acetate, Chlorides, and Bromides

Lead acetate (Table 3) is too soluble for use in a gravimetric determination. Lead

TABLE 3
Pb Formation Constants

$$Pb + L \rightleftarrows PbL \qquad K_1$$
$$PbL + L \rightleftarrows PbL_2 \qquad K_2$$
$$PbL_{n-1} + L \rightleftarrows PbL_n \qquad K_n$$

Ligand, L	Name	log K_1	log K_2	log K_3	log K_4
Cl^-		1.55	0.6	−0.4	0.7
Br^-		1.77	0.8	0.4	−0.7
I^-		1.92	1.3	0.7	0.6
OH^-		6.4	4.5	3.0	
SO_4^{2-}		2.69			
$CH_3CO_2^-$	Acetate	2.33	1.27	0.0	−0.7
$C_2CO_4^{2-}$	Oxalate	4.91	1.85		
	Citrate	5.7			
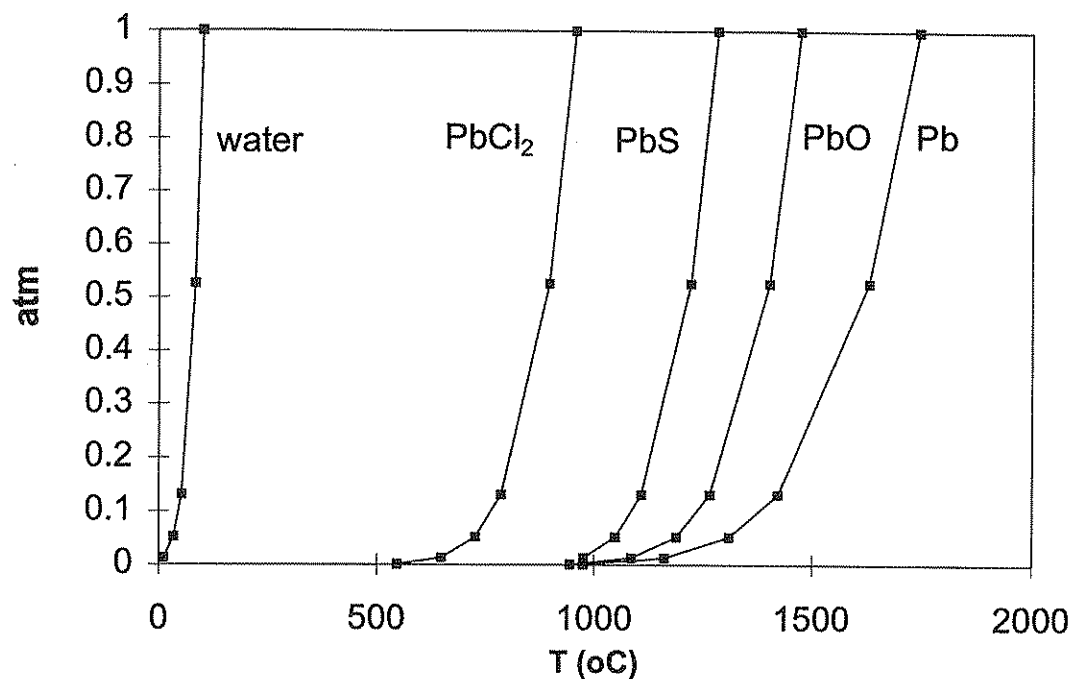
FIGURE 4. Plot of the vapor pressure of lead compounds as a function of temperature.
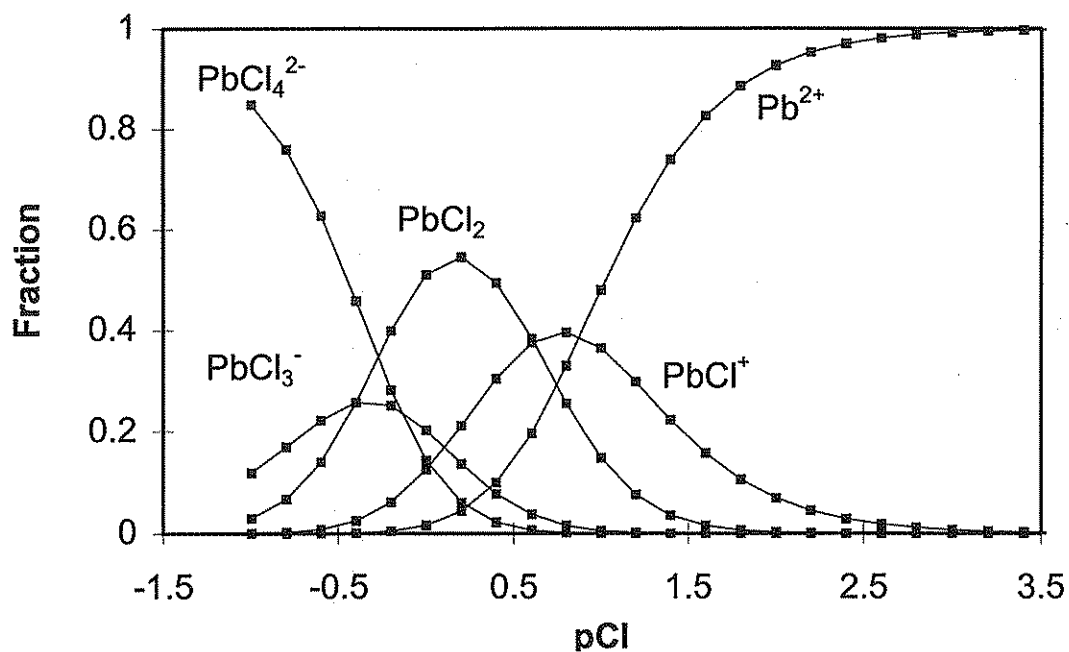
FIGURE 5. Plot of the fraction of lead in various chloride species as a function of the total chloride concentration.

acetate is known as sugar of lead, and was a major component of the Roman sweetener known as sapa. It found use as a preservative or antioxidant for wines. Lead tetraacetate is less soluble and is a common oxygen carrying reagent in organic chemistry. The lone pair in lead tetraacetate is stereochemically active.
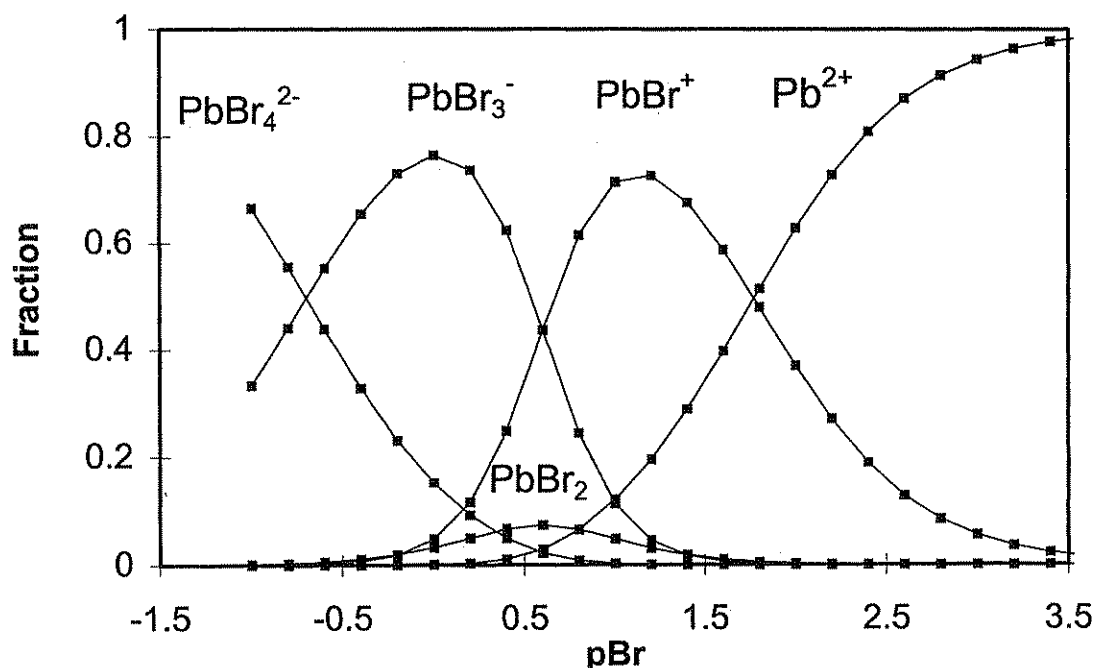
FIGURE 6. Plot of the fraction of lead in various bromide species as a function of the total bromide concentration.

TABLE 4
Lead Chelation Data

Metal cation ionic radii/pm Chelate		log K(ML) or K(MHL)						
		Pb 133	Ca 114	Cd 109	Zn 88	Cu 87	Mg 86	Ni 83
Name	**Ligands**							
Pyrocatechol	O	13.25		8.13	10.41	16.47	4.42	9.35
Tiron	O	11.95	5.8	7.69	10.19	14.53	6.86	9.96
Betadiketones AA	O	8.6		7.79	9.52	12.46	3.36	5.96
Betadiketones BzA	O	8.84		12.02	9.62	9.42	7.84	10.3
Betadiketones Dbm	O	9.75		8.67	10.23	12.98	8.54	10.83
Sulfarsazen	N, O	10.5		9.8	10.8	5.09		8.1
PAR	N, O	11.9		10.5	10.5	14.8		13.2
TAR	N, O	8.34	3.5	6.96	7.19	11.56	<3	12.94
EDTA	N, O	18.04	10.96	16.46	16.5	18.80	8.69	18.62
MTB	N, O	6.4	5.5	3.3	5.5		5.2	
Alizarin	N, O	11.69			12.19	14.75		12.23
8-hydroxyquinoline	N, O	10.61	7.3	9.43	9.96	13.49	6.38	11.44
Nitrosnaphtaline	N, O	9.73		6.18	9.32	12.52	6.05	10.75
Dioxime	N	7.3		5.7	8.1	11		11.16
Thioxine	S N	11.52		10.79		12–14		10.95
Diethyldithiocarbamate	S	18.3			11.4	28,8		12.9

Lead chloride can be used as the chemical basis for separation (column) methods, but otherwise presents a problem because of its high volatility, a fact that was made use of in gasoline chemistry (Figure 4). The high volatility makes lead chlorides the basis to
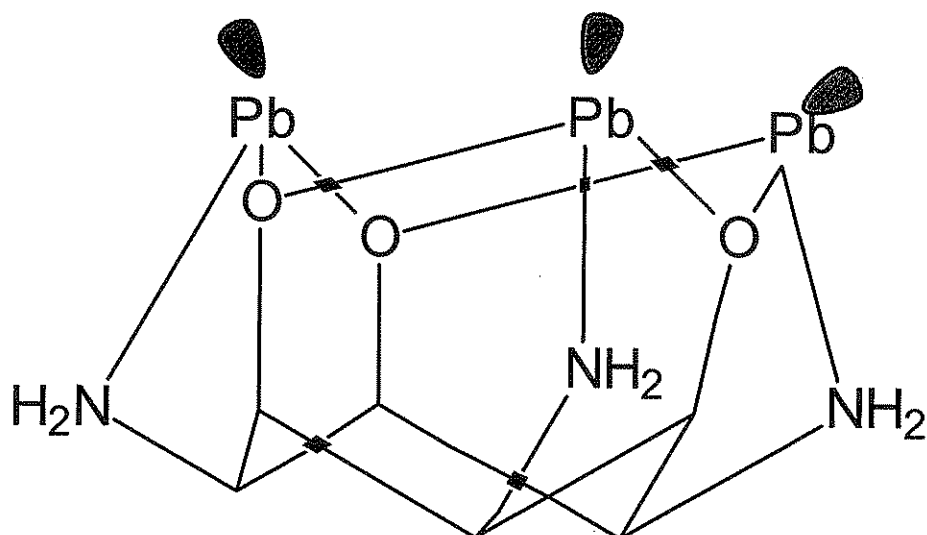
FIGURE 7. Figure showing the stereochemically active 2s lone pair on Pb^{2+} in the compound 1,3,5-triamino-1,3,5-trideoxxy-*cis*-inosital.

lead exposure from soldering industries and incinerated wastes. Figure 5 shows a plot of the various forms of lead as a function of the chloride concentration. This has implications for the ability to do "good" analysis on ocean waters.

Bromide complexes with lead are slightly more stable than those of chloride, consistent with the larger size of Br^- compared with Cl^- (Figure 6). The small change in stability is sufficiently large that a method of preparative separation for lead is based on $PbBr_3^-$ chromatographic exchange.

B. Chelates and Molecular Recognition

A variety of chelates have been designed, but few have been genuinely selective for lead. There are few clues to be gained from a general survey of lead chelates. There is no particular generic preference of lead for N-, S-, vs. O-containing chelates that can be observed from Table 4. Examples of strong binding of lead to all N-, S-, and O-containing ligands can be observed.

This suggests that the strength of binding lies not just in the type of ligand but in the geometry of the binding site. In nitrogen-containing complexes, the short bond length (due to covalency) can activate the lone pair.[5] Where the Pb-N bond length is 2.37 to 2.56 Å the lone pair is active, while the bond length of 2.62 to 2.88 Å results in an inactive lone pair. This is consistent with the requirement that the ligand penetrate deep enough to the central metal atom to cause distortions in its electronic structure.

Lead in 1,3,5-triamino-1,3,5-trideoxxy-*cis*-inosital becomes stereochemically active,[6] as shown in Figure 7. In the configuration each lead has 2 O and 1 N in a distorted pyramidal shape. A nitrato ligand fills the 4th C. N. Site (C. N. #4). A similar effect is noted when lead binds to S. A review of lead coordination in PbS_4 compounds as influenced by structural constraints imposed by the chelates has been given recently.[7] The activation of the lone pair of electrons is expected when the Pb-S bond is longer and the S-Pb-S bond angle is larger than expected. The lone pair should occupy the apex of a pyramid opposite the S atoms and be stereochemically active. The pyramid has equal trans angles (113.3°). Another example of the lone pair effect is given by *bis*(6-(diethylcarbamoyl)-1 hydroxy- 2(1H)-pyridine-2-thionato-O,S)-lead (II) (Figure 8).[8]
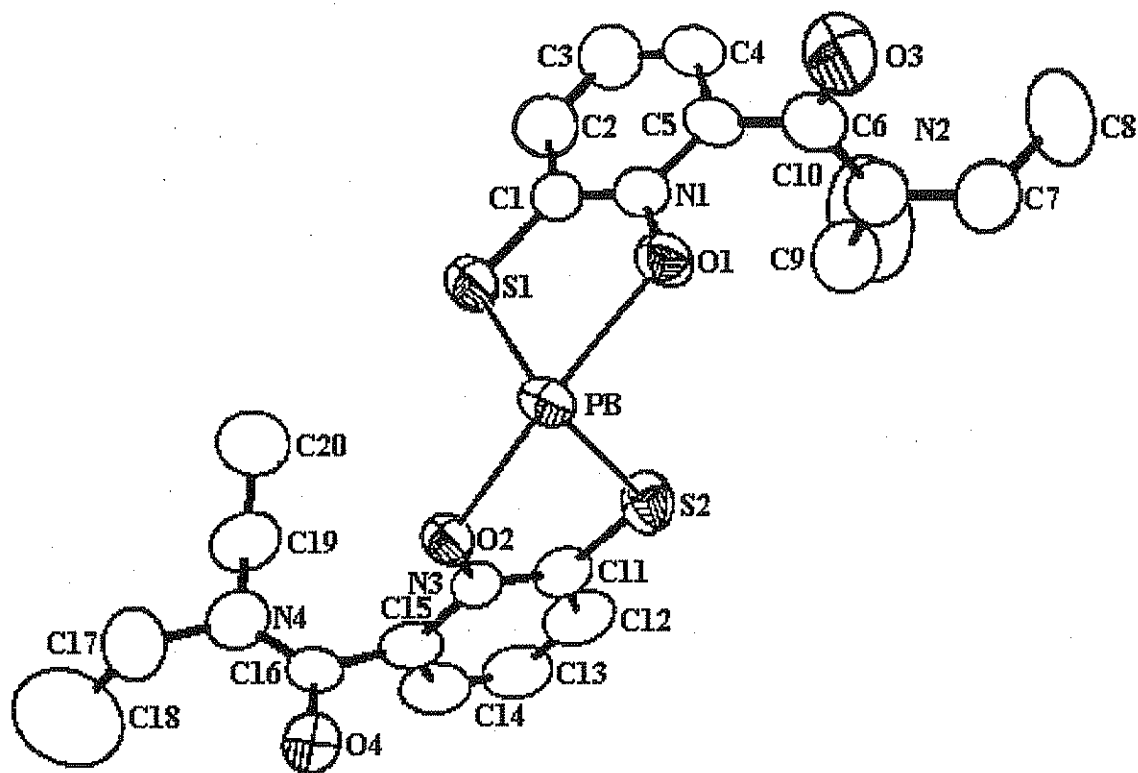
FIGURE 8. Figure showing the stereochemically active 2s lone pair on Pb²⁺ in the compound *bis*(6-(diethylcarbamoyl)-1 hydroxy- 2(1H)-pyridine-2-2thionato-*O,S*)-lead(II). The compound is viewed along the direction occupied by the lone pair on Pb²⁺. (From Kama Abu-Dari, T. B. Karpishin, and K. N. Raymond, *Inorganic Chemistry* 1993, **32**, 3052–3055.)

In an oxygen environment where bond strength is midway between covalency and ionicity, lead adopts different coordination numbers depending on the flexibility of the ligand site (which could be related to the rigidity of the chelate in forcing the lone pair out of the way). The greater flexibility and weakness of binding make the oxygen-based site attractive for chelation-based analysis, where multiple use of the chelate is important. A variety of ionophores have been synthesized that have a reasonable strength of binding to lead. Crown ethers have an open oxygen environment capable of multiple coordination with ions. Of the two crown ethers shown, the larger ring (18-crown with 6 binding oxygen) did not show involvement of the lead lone pair (Figure 9).[9,10] The dimeric 12-crown ring with each 4 oxygen binding sites (total of 8) indicated involvement of the lone pair.[11] Other ionophores

that have been used in lead separations include ethylenedi(oxy-*o*-phenoxyacetic acid) EDPAR (Figure 10)[12] and similar crown ether-like structures that are "open" at one side.[13] Some of these compounds do very well at selectively transporting lead over copper in organic matrices.

One reagent that is moderately selective for lead is meso 2,3 dimercaptosuccinic acid (DMSA). Binding of lead will occur either between the terminal oxygen and its adjacent sulfur or between the two sulfur groups. Which bond forms depends on the stereoisomer of the chelating agent present. The two stereoisomers shown in Figure 11 have similar structures but have a transposition of the bottom O and OH around the carbon. The stronger bond to lead is a single S bond, showing preference to the O-Pb-S link.[14,15] This form is also the more soluble for of the chelate.[16,17] The more effective chelate is the

NO₃ ··· 18-crown

12-crown dimer
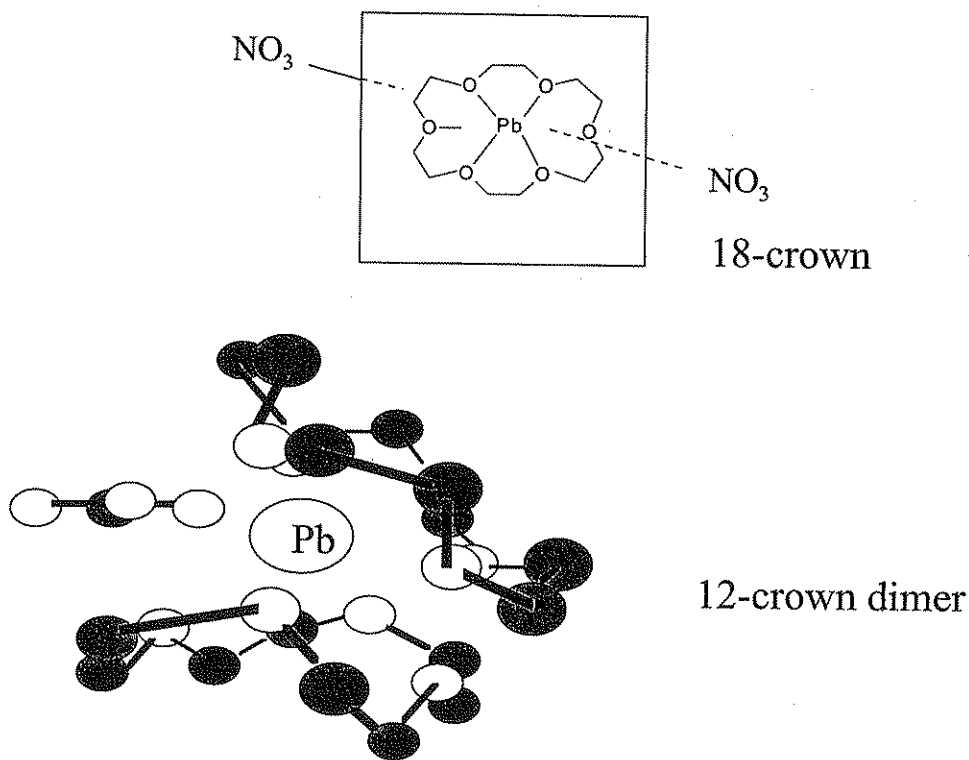
FIGURE 9. (A) 18-crown ether has been used as a lead ionophore but does not exhibit stereochemical activity of the 2s lone pair on Pb^{2+}. In this figure the Pb(18- crown-6) cation and its 2 NO_3^- anions are viewed almost perpendicularly (M. G. B. Drew, D. G. Nicholson, I. Sylte, and A. K. Vasudevan, *Acta Chem. Scan.* 1992, 46, 396-398). (B) The dimeric 12 crown ether used as a lead ionophore does exhibit stereochemical activity of the 2s lone pair on Pb^{2+}. (D. G. Nicholson, I. Sylte, A. K. Vasudevan, and L. J. Saethre, *Acta Chem. Scan.* 1992, **46**, 358-362.) One site is occupied by the lone pair and another by NO_3^-.

racemate. This is because the meso form in solution can chelate to form a double chair configuration, which has few ionic groups giving solubility, Figure 11B.

The unique geometry of the lead in this compound gives rise to a reasonable selectivity for lead over other metals (Table 5).To date, there has been no attempt to use this chelate in an analytical determination, as opposed to a therapeutic situation.

C. EDTA-BASED Methods

The most common chelation method for determination of lead is that involving the use of the Ethylene Diamine Tetraacetic Acid (EDTA) shown in Figure 12. This reagent was first put on the market in the 1930s by I. G. Farben under the tradenames Trilon A and Trilon B. Its use as a titration reagent was pioneered in the late 1940s by Schwarzenbach and co-workers.[18] The acid form of the complex H_4Y has a molecular weight of 292.1 and a low solubility in water (0.02 g in 100 ml water at 22°C[19] and 11.1 g of $Na_2H_2Y\cdot2H2O$ g/100 g water at 21°C). The protonated species can exist in a variety of forms, some of which minimize the solubilizing effect of the carboxylic acid by forming internal hydrogen bonded rings within the compound (Figure 12).

The tetraprotic chelate without metal, C_y, can exist in five separate species in solution:

$$C_Y = [H_4Y] + [H_3Y^-] + [H_2Y^{2-}] + [HY^{3-}] + [Y^{4-}]$$

$$(15)$$
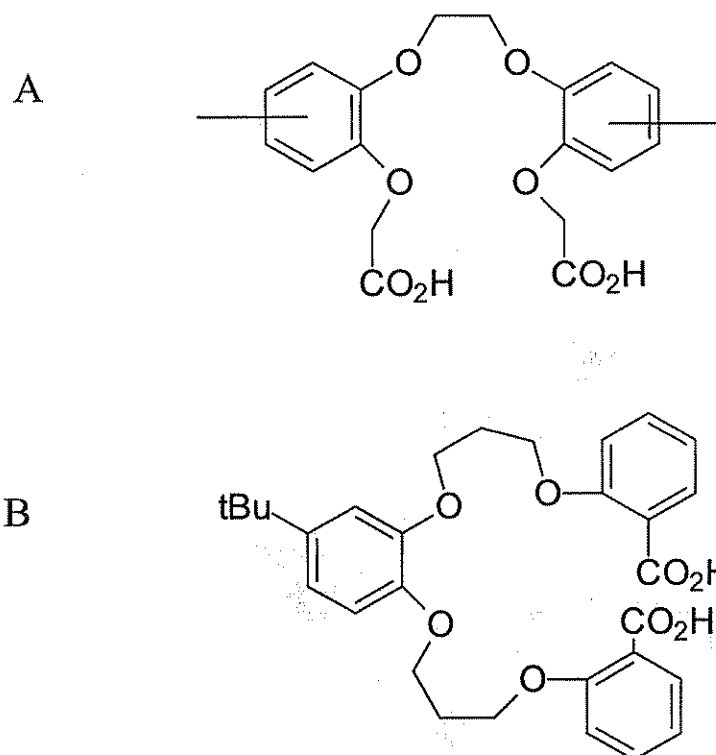
FIGURE 10. Structures similar to the crown ethers in Figure 9, but with open edges that have been used for lead selectivity.

with the fraction of each species depending on the pH. The structure of the diproton species is thought to be a resonance structure in which the sodium is shared through the carboxylic acid causing a strong stability preventing the removal of the third proton (Figure 12). The last proton pKa value is consistent with association with the nitrogen, suggesting that the remaining proton moves to the nitrogen (Figure 12).

The acid dissociation reactions for EDTA are

$$H_4Y \leftrightarrows H_3Y^- + H^+ \qquad K_{a1} \quad 10^{-2.0} \qquad (16)$$

$$H_3Y^- \leftrightarrows H_2Y^{2-} + H^+ \qquad K_{a2} \quad 10^{-2.67} \qquad (17)$$

$$H_2Y^2 \leftrightarrows HY^{3-} + H^+ \qquad K_{a3} \quad 10^{-6.16} \qquad (18)$$

$$HY^{3-} \leftrightarrows Y^{4-} + H^+ \qquad K_{a4} \quad 10^{-10.3} \qquad (19)$$
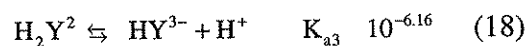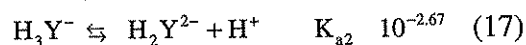
The equations can be used to express each of the species of EDTA as a function of the tetravalent form:

$$[HY^{3-}] = [Y^{-4}][H^+]/K_{a4} \qquad (20)$$

$$[H_2Y^{2-}] = [HY^{3-}][H^+]/K_{a3} = [Y^{-4}][H^+]^2/K_{a3}K_{a4} \qquad (21)$$

$$[H_3Y^-] = [H_2Y^{2-}][H^+]/K_{a2} = [Y^{-4}][H^+]^3/K_{a2}K_{a3}K_{a4} \qquad (22)$$

$$[H_4Y] = [H_3Y^-][H^+]/K_{a1} = [Y^{-4}][H^+]^4/K_{a1}K_{a2}K_{a3}K_{a4} \qquad (23)$$

Using these expressions the total uncomplexed EDTA, C_y, can be written as

$$\alpha_4 = [Y^{4-}]/([Y^{4-}] + [HY^{3-}] + [H_2Y^{2-}] + [H_3Y^-] + [H_4Y] \qquad (24)$$
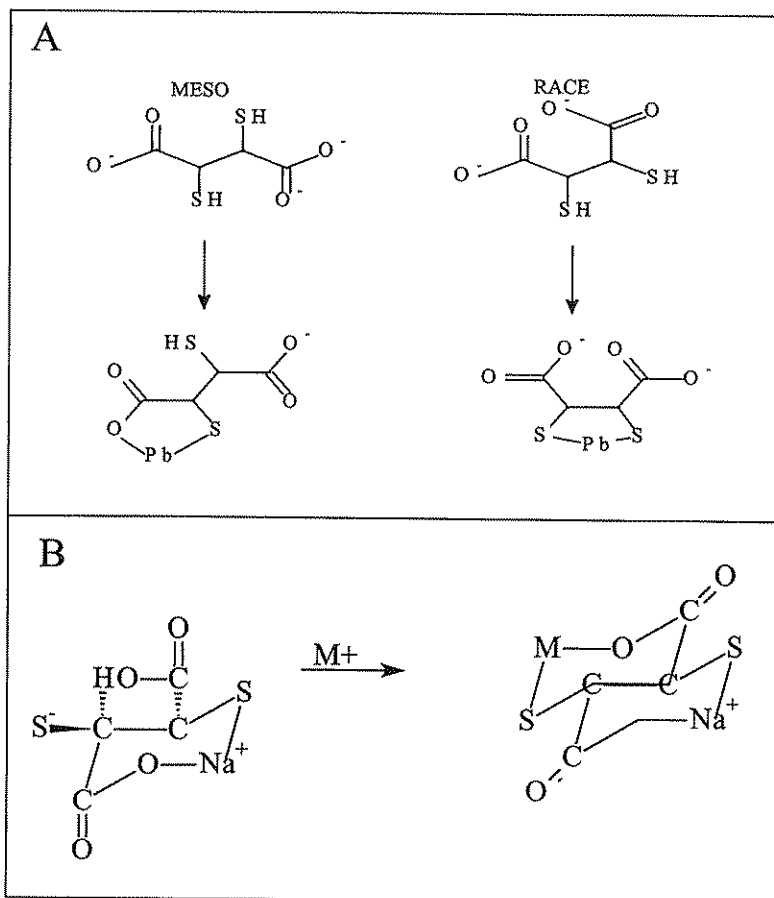
FIGURE 11. **(A)** The stereoisomeric forms of di-mercaptosuccinic acid (DMSA) used in selective lead chelation therapy. **(B)** The meso stereoisomer of DMSA ML_2 form results in a double chair configuration with low solubility, resulting in a less effective therapeutic reagent.

TABLE 5
Formation Constants with
EDTA and DMSA

Metal	EDTA K ML	DMSA K (ML)	K (ML$_2$)	K M$_2$L
In^{2+}		4.8×10^{21}		
Cu^{2+}	6.31×10^{18}			
Ni^{2+}	3.98×10^{18}	4.9×10^{11}		4.4×10^2
Cd^{2+}	3.16×10^{18}			
Pb^{2+}	7.9×10^{17}	2.9×10^{17}	1.6×10^{27}	
Zn^{2+}	3.16×10^{16}	2.6×10^4	1.2×10^4	2.1×10^3
Ca^{2+}	5.01×10^{10}			
Mg^{2+}	5.01×10^8			
Ba^{2+}	6.3×10^7			

$$\alpha_4 = [Y^{4-}]/([Y^{4-}]+[Y^{-4}][H^+]/K_{a4}+[Y^{-4}][H^+]^2/K_{a3}K_{a4}$$
$$+ [Y^{-4}][H^+]^3/K_{a2}K_{a3}K_{a4} +[Y^{-4}][H^+]^4/K_{a1}K_{a2}K_{a3}K_{a4} \quad (25)$$

$$\alpha_4 = K_{a1}K_{a2}K_{a3}K_{a4}/(K_{a1}K_{a2}K_{a3}K_{a4} + K_{a1}K_{a2}K_{a3}[H^+]$$
$$+ K_{a1}K_{a2}[H^+]^2 + K_{a1}[H^+]^3 + [H^+]^4) \quad (26)$$

The denominator can be defined as:

$$D = K_{a1}K_{a2}K_{a3}K_{a4} + K_{a1}K_{a2}K_{a3}[H^+]$$
$$+ K_{a1}K_{a2}[H^+]^2 + K_{a1}[H^+]^3 + [H^+]^4 \quad (27)$$

from which the various alpha fractions can be written:

$$\alpha_0 = [H_4Y]/C_y = K_{a1}K_{a2}K_{a3}K_{a4}[H^+]^4/D \quad (28)$$

281

H₂YPb   HYPb⁻   YPb²⁻

YPbM
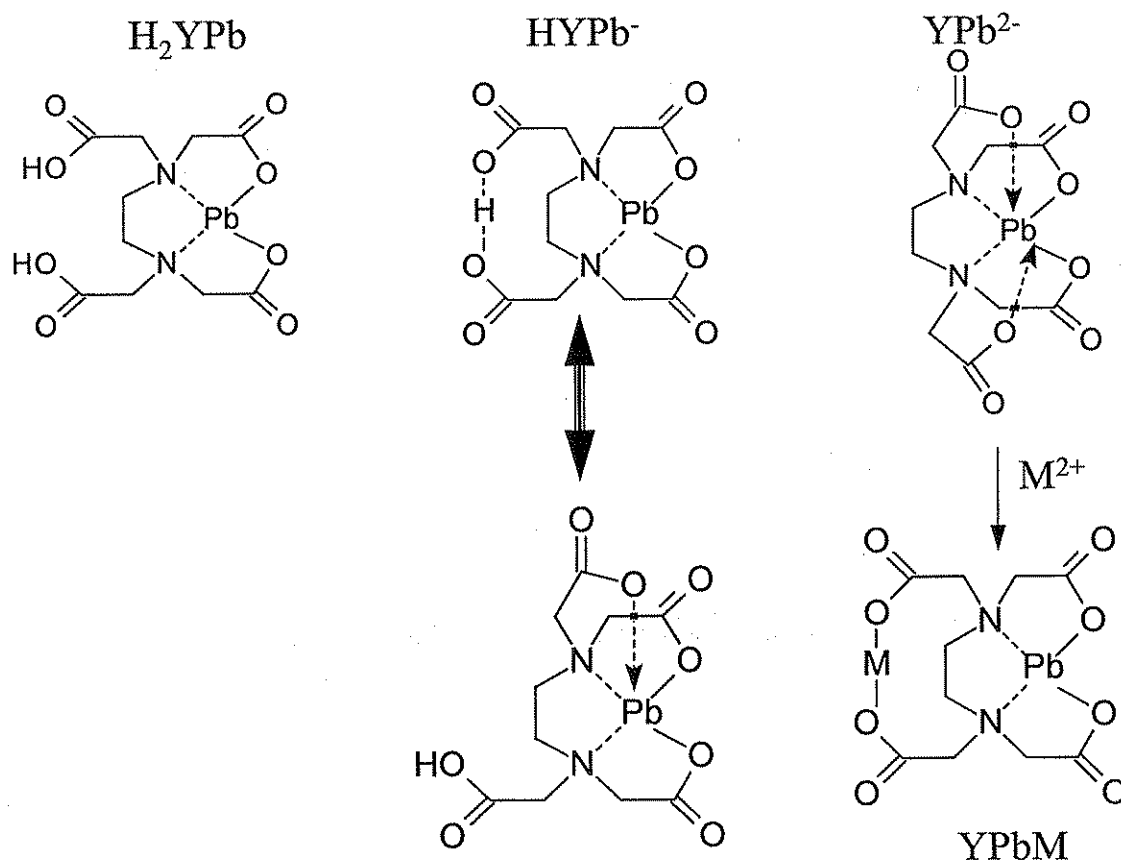
FIGURE 14. Structures of EDTA metal complexes showing the tetra- and pentacoordinated form of the metal chelate. The uncoordinated carboxyl groups maintains solubility of the EDTA chelate in solution. In the tetracoordinated form, the two remaining arms can share a proton at higher pH values.

From which one can write

$$\delta = [Pb^{2+}]/C_M = 1/(1 + K_1[X^-] + K_1K_2[X^-]^2) \quad (40)$$

A new conditional constant can be written:

$$[PbY^{2-}]/C_MC_Y = \alpha_4\delta K_f \quad (41)$$

If this conditional stability constant is large, a good endpoint in the titration is achieved.

The endpoint can be detected with either an indicator or with changes in the UV-Vis spectrum. The UV-Vis spectrum for the lead EDTA complex at pH 2 is shown in Figure

15.[18] The UV-Vis peak for Pb-EDTA at 240 nm is related to an optical transition involving the N lone pair electrons that are perturbed by the vicinty of the large lead electron cloud. For most ions the UV-Vis spectra of the complex with EDTA is "silent". In this case an indicator that changes color with chelation with lead is used. The indicator Erio T reacts with lead in an ammoniacal (high pH) solution. This causes a problem due to the precipitation of lead, so tartarate is added to keep lead in solution. The lead-tartrate complex is stable enough to keep the lead in solution but does not interfere with the reaction with the indicator. The color of the indicator is bluish violet in
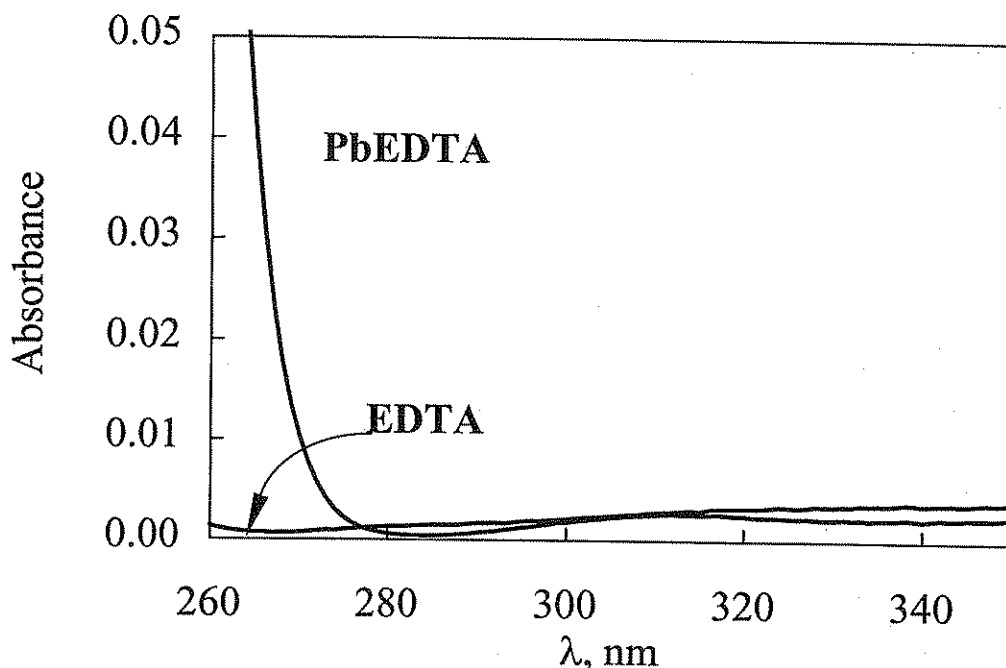
FIGURE 15. The UV-Vis spectrum of free EDTA and lead EDTA in the UV region. The change in the absorption 260 nm is attributed to perturbations of the electrons on the nitrogen.

the present of the lead. With the disappearance of lead, the color also disappears.

EDTA chelation of lead was used extensively for therapeutic purposes; however, it is non-selective, that is, it binds strongly with other metals (Table 5), resulting in their removal from the body creating side effects. In addition, it binds so strongly to lead that it mobilizes lead from the bone, resulting in an elevation of blood lead levels, and it may serve as a cross-linking reagent from metal enzyme site to a second metal site inactivating a variety of important biological functions (Figure 4, MYPb dimer).

A cadmium EDTA chelate has a sufficiently unique structure that a monoclonal antibody can be raised against the chelate. The tagged antibody can be monitored as a test for the metal cadmium. It is likely that this methodology will be extended in the future to lead.[23]

IV. DETERMINATIONS BASED ON ALLOYS/METAL FORMATION

A. Anodic Stripping Voltammetry

Lead oxides or metallic lead can be formed by oxidation or reduction reactions from the divalent lead:

$$Pb^{2+} + 2H_2O \leftrightarrows PbO_{2(s)} + 4H^+ + 4e \quad (42)$$

$$Pb^{2+} + 2e \leftrightarrows Pb_{(s)} \quad (43)$$
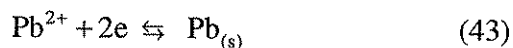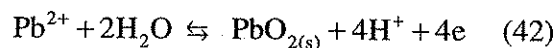
The second reaction involves reducing soluble divalent lead to the metal. This is a method known as cathodic (reductive) electrolysis of lead. The lead can either be directly collected, or, for very sensitive determination of the amount of lead, it can be

deposited as an alloy in a mercury drop or film to preconcentrate it. Once concentrated, the lead can be re-oxidized to form the soluble divalent species and the current for that reaction monitored amperometrically through a process called anodic (oxidation) stripping voltammetry.[24,25,26]

$$Pb_s + Hg_1 \leftrightarrows PbHg \qquad (44)$$

$$PbHg \leftrightarrows Pb^{2+} + 2e + Hg_1 \qquad (45)$$
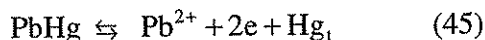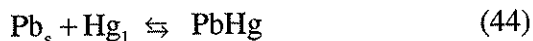
The limits of detection for this method are quite low (Table 1) and can be controlled by the preconcentration step of the lead/mercury alloy formation. The selectivity of the method arises from the potential dependent oxidation of the lead, which is resolved from other similar heavy metal, soft, ions such as Cd^{2+} (Figure 16) and Hg^+ as well as from hard ions like Zn^{2+} or Cu^{2+}, as can be

observed by a list of oxidation/reduction potentials shown in Table 6. One difficulty in this measurement comes from tin, which has its redox potential close to that of lead.

Because of the Lewis acid complex formation chemistry of chlorides and bromides the potential of lead (and other metals) shifts in the presence of chloride and bromide. The presence of the ligand stabilizes the cationic form over the reduced metal. An additional complexity is that Cl^-, Br^-, and I^- not only change the solution phase chemistry of the metal, but adsorb to the surfaces of electrodes, altering the rate of electron transfer. Figure 17 shows an example of the effect of bromide on the Indium signal.[27]

Because tin is only a few mV away from lead in reduction potential the anodic stripping voltammetry wave for lead and tin can overlap.[28,29] They can be resolved by the addition of a weak chelating reagent for lead that shifts the potential of lead further away from
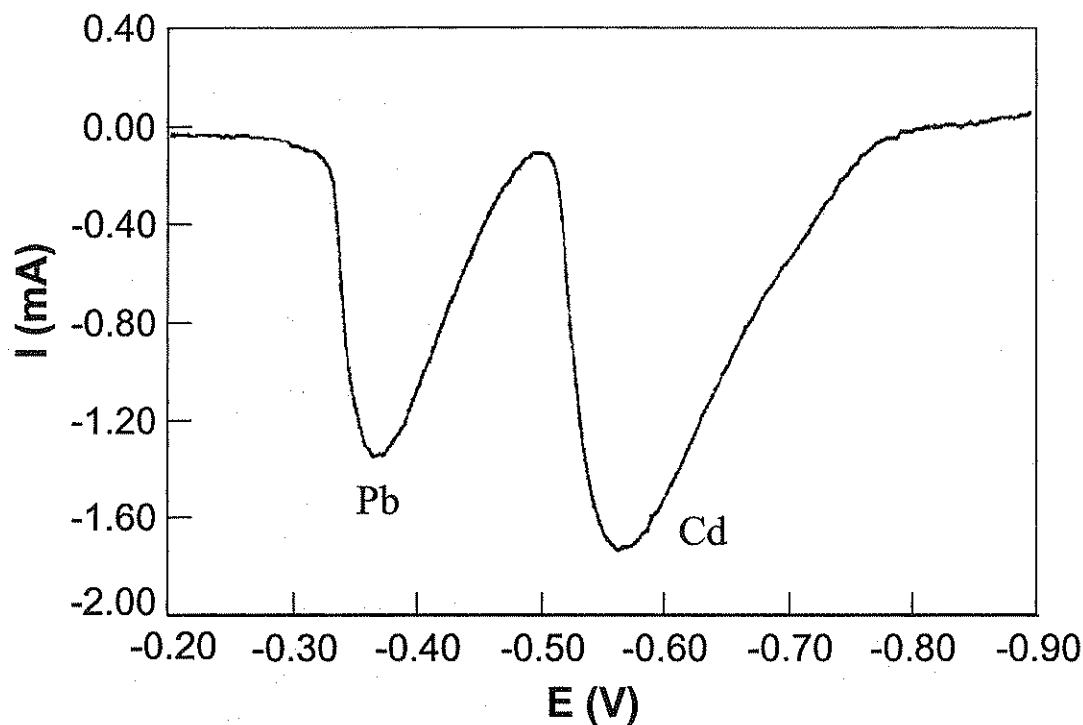
FIGURE 16. Anodic stripping voltammogram of lead (located at −0.35 V) in the presence of cadmium (at −0.6 V). Deposition of lead cation to lead in the mercury film (on Pt) was accomplished at −0.9 V.

TABLE 6
Reduction Potentials for Metals

Reaction		V vs. NHE, water
$Cd^{2+} + 2e \rightleftarrows$	Cd	−0.402
$Sn^{2+} + 2e \rightleftarrows$	Sn	−0.141
$Pb^{2+} + 2e \rightleftarrows$	Pb	−0.127
$In^{+} + e$	In	−0.126
$Cu^{2+} + 2e \rightleftarrows$	Cu	+0.161

that of tin. A typical procedure is to add sodium citrate $(HO_2CCH_2C(OH)(CO_2H)CH_2CO_2H)$ (Figure 18) buffer (0.07 M Na citrate), which will separate Sn and Pb by 70 to 240 mV. The formation constant for lead citrate is $10^{5.7}$, while citrate does not appreciably react with the tin (Table 7). The potential shift in the reduction of lead is therefore:

$$\Delta G$$
$$PbHg \rightleftarrows Pb^{2+} + 2e + Hg_1 \quad E° \quad -nFE° \quad (46)$$

$$\underline{PB^{2+} + citrate \rightleftarrows Pbcitrate} \quad K \quad \underline{RT \ln K} \quad (47)$$

$$PbHg \rightleftarrows Pb\text{-citrate} +2e + Hg -nFE° + RT \ln K$$
$$(48)$$
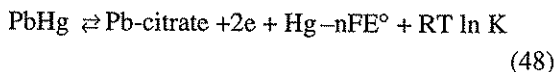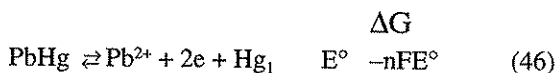
The formal potential for the overall reaction $E°'$ is

$$E°' = E° - \frac{RT}{nf} \ln K = E° - .0128 \ln K = E° - 0.0128(5.6) = E° - .0719V$$
$$(49)$$

As K is pH dependent (citrate/citric acid equilibrium) as well as citrate concentration
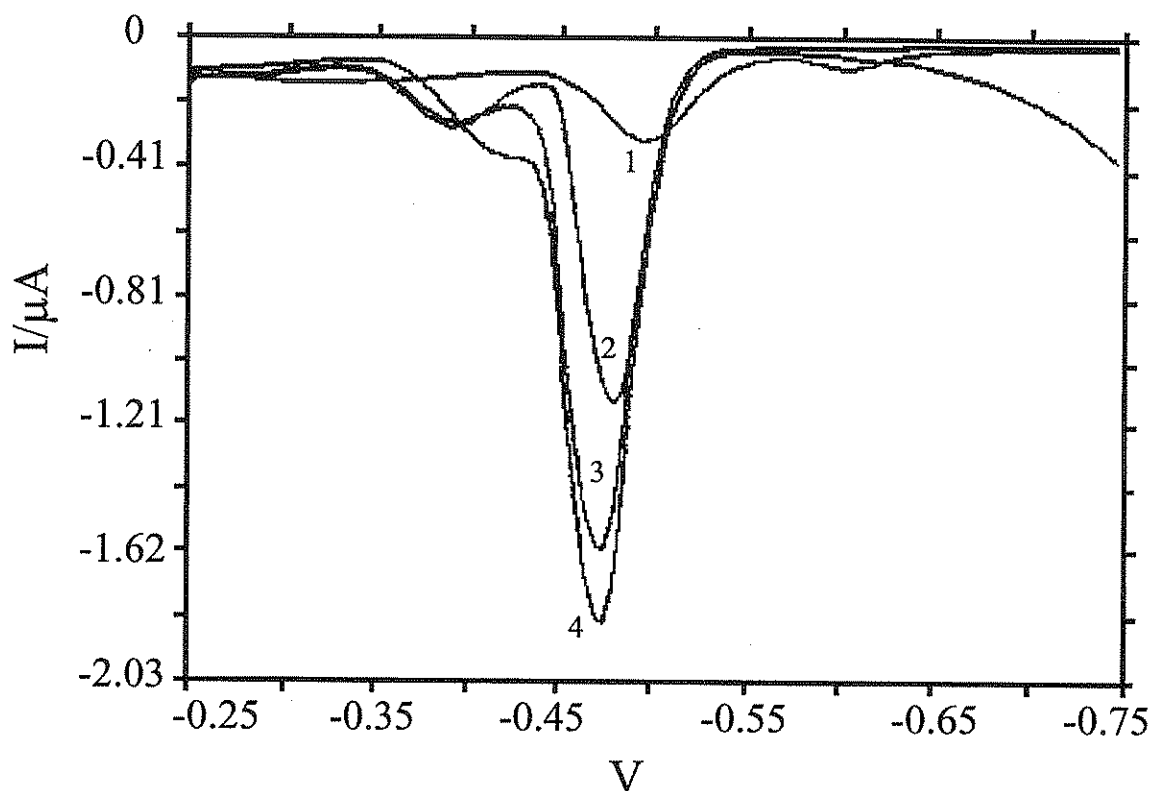
FIGURE 17. Square wave anodic stripping voltammogram of 10 ppb Pb and 150 ppb In from a solution containing 1.2 M HCl and variable concentrations of NaBr (0.0; 1.0, 1.5, and 2.0 M). As the bromide concentration is increased, the peak sharpens and shifts to more positive potentials. (From Liu, T. Z., D. Lai, and J. D. Osterloh, *Anal. Chem.*, 1997, **69**, 3539–3543.)
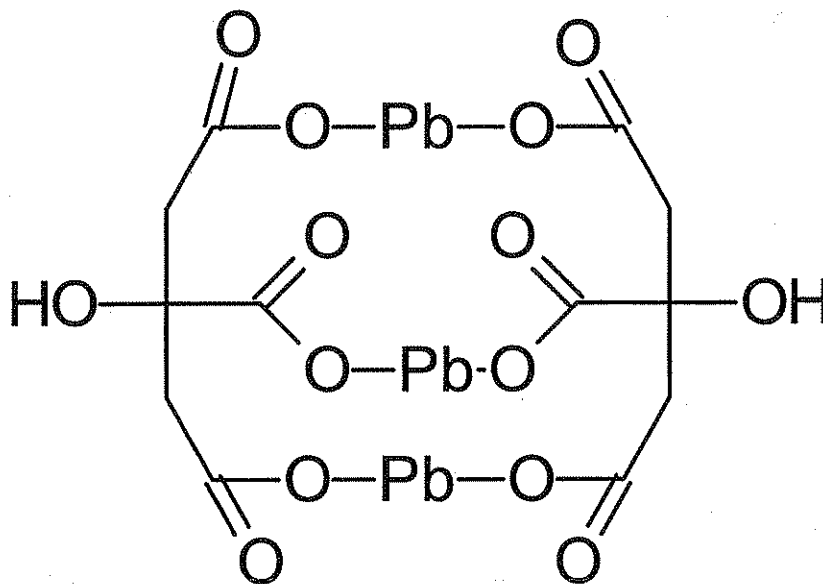
FIGURE 18. Lead II citrate complex consists of an LM_3 complex. Citrate is used to modulate the potential at which lead is reduced in order to resolve the lead peak from the tin peak in anodic stripping voltammetry.

TABLE 7
Formation Constants of Metal/Citrate Complexes

$$M^{n+} + xCitrate \rightleftarrows Mcitrate^{x-n}$$

Metal	$logK_f$
Cd^{2+}	4.2
Ca^{2+}	3.2
Cu^{2+}	14.2
Pb^{2+}	5.7
Sn^{2+}	—

dependent, the shift can be larger or smaller than the value shown above.

One interesting appplication of ASV is as a preconcentration/selective step for other more sensitive techniques such as ICP-MS.[30] The method was used extensively in the 1970s and early 1980s as a means of determining the speciation of Pb^{2+}, Pb-Ligand, Pb-solids in aquated samples. Speciation is important in determining toxicity.[31,32] Many studies investigated the role of large organic materials (humic and fulvic acids) and

surfactents in distorting the Pb^{2+} measurement vis ASV.[33,34]

While this method had been a standard method (EPA Methods 7472, 7063 for Cr and Hg) of analysis, it was never as popular as others, in part due to the necessity of working with large amounts of liquid mercury to form the mercury drop into which the lead is deposited. This drawback had been overcome in the 1980s by the introduction of mercury film electrodes, where a thin film of mercury is deposited onto a support electrode. The film can be as thick as 0.082 mm with a volume of 1 mm³. A drop of mercury that size would have a radius 0.5 mm. As a result, lead metal within the mercury drop would need to travel nearly 50 times the distance to arrive at the edge from the center. This means that the film electrode has a more efficient rate of stripping (or removal) of lead on the oxidation (Equation 45) step, leading to larger currents and lower limits of detection.

A modern variant of this method is a gravimetric determination of the lead via

288

quartz crystal microbalance. The frequency of the crystal is affected by the shear plane at the quartz crystal surface with the surface coating of mercury. When the weight of the coating increases, the resonant frequency shifts and can be calibrated for a sensitive weight measurement. The method has been applied to lead analysis but is subject to some of the same chemistry associated with bulk electrolysis of lead.[35]

Despite the lower amount of mercury used, ASV, anodic stripping voltammetry, still has remained unpopular in commercial laboratories. One way to alleviate this drawback is to have the stream of mercury be self-contained. The mercury thread electrode is a flow cell system in which the mercury reservoir is connected to the sample stream through a permeable membrane. The mercury is automatically recycled back to the waste bottle.[36,37] The disadvantage is the time required for diffusion across the membrane. The advantage is that the method is nondestructive, which means that the sample can be retrieved uncontaminated for further analysis.

Adsorptive stripping voltammetry involves depositing a chelate of the metal on the electrode and anodically stripping it off.[38,39,40] An example is that of a metal electrode (often Pt or graphite) coated with a perfluorinated ion exchange membrane (Nafion) that contains a chelating reagent such as 2,2-bipyridal[41] or with the neutral reagent PAN (Figure 19).[42] The mechanism would be based on the following reactions:

$$PAN_{Nafion} + nNa^+X^{n-} + Pb^{2+}_{aqueous} \leftrightarrows [Pb-PAN] \bullet X_2 + Na^+_{aqueous} \tag{50}$$
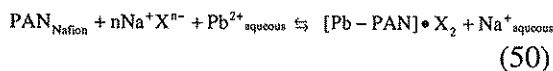
where X is the anion exchange sites on the Nafion. Reaction 50 indicates that the process involves a slow ion exchange/chelation step into the film with concurrent charge expulsion. Because the chemistry depends on a slow uptake process into the membrane

the method is significantly slower than reductive deposition of lead to the mercury. The response time of the PAN electrode was 10 min.

The lead within the film is next reduced:

$$Pb-PAN \bullet X_2 + 2Na^+_{aqueous} + 2e \leftrightarrows Pb^\circ + PAN_{Nafion} + 2Nax \tag{51}$$
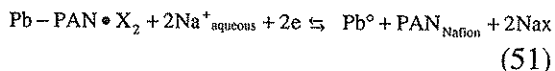
Reactions 51 and 52 both represent a preconcentration step, with the overall selectivity for the reaction being enhanced by the presence of the PAN. The analysis step involves an anodic stripping wave where the lead metal is reoxidized to the divalent species. The PAN containing modified electrode was able to achieve a limit of detection of 1×10^{-8} (0.2 μg Pb/dl) using square wave voltammetry. In these methods selectivity is **not** achieved by the redox potentials of the metals shown in Table 7, but is driven by the chelation reaction. As a consequence interferences will include species with similar overall redox potentials (modulated by the chelation reaction).

A similar methodology was achieved by incorporating crown ethers into graphite paste electrodes.[43]

B. PbO₂ Electrolytic Deposition

Another driving force to move away from mercury films is that sensors based on mercury cannot be successful in the clinical or home market due to problems of disposal. These problems have been addressed by the development of cathodic (reductive) stripping voltammetry. In cathodic stripping voltammetry lead is deposited as the tetravalent lead oxide PbO_2 onto gold or graphite (or lead). Bulk amounts of the lead oxide can be scraped from the electrode and measured gravimetrically, a method common in the 1960s. It has been used for preconcentration and purification for thermal ionization mass
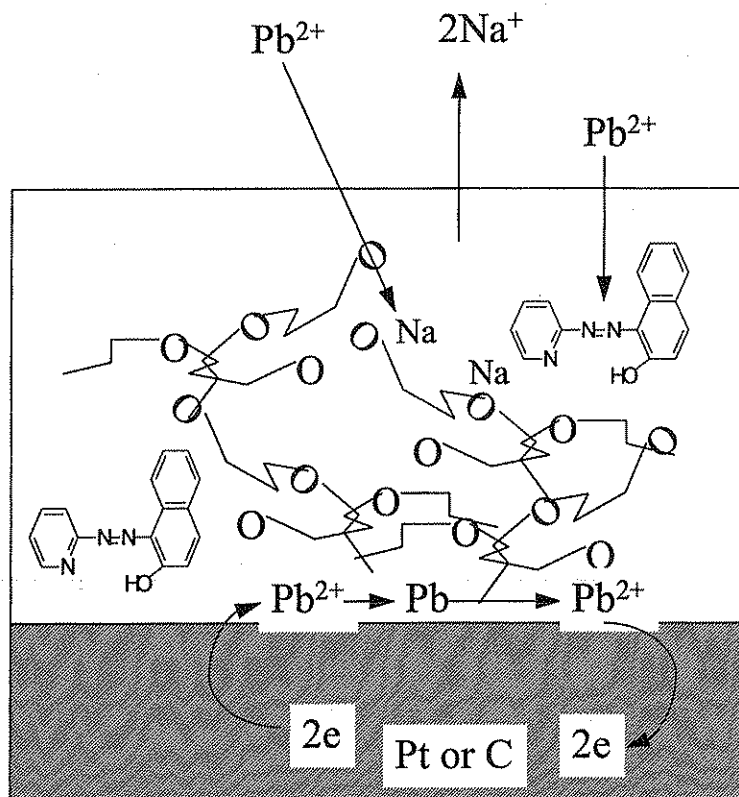
FIGURE 19. The ligand 1-(2-pyridylazo)-2-naphthaol (PAN) can be used to impart additional selectivity and concentration effects in modified electrode-based stripping voltammetry. The mechanism for the process is shown schematically where lead is coordinated by the neutral reagent enhancing its concentration selectively at the electrode surface before the reduction to metal. After reduction to the metal the lead is measured by its reoxidation signal.

spectrometry.[44] Two forms of lead can be deposited, tetragonal or orthorhombic, although from a nitric acid solution the tetragonal form is most common.[45] The reaction is performed in a nitric acid solution to prevent chlorine gas formation that occurs at about the same potential as the anodic deposition of lead dioxide:

$$PbO_2 + 4H^+ + 2e \leftrightarrows Pb^{2+} + 2H2O \qquad 1.456V$$
(52)

$$Cl_2 + 2e \leftrightarrows 2Cl^- \qquad 1.358V. \qquad (53)$$
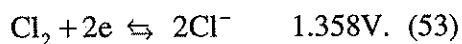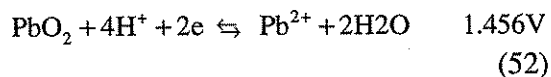
A problem with this method is that the gravimetric factor (weight of lead dioxide to weight of lead) is not always constant and is dependent on the method of electrolysis.[46,47]

C. Cathodic Stripping Voltammetry

Alternatively, the lead dioxide film can be monitored not by a weight measurement but by a stripping analysis. Because lead dioxide does not passivate (stop charge transfer), an important property in its use in lead acid batteries, it can be electrochemically probed. Lead is deposited as lead dioxide

290

onto gold or carbon. Once deposited it can be efficiently stripped from the surface by a reductive step to the divalent cation.[48,49,50] This method has the advantage that it can be miniaturized and powered by a watch battery. No purge gases are necessary for the removal of oxygen whose reduction interferes with anodic stripping voltammetry. Projected costs of blood lead measurements by this method are $2 to $3, making on site measurements feasible.

D. PbS/Ag$_2$S Alloys (Ion-Selective Electrodes)

Another use for lead metal/alloy forming behavior is in the use of the niello eutectic. PbS forms an alloy with Ag$_2$S. Historically, the association of lead sulfide (galena) with small amounts of silver (2 oz per 2 tons) drove the mass dispersion of lead into the atmosphere by Greek, Roman, and German silver mining. The eutectic of lead sulfide with silver sulfide provides the lowest melting point (Table 8). If a thin membrane is made of this solid material then either Pb^{2+}, Ag$^+$, or S^{2-} can hop through the solid. The hopping rate depends on the size of the moving ion with respect to the lattice structure of the crystal. The more open the lattice, the less motion required of the lattice to accommodate motion of the ion. In the PbS/Ag$_2$S alloy, Ag$^+$ is very mobile. An analytical method can be devised based on the mobility of silver in the niello. When charge separation across the membrane occurs, or when there is a concentration gradient, a potential is developed. A schematic of the mechanism is shown in Figure 20.

Because the signal developed is a potential in response to interfacial equilibria and in response to mobility within the membrane, the measurement is related to the energy of the system, not directly to the concentration. The free energy of the system is related (by

TABLE 8
Historical Recipes for Niello

Author	%Ag$_2$S	%Cu$_2$S	%PbS	Melt range °C
Pliny	53.4	46.6		700
Theophilus	55.7	30.3	14.0	430–560
Eraclius	32.3	35.2	32.5	440–460
Cellini	16.2	35.2	48.7	440–640
Eutectic	25	35	39	440

anology to a Boltzman distribution) in a log fashion to concentration. Consequently, the standard curve should be predicted from the Nikolsky equation:

$$E = constant + (RT/z_iF)(2.303) \log (a_i + k_{ij}a^{(zi/zj)})$$
(54)

where z_i is the valence of the ion measured (Pb^{2+}), R is the natural gas constant, T is the temperature in Kelvin, and F is Faraday's constant. Assuming room temperature and combining constants.[51]

$$E = constant + (59.16 \text{ mV}/z_i) \log (a_i + k_{ij}a^{(zi/zj)})$$
(55)

that is, the potential is related to the activity of the species of interest (a$_i$) in the log term, with the slope of the line 59/z mV. Because lead is divalent, a 28.5-mV slope in the line is expected.

Equation 56 also indicates that other elements can interfere with the measurement. Because the potential is developed due to equilibrium at the interface (solubility of PbS, which controls the solubility of Ag$_2$S, which controls the concentration of Ag$^+$, which controls the mobility of Ag$^+$ in the membrane, which controls the potential developed) any ion in solution that interferes with PbS solubility, Ag$_2$S solubility, or Ag$^+$ concentration or activity will interfere in the method. The interference will be noted as a shift in the

onto gold or carbon. Once deposited it can be efficiently stripped from the surface by a reductive step to the divalent cation.[48,49,50] This method has the advantage that it can be miniaturized and powered by a watch battery. No purge gases are necessary for the removal of oxygen whose reduction interferes with anodic stripping voltammetry. Projected costs of blood lead measurements by this method are $2 to $3, making on site measurements feasible.

D. PbS/Ag$_2$S Alloys (Ion-Selective Electrodes)

Another use for lead metal/alloy forming behavior is in the use of the niello eutectic. PbS forms an alloy with Ag$_2$S. Historically, the association of lead sulfide (galena) with small amounts of silver (2 oz per 2 tons) drove the mass dispersion of lead into the atmosphere by Greek, Roman, and German silver mining. The eutectic of lead sulfide with silver sulfide provides the lowest melting point (Table 8). If a thin membrane is made of this solid material then either Pb^{2+}, Ag$^+$, or S^{2-} can hop through the solid. The hopping rate depends on the size of the moving ion with respect to the lattice structure of the crystal. The more open the lattice, the less motion required of the lattice to accommodate motion of the ion. In the PbS/Ag$_2$S alloy, Ag$^+$ is very mobile. An analytical method can be devised based on the mobility of silver in the niello. When charge separation across the membrane occurs, or when there is a concentration gradient, a potential is developed. A schematic of the mechanism is shown in Figure 20.

Because the signal developed is a potential in response to interfacial equilibria and in response to mobility within the membrane, the measurement is related to the energy of the system, not directly to the concentration. The free energy of the system is related (by

TABLE 8
Historical Recipes for Niello

Author	%Ag$_2$S	%Cu$_2$S	%PbS	Melt range °C
Pliny	53.4	46.6		700
Theophilus	55.7	30.3	14.0	430–560
Eraclius	32.3	35.2	32.5	440–460
Cellini	16.2	35.2	48.7	440–640
Eutectic	25	35	39	440

anology to a Boltzman distribution) in a log fashion to concentration. Consequently, the standard curve should be predicted from the Nikolsky equation:

$$E = \text{constant} + (RT/z_iF)(2.303) \log (a_i + k_{ij}a^{(zi/zj)}) \tag{54}$$

where z_i is the valence of the ion measured (Pb^{2+}), R is the natural gas constant, T is the temperature in Kelvin, and F is Faraday's constant. Assuming room temperature and combining constants.[51]

$$E = \text{constant} + (59.16 \text{ mV}/z_i) \log (a_i + k_{ij}a^{(zi/zj)}) \tag{55}$$

that is, the potential is related to the activity of the species of interest (a_i) in the log term, with the slope of the line 59/z mV. Because lead is divalent, a 28.5-mV slope in the line is expected.

Equation 56 also indicates that other elements can interfere with the measurement. Because the potential is developed due to equilibrium at the interface (solubility of PbS, which controls the solubility of Ag$_2$S, which controls the concentration of Ag$^+$, which controls the mobility of Ag$^+$ in the membrane, which controls the potential developed) any ion in solution that interferes with PbS solubility, Ag$_2$S solubility, or Ag$^+$ concentration or activity will interfere in the method. The interference will be noted as a shift in the

FIGURE 20. (A) Schematic of the mechanism by which a lead/silver sulfide membrane senses lead. A potential is developed in response to silver mobility within the eutectic PbS/Ag_2S alloy. The membrane is sensitive to any reagent modulating the surface silver ion concentration, including lead. (B) Schematic of the mechanism by which a polymeric-based lead-selective ion-selective membrane is constructed. The neutral lead/chelate species is soluble in the membrane and diffuses across the membrane in the process developing a concentration-based potential.

control of the potential from the lead system to the interfering ion system. It is expressed as k_{ij} in Equation 55. The stability of the PbS electrode depends on the same chemistry as the stability of the ore galena, PbS. The chemistry of the interference at the lead ion-selective electrode can be predicted from the chemistry of PbS and from any complexation chemistry of lead and or silver.

Potentiometric methods are easily used and very reliable, particularly when the system to be analyzed is more or less constant in composition, for example, a waste stream from one part of a particular industrial process. An ISE is highly useful as an on site continuous monitor of changes in industrial process.

However, it depends on a logarithmic relationship with concentration and is not as sensitive to the type of threshold measurements that are of interest biologically: the 100 or 20 ppb level. Furthermore, the limit of detection of the ISE is often around 10^{-6} M (~2 ppm).

1. Other Ion-Selective Electrodes

To overcome the interference problems of the sulfide alloy-based ion-selective electrode, several attempts have been made to introduce polymeric-based lead-selective membranes.[52] One such membrane is a poly(vinyl)chloride polymer that has been

plasticized with an ether to make it more porous and flexible. In addition, the polymer has added to it an anion excluder (negative charged polymer). Lead is chelated with a moderately selective lead chelate which is also insoluble in water but soluble in the polymer. This creates a carrier for the lead, much like organolead served as a carrier for chloride ions in the cell membrane. Figure 20 illustrates the concept.

V. DETERMINATIONS BASED ON ELECTRONIC TRANSITIONS

A. Introduction

There are a wide range of spectroscopic transitions that could potentially be used to monitor lead. In all of the methods the sample either absorbs or emits radiation. Absorption of electromagnetic radiation can result in (1) a charge transfer band (essentially an electron transfer reaction within the compound), (2) movement of an electron from the valence shell of the atom from a low-energy state to a high-energy state, (3) movement of an electron from the lowest occupied molecular orbital to the highest occupied molecular orbital of a molecule to which lead is bound, (4) movement of a bond vibration to a higher frequency mode, or (5) a spin flip of either an electron or a nucleus. The species may emit light in order to relax to a lower energy state (electronic, vibration, or spin). The higher energy state can be achieved from heat input (emission) or from a prior photon input (fluorescence).

B. Charge Transfer-Based Analysis (PbI_2)

Lead is used in two of the three primary colors pigments, red and yellow. The color in these compounds arises from an internal oxidation reduction reaction, a ligand to metal charge transfer band in which oxygen gives up electrons to either lead or some other ion (antimony, or tin or chromium) within the inorganic crystal. For red lead, Pb_3O_4, Pb^{2+} donates electrons to Pb^{4+}, for yellow lead oxygen donates electrons to chromium, and for yellow tin oxygen donates electrons to tin or antimony. Lead is important in structural rearrangements of the crystal that allow the acceptor ion to be in close enough proximity to oxygen to accept electrons. None of these reactions have been exploited analytically, most probably due to the requirement that the color forming inorganic crystal be made and then observed in the solid state

A similar type of charge transfer reaction is observed for lead iodide. Lead iodide forms a yellow color via the process:

$$Pb^{2+}(I^-)_2 \leftrightarrows Pb^+I^- + I \qquad (56)$$
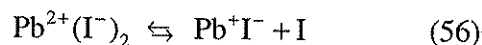
Light is absorbed at 450 nm. The crystals of lead iodide are observed as bright yellow hexagonal plates. Interferences are other insoluble iodides (Table 9). This method was used in some mid-20th century measurements of lead in paintings, but has not been exploited significantly in a commercial application.

C. Atomic Valence Electrons

1. Atomic Absorption (Graphite Furnace: EPA 200.9)

Probes of the valence shell electrons of lead are limited to the s/p transitions due to the filled d shell of lead. As a consequence, these transitions tend to be of very high energy (short wavelengths) for the UV-Vis domain (150 to 800 nm). In atomic absorption the soluble lead ion is converted to a gas phase atom and interrogated with a light

293

**TABLE 9
Solubility Product Constants
of Metal Iodides**

Species	Constant
Cu_2I	1.1×10^{-12}
PbI_2	7.1×10^{-9}
Hg_2I_2	4.5×10^{-29}
AgI	8.3×10^{-17}
SnI_2	$10^{-5.08}$

beam (Figure 21). In order to analyze for lead several steps must take place.

The sample must be dried (300°C). This step constitutes a natural concentration step because the total volume is diminished. Interfering organics must be removed (ashing), and the vapor phase containing predominately lead atoms must be formed. Once in the vapor phase a selected beam of light must be passed through the sample and the decrease in its intensity measured.

The sample is ashed at temperatures between 500 and 800°C. The chemistry of the ashing process drives the choice of wet digestion methods. Samples are generally prepared in a nitrate matrix (Figure 22).[53] The nitrates decompose to stable oxides at low temperatures:[54,55]

$$Pb(NO_3)_2 \leftrightarrows PbO + 2NO_2(g) + {}^1/_2O_2 \quad (57)$$
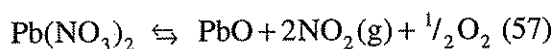
The oxide formed is stable to very high temperatures (Table 10; Figure 23). The chlorides, on the other hand, dry then sublime after drying. As a consequence, a standard procedure is the addition of either $Mg(NO_3)_2$ or $NH_4H_2PO_4$ helps to prevent premature volatilization of the lead species.[56] (The chemistry involved in the production of the lead atom vapor phase is important not only in its analysis, but in the release of lead during waste incineration of plastics containing chlorine.)

Finally, the lead atom vapor phase is formed by volatilization of solid PbO, a process that involves a donation of electrons from the surface (carbon) to the PbO.

$$PbO - C(s) \rightarrow Pb(g) + CO_2, CO(g) \quad (58)$$
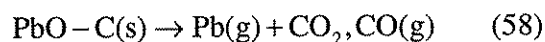
The temperature of atomization is generally 2300°C. If the sample consists of several species with different temperatures of volatilization part of the sample can be removed into the gas phase, while the remainder is still heating (Figure 24). This leads to an undermeasurement of the sample present.

The time sequence of the evolution of the lead atom vapor phase is driven by the fact that the furnace is changing temperature with time, which in turn changes the rate of volatilization of the various species. The rate of volatilization will depend in part on the oxidation state of the carbon surface and the degree to which lead moves into the interior of the graphite tube.[57] Some researchers have suggested that even with good oxide formation double peaks will be observed reflecting polymorphic oxide formation (αPbO, litharge, transforms to βPbO, massicot, at 489°C).[58] The number and location of the lead peaks depended on the number of firings of the graphite tube, suggesting that the tube surface was involved in the production of the peaks.[60]

Other methods to improve the production of the vapor phase involve stabilizing lead as an intermetallic compound with palladium. This keeps the lead present during the decomposition process of the nitrate and chloride salts while preventing the formation of the variable oxides salts by acting as a low-temperature reductant of Pb^{2+} to a metal, which subsequently undergoes Pb-Pd bond formation.[60]

A common method of producing the vapor phase is through generation of the lead hydride, plumbane, PbH_4.[61] Reaction to the
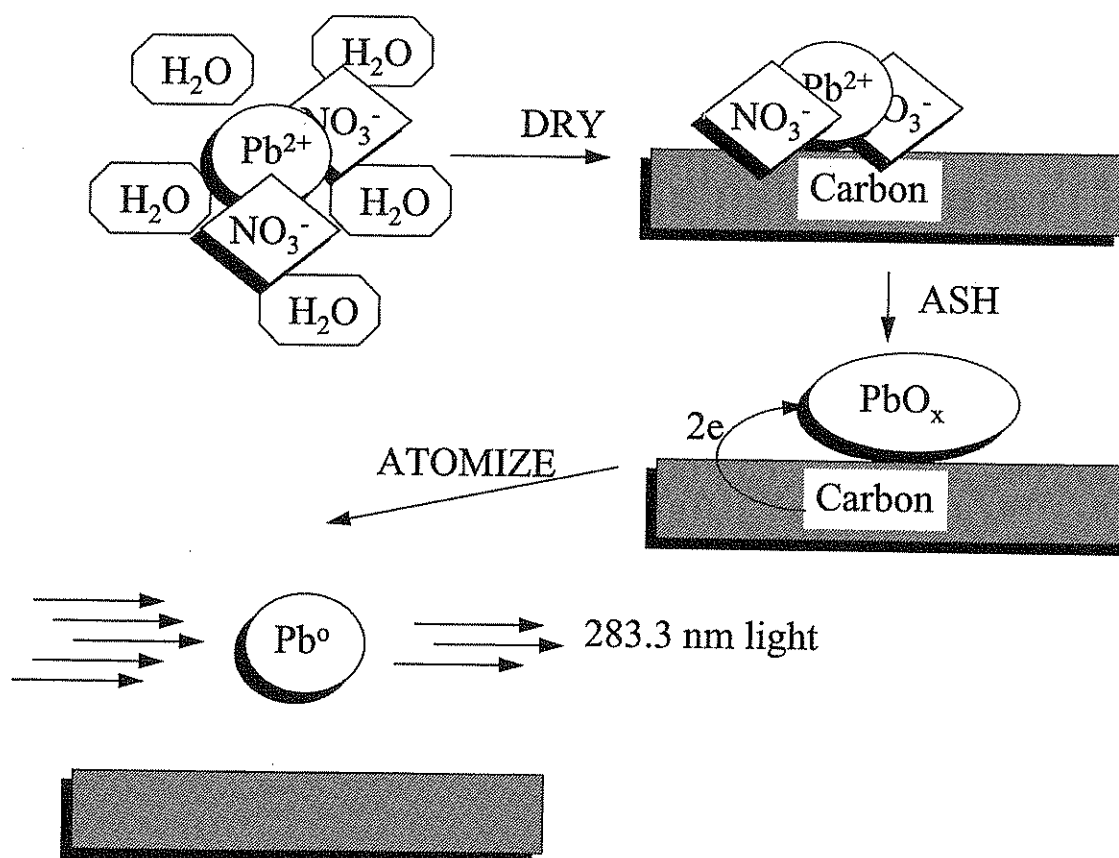
FIGURE 21. Schematic of the steps required to bring the gas phase from solution. The lead, as a nitrate, is desolvated during the drying cycle. During the ashing cycle used to remove organics, the lead nitrate decomposes to an oxide, which is reduced by the carbon support during the vapor-producing phase.

hydride requires an acid media, an oxidant, and $NaBH_4$ as the hydride source:

$$Pb(II) \xrightarrow{\text{oxidant}} Pb(IV) \xrightarrow{NaBH_4} PbH_{4(gas)}$$

$$(59)$$
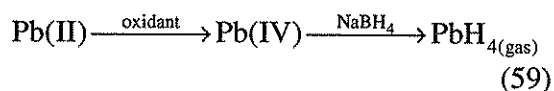
The reaction essentially involves a preparative step (oxidation of the sample) and a collection step (formation of the gas) serving as a preconcentration of lead from the matrix. As a result, the method is free from some of the background effects present in thermal production of the gas phase but has introduced other matrix ef-

fects. On the other hand, the lead within the sample has been concentrated, resulting in lower limits of detection than are achieved by flame atomization (Table 11).[62,63,64,65,66,67]

For organolead compounds some work has been done on direct injection of vapors into the path for AA, but validated methods involve a transformation of the sample from the vaporous gas, to an aquated sample, to a dried sample, as described by the ASTM method D3237. The reaction is based generically on the conversion of tetraalkyl lead to dialkyldihalogenated species, as shown below for chloride:
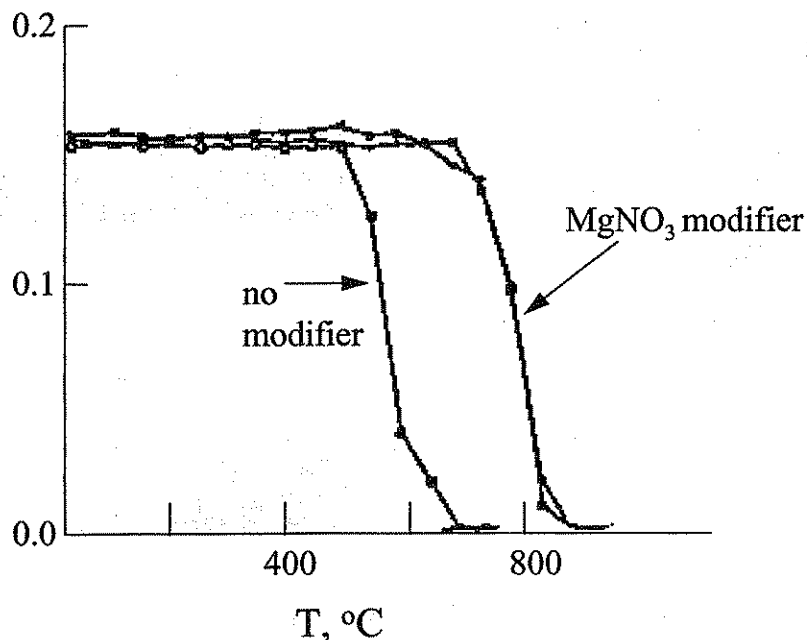
FIGURE 22. The temperature at which the lead is volatilized as a gas is modified by the presence of the nitrate (see Figure 4), which produces lead oxide. In normal solution lead may volatilize at very low temperatures due to the presence of halides. The presence of the oxide raises the temperature of volatilization. (From A. Deval and J. Sneddon, *Microchemical Journal*, 1995, **52**, 96–100.)

$$Bu_4Pb + 2Cl_2 \leftrightarrows Bu_2PbCl_2 + 2RCl \quad (60)$$

TABLE 10
Boiling Points of Various Chlorides, Oxides and Nitrates

d = decompose, subl = sublimes

Metal, Row 4	Chlorides	Oxides (m.p.)	Nitrates	
K^+	Subl 1500	d 350	d 400	
Ca^{2+}	>1600	2850	d 132	
Cr^{3+}	Subl 1300	4000	d 100	$Cr(NO_3)_3$–$9H_2O$
Zn^{2+}	1190		129.4	$Mn(NO_3)_3$–$4H_2O$
Fe^{3+}	d 315	(1565)	d 125	$Fe(NO_3)_3$–$9H_2O$
Co^{2+}	1049	(1795)	55	$Co(NO_3)_2$–$6H_2O$
Ni^{2+}	Subl 973	(1984)	136.7	$Ni(NO_3)_2$–$6H_2O$
Cu^{2+}	d 993 to CuCl	(1326)	–HNO_2, 170	
Zn^{2+}	732	(1975)	–$6H_2O$, 105–131	$Zn(NO_3)_2$–
$6H_2O$				
Pb^{2+}	950	(886)	d (470)	
Cd^{2+}	960	sub 1559	132	$Cd(NO_3)_2$–$4H_2O$
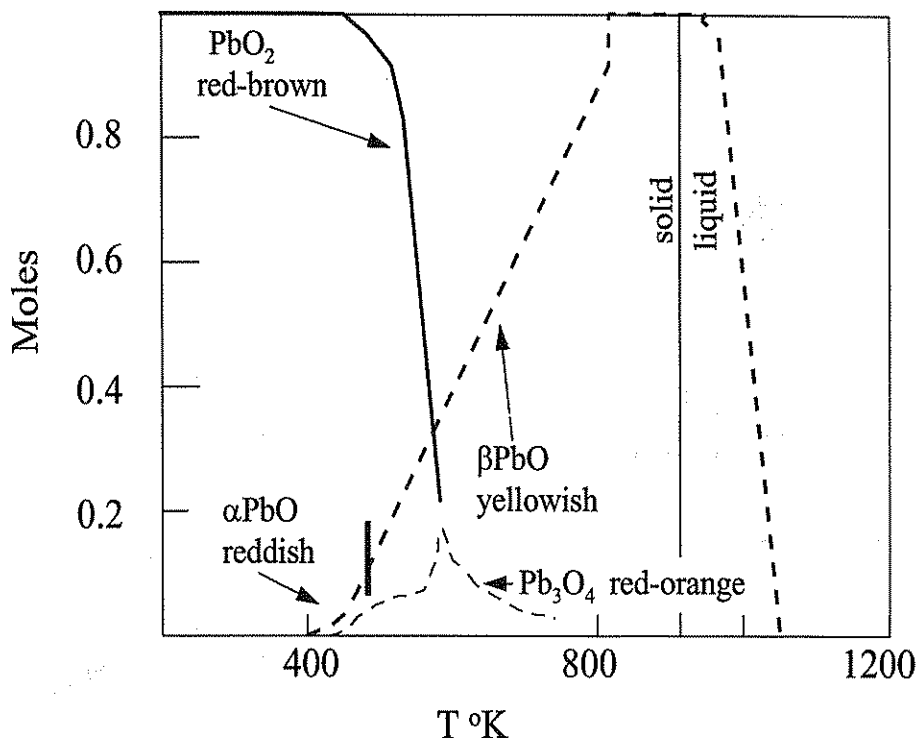
FIGURE 23. The rate of volatilization depends on the solid phase present. Four different lead oxide phases may be present as the atom vapor phase is initiated, which may affect temperature at which the gas phase is formed.

The butyl lead salt is more soluble in water than in benzene (Table 12).[68] In the ASTM method ICl is reacted with the gas phase containing tetraalkyl lead to form the water-soluble salt of iodide. After extraction from the gasoline into water, the lead containing mixture is reacted with nitric acid to form a lead nitrate species which can be titrated by EDTA or measured by AA.

Once an atom vapor phase is formed, a selected beam of light is passed through the sample and its attenuation measured. Figure 25 shows the relative intensities of the more prominent of the approximately 370 possible electronic transitions available to atomic lead. It should be noted that most of the

transitions are from the ground $6p^2$ state (lead = $[Xe]6s^24f^{14}5d^{10}6p^2$) to the next highest s orbital (7s). Of the available lines some of the most intense are those that do not involve an electron spin flip. The most intense line is at 405.7 nm involving a triplet state excitation from $6p^2$ to 7s.

The most customary line to use is the 283.3 nm line corresponding to a p^2 to 6d transition. The reason for this is spectral interferences, the presence of other species present in high concentration that absorb at very nearly the same wavelength. A common species in the solution is expected to be K (electronic transitions at 404.4 and 404.7 nm) and, for metal-contaminated soils,
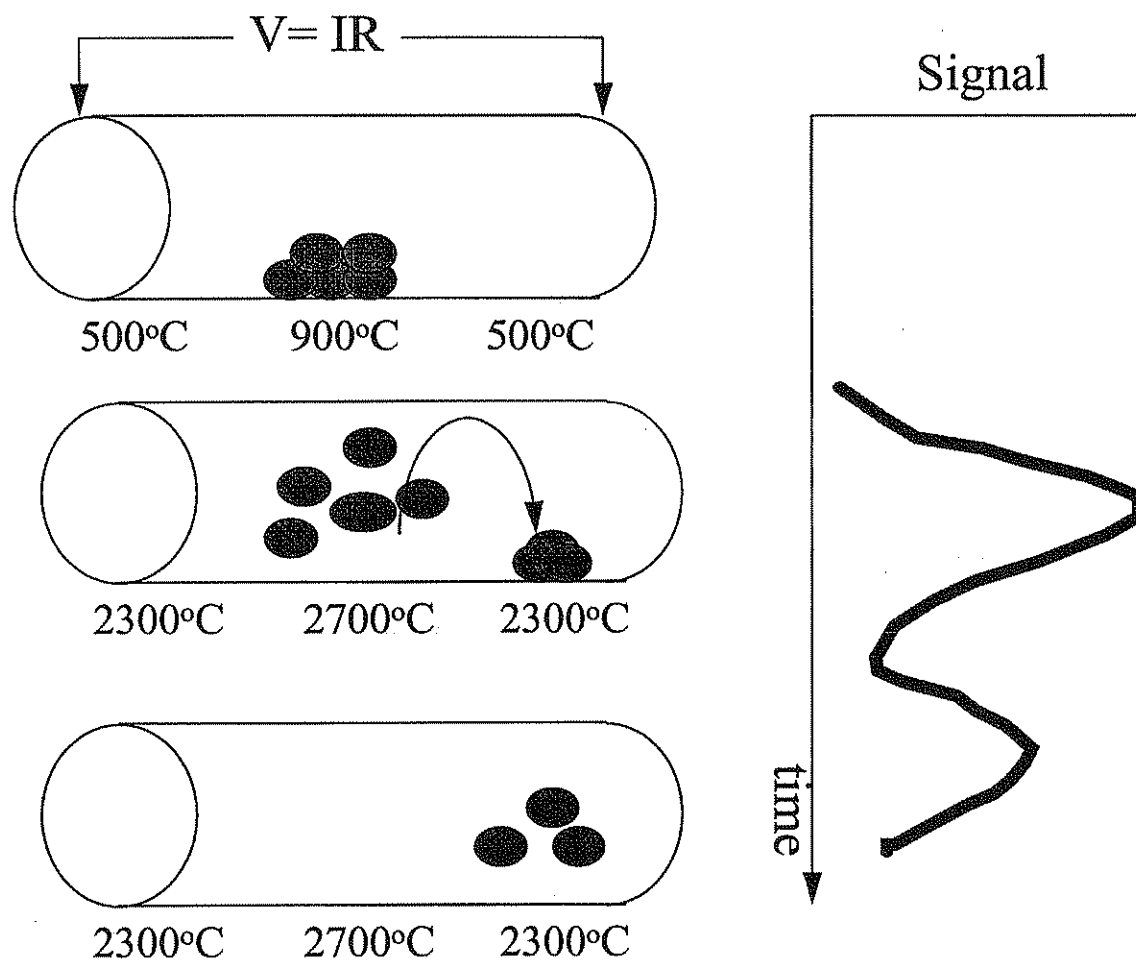
FIGURE 24. When different lead species volatilize at different temperatures, multiple peaks of maximum lead concentration may be observed as a function of time. The result is to lower the total amount of lead in the analyte signal.

TABLE 11
Hydride Generation Atomic Absorption

Oxidant	Name	LOD for Pb
H_2O_2	Hydrogen peroxide	0.1 µg/l
$(NH_2)_2S_2O_8$	Ammonia peroxodisulfite	1.2 ng
$K_2Cr_2O_7$		0.04–0.7 µg/l
Ce(III)		0.04 µg/g

TABLE 12
Solubility of Bu_2PbCl_2

Solvent	Solubility (g/l)
Water	6.4
EtOH	26
Tetrahydrofuran	52
Dioxane	13
Acetone	33
Chloroform	2
Benzene	0.3
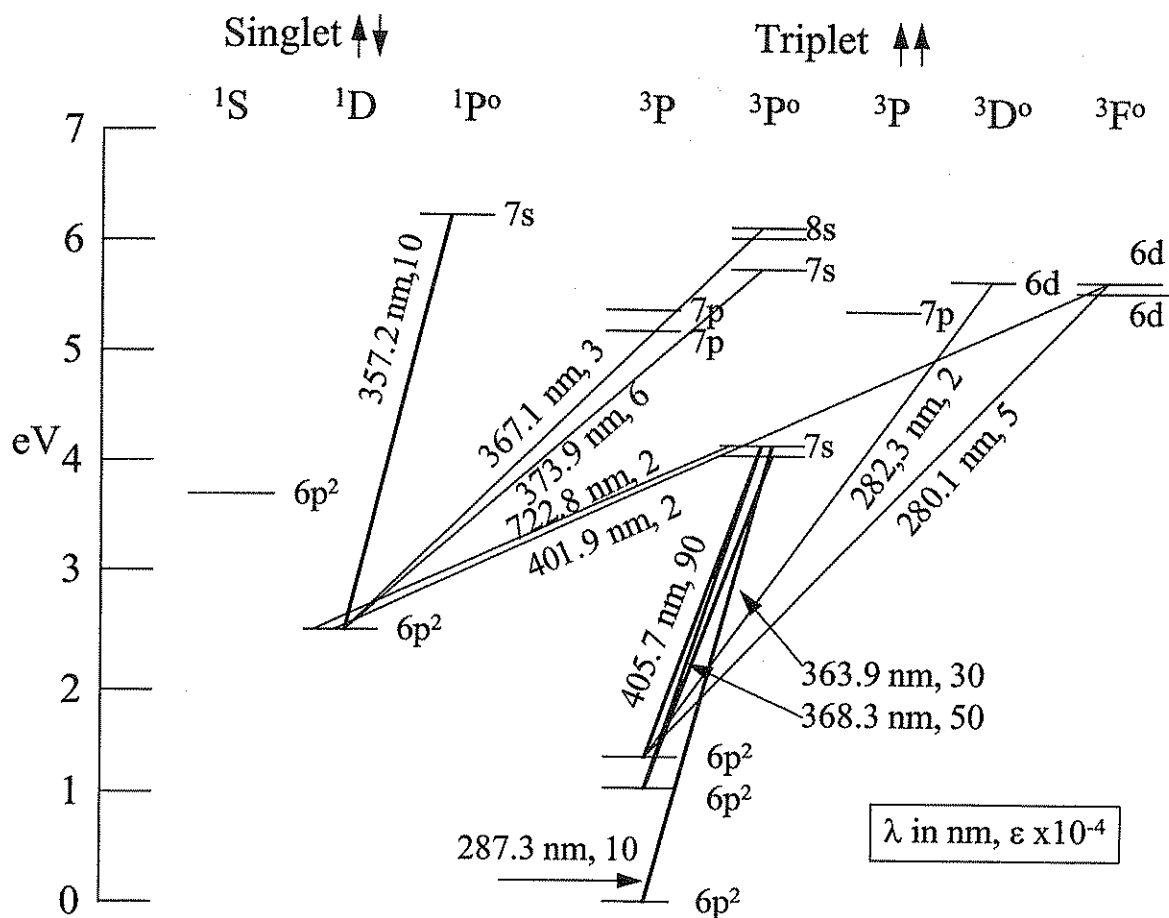
FIGURE 25. Diagram of some of the major electronic transitions of lead. The darker the line, the more probable or intense the line.

Mn (electronic transitions at 403.1, 403.3, and 403.5 nm) may also be present.[69]

In selecting the 283.3-nm line atomic line, interferences are minimized. Other potential absorbing species, however, are the molecular oxides that absorb in molecular bands. In order to measure the contribution of these bands to the total measured absorption at 283. 3 nm, it is necessary to monitor the absorption very close to the 283.3 nm line for the same sample in the absence of lead absorption (Figure 26). Two main strategies are employed.[70,71,72,73,74,75,76,77] In older instruments, if one assumes that the broad band absorber absorbs equally well over a range of wavelengths near 283.3, then one measures the background absorbance by

sitting off line slightly. This can be accomplished by operating the source lamp under self-reversal conditions.

In other instruments the broadband contribution at 283.3 nm is directly measured by temporarily making lead invisible to the 283.3 nm light. This is accomplished by applying a magnetic field across the atom vapor sample phase. The applied magnetic field splits the lead line into three different energy states due to spin-coupling effects. The energy levels are split into a center band at the original 283.3 nm, π, which is plane polarized with light parallel to the magnetic field. Two side bands are created, σ, which are sensitive to light polarized perpendicular to the magnetic field.
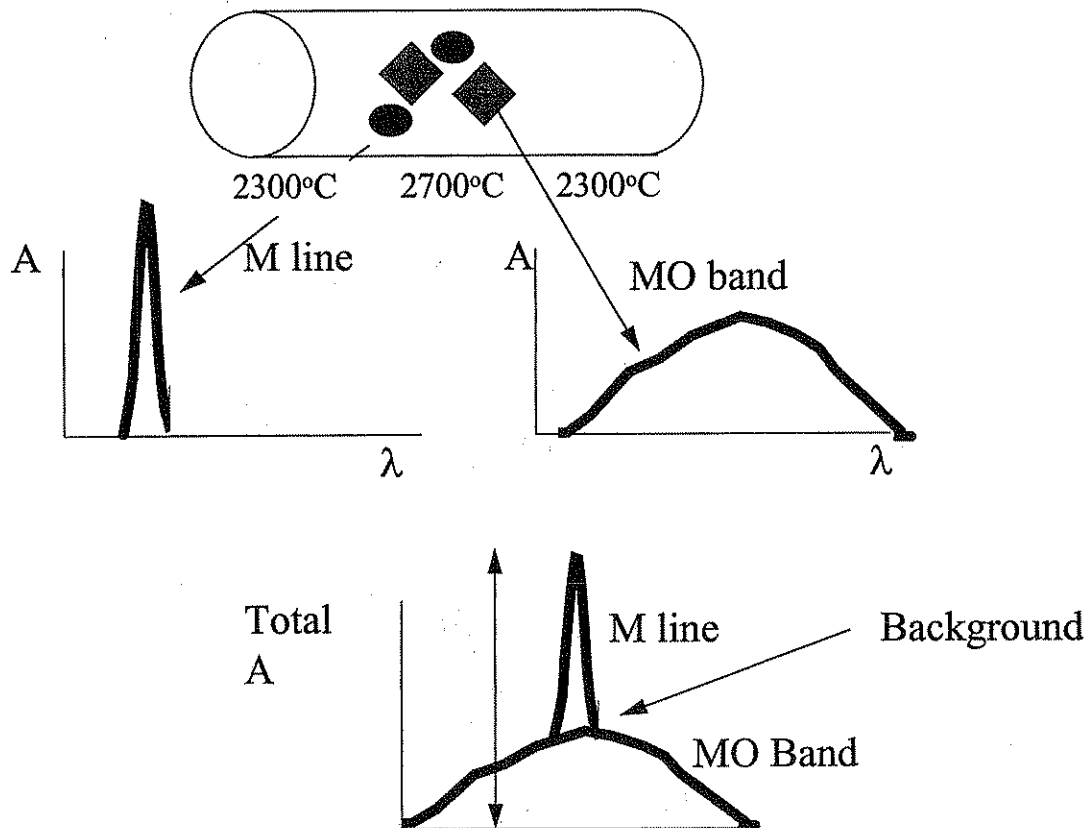
FIGURE 26. Background effects in atomic absorption are the result of spectral or line interferences or of molecular species, such as oxides. To remove the signal contribution from the molecular species, absorbance must be measured at the line center (283.3 nm) and just off line center. The off line center measurement is background and may be subtracted from the total absorbance at 283.3 nm to obtain a measure of atomic lead.

Figure 27 shows the π and σ bands for 282.2 nm lead line. Note that the π line does not lie exactly at dead center (282.2 nm) because of spin orbit coupling that occurs with heavy atoms. This splitting of orbitals would be of little interest except for the fact that the π and σ bands absorb differently polarized light. Absorption of the broadband absorbers can be monitored by passing perpendicular polarized light at 282.2 nm through the sample. Lead will not absorb light because it may only absorb parallel polarized light when bathed in the magnetic field. The absorption of the total sample can be monitored by passing parallel polarized light at 283.3 nm through

the sample. The difference between these two values is the absorption of light due to the presence of lead. Interferences for lead in the Zeeman correction are S_2 at 283.3 nm in coal,[78] PO at 217.0, 239.4, and 283.3 nm,[79] and Co at 261.4 nm.[80]

The GFAA method (EPA 200.9) is one of the "standards" next to Anodic Stripping and ICP-MS or ICP-AES. For a comparison of methods see Table 1. GFAA is highly reliable and very sensitive due to the concentrating of the sample and the rapid production of the atom vapor phase. GFAA can be used for mass number of samples if connected with an autosampling device.
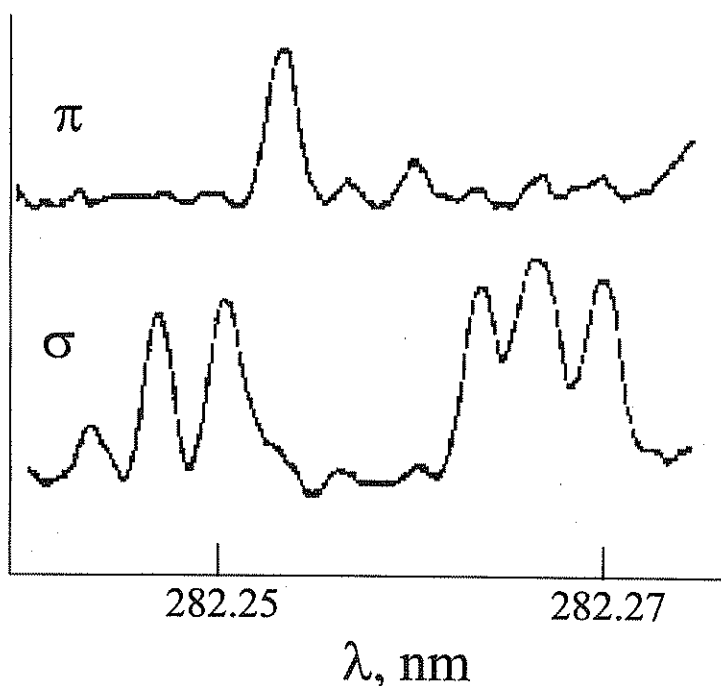
FIGURE 27. In the presence of a magnetic field, the lead line at 282.2 nm is split into bands at 282.25 and 282.27. Application of a magnetic field leaves the lead atom non-absorbing at 282.2 so that any absorption measured is a measure of the background or blank. (Redrawn from Wood D.R. and K. L. Andrew, *J. Opt. Soc. Am.,* 1968, **58**, 6, 830.)

GFAA is not a method of choice for on site blood lead screening because it is not portable. The requirements of the furnace, the voltage regulators, cooling apparatus, and gas cylinders render it a bulky and costly method of analysis. The cost of an AAS analysis runs anywhere from $10 to $70 a sample for blood. This has important implications for a public health policy that required routine blood lead sampling.[48]

a. Other Atomic Absorption Experiments

There are a variety of other ways of delivering the gas vapor into the atomic absorption instrument. These include plasmas, laser desorption, and thermal slow heating.[81] None of these is, as of yet, common. Laser ablation as a means of delivering the sample to the atomic absorption cell is intriguing because it allows spatial sampling of a given material. Laser ablation has been particularly adopted by the geochemical community to image complex rock matrices.[82]

2. Atomic Emission

Just as the light absorbed by lead in its electronic transitions from p to higher lying s orbitals can be monitored, so too can the relaxation of electrons from those excited states. These methods give rise to atomic emission methods of analysis. The most common method of atomic emission in the 1970s was desolvation of the sample by a flame and excitation of the atom by the flame from a 6p to a 7s electron state. The method was not particularly good, however, because the energy required for the excitation was above

the reach of the flame temperature. The advent of alternative heating methods, such as graphite furnace, laser beams, and plasmas, has allowed atomic emission of lead to be quite reliable. In the plasma method the sample is desolvated, brought to an atomic gas phase, and electrons within the atoms excited by the process of the plasma.

Inductively coupled plasmas (ICP) can reach very high temperatures capable of ionizing most of the elements with the exception of the halogens. The plasma is obtained by coiling a wire around the glass injection tube for the water vapor plus argon gas. A high-voltage, high-frequency source is applied to the wire, causing a magnetic field to be sensed within the sample chamber (Figure 28). Any ions present begin to move in response to the magnetic field, colliding and ionizing other species, until a plasma is obtained. The plasma is a delocalized source of electrons with the ion cloud. The motion of these ions is sufficiently rapid that kinetic heating (4000 to 7000°K) of the sample takes place and the atoms both excited and ionized.

When the gas exits the plasma, cooling takes place and light can be emitted when the excited electrons fall back to a ground or unexcited energy level. The light emitted can be monitored. The total amount of light emitted is proportional to the amount of the atom in the gas phase, making a measure of concentration. The method has relatively low detection limits (ppt) due to the ability to select the ion to be monitored, and the lack of flicker of the flame in the plasma, contributing to background effects.

Historically, ICP was developed to create an excitation source for atomic emission experiments. Because the emission of ions gives one a greater range of wavelengths to monitor (atoms pluse their ions) nearly all elements could be resolved. At least one ion line will emit in a background free portion of the spectrum. In order to accomodate the large number of wavelengths to be monitored, a large Rowland circle detector is used. In effect, the instrument is operated in a manner similar to a diode array UV-Vis instrument or an FTIR in which all wavelength
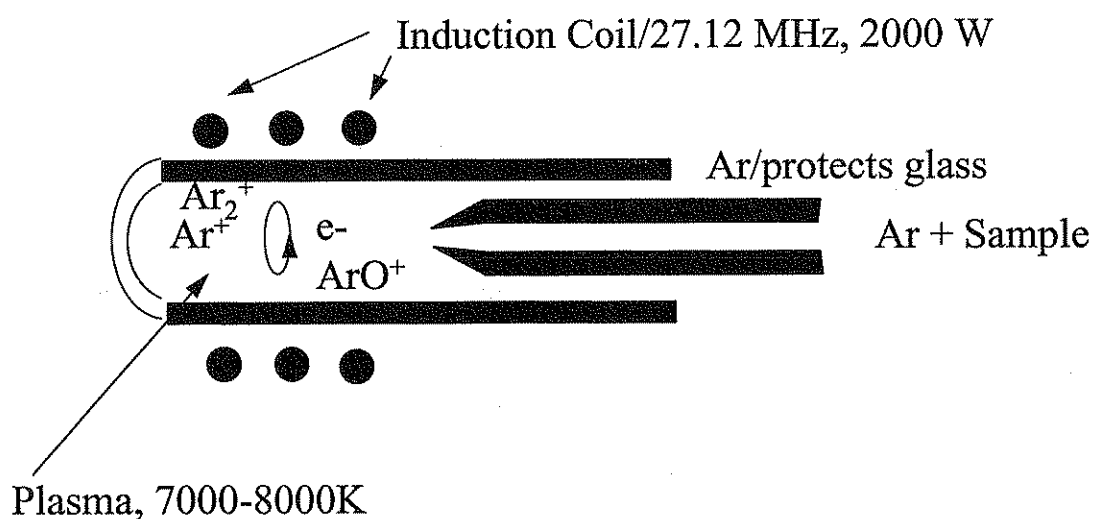
FIGURE 28. A plasma can be formed by inductively coupling a radio frequency to an argon gas. Ionized argon species and electrons move in response to the external electric field. The motion of the ions raises the temperature to 7000 to 8000°K, ionizing both atomic and molecular species. The plasma is controlled and shaped by a flow of argon gas.

302

TABLE 13
Typical Operating Conditions
for the ICP-AES

Wavelength	220.35 nm
Viewing height	15–20 mm above load coil
Auxiliary gas flow	<1.0 l/min
Plasma gas flow	15 l/min
Nebulizer pressure	20–40 psi
Induction RF	1250 W
Reflection power	<5 W
Sample uptake	0.5–20.0 ml/min

emission intensities are acquired simultaneously, resulting in a high sample throughput.

Typical operating conditions for the ICP-AES method are shown in Table 13.[83] The wavelength for monitoring the emission is the 220.35 line due to various interferences (Table 14).

a. Other Atomic Emission Experiments (Laser-Induced Breakdown Spectroscopy or LIBS)

In order to create a more mobile instrument, plasmas can be generated using laser spectroscopy. These localized plasmas can then be probed by atomic emission of the lead lines. The intense 405.78-nm line can be used for calibration.[84] The advantage of these methods is the anticipated portability of the instrument. In laser-induced breakdown spectroscopy, a 10-ns pulse from a 100-µJ laser delivers a peak power of 10 MW, or, if focused to 100 m diameter, 130 GW/cm². Under this intense energy delivery a plasma can be formed and swept into a variety of detectors (ICP-MS, AES, GC). In the spectroscopic mode, the gas phase is focused into a spectrometer and the emission line monitored for lead.

This method has been pursued with an eye to a field mobile instrument for paint and soil analysis. The instrument described had a weight of 35 lb and required 115VAC.[85]

TABLE 14
Interferences in ICP-AES

Pb line monitored	LOD μg/l	Interference
217.00	50	Fe, Al
220.35 nm	25	Al
280.20	150	Mn
283.31	100	Fe

A detection limit of lead in paints was found to be 0.014%Pb (wt/dry weight), which is better than the detection limits obtained for portable X-ray fluorescence (XRF) measurements. It has the additional advantage of sampling below the surface paint layer, something that X-ray fluorescence cannot do and that contributes a large degree of uncertainty to the XRF method. One difficulty is that the sample does not vaporize homogeneously due in part to the sample itself and to reproducibility of the laser sparks.[86]

3. Atomic Fluorescence

Atomic fluorescence involves a similar process to atomic emission, except that excitation is obtained by an absorption event. Atomic fluorescence for lead is a very new method (since 1990) in which a lead atom in a gas is excited with a XeCl eximer that uses second harmonic generation to lase with 3 kW power at the lead absorption line of 283.3 nm (transition $6 \ p^{23} \ P_o \rightarrow 7 \ s^3 \ P_1{}^o$). After excitation, the atom emits at 405.8 nm (transition $6 \ p^{23} \ P_o \rightarrow 7 \ s^3 \ P_1{}^o$). The intensity of the excitation beam leads to the high emission intensities allowing a very low limit of detection, LOD. The gas is obtained by the graphite furnace method. Figure 29 shows a typical instrumental scheme for this system.[87,88]

A variant on this method involves the use of two lasers, one to create the plasma (laser induced plasma (LIP) or LIB[89]) and a second to excite the lead atom for the emission experiment. Because of the low limits
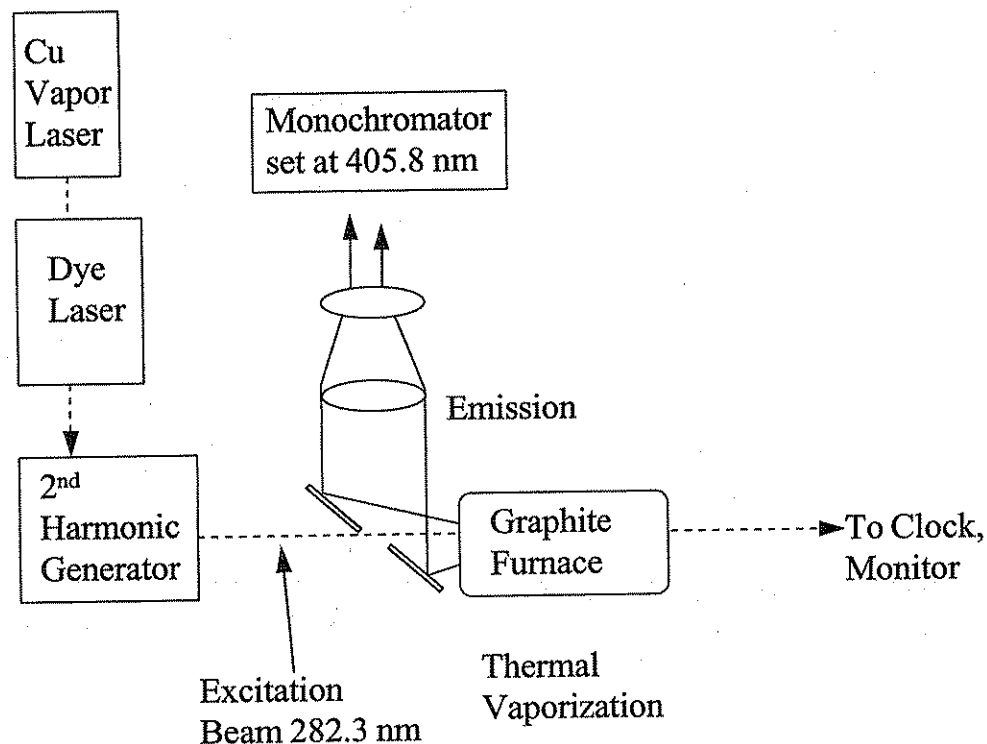
FIGURE 29. Generic schematic of a laser excitation atomic absorption spectrometer. A graphite furnace is used to create the vapor phase, and a laser is used to create the excited atomic state that is monitored at right angles to the excitation.

of detection, air flow in a normal lab can contaminate samples. The entire system is run in a clean room.

D. Molecular Bond (Valence) Electronic Transitions

1. Molecular Absorption of Light by Valence Electrons (Dithizone)

Lead is "silent" in the Vis region due to its filled d shell. As a result, it can be probed only by coordination to an active species, such as a chelate. The method relies for selectivity not on the inherent nature of lead valence shell electrons, but on the chelation selectivity. Chelation selectivity for lead is not well understood, neither have many

rationally designed lead selective chelates been constructed. The most common method for lead (used extensively from the late 1927 to the 1960s) is the dithizone method.[90] The dithizone reagent has been reviewed extensively in 1977 on the occasion of the 50th anniversary of its introduction as an analytical reagent by Hellmuth Fischer.[91] It is the first organic chemical really put to use in analytical chemistry. Earlier reagents had been introduced by the late 1800s, following the birth of organic chemistry. Table 15 shows a timeline for some early organic reagents. Siemens German Chemical company needed highly pure metals that drove the development of analysis.

Figure 30 shows the structure of dithizone. The uncomplexed reagent (proton monomer) has two absorption bands possibly

TABLE 15
Early Analytical Organic Reagents

Reagent	Authors	Date of Introduction
α-nitroso-β-naphthol	Ilinsky M. and G. Von Knorre	1884–1885
Dimethylglyoxime	L. H. Tsuchugaeff	1905
Cupferron	O. Baudische	1909
Spot test	F. Feigl	1891
Diphenylcarbazide	Cazeneuve	1900
Dithizone	Hellmuth Fischer	1925

Thione, 450 nm?   Thiol, 620 nm?

Complex, 555 nm
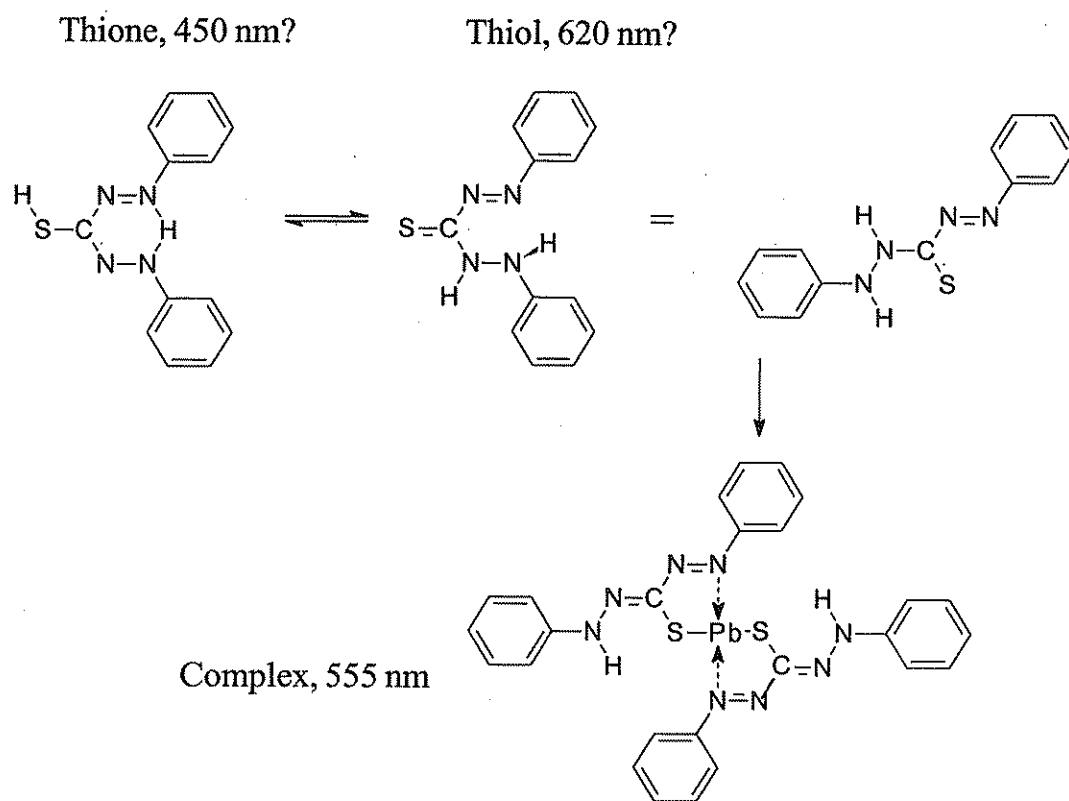
FIGURE 30. The reagent dithizone or diphenylthiocarbazone. The uncomplexed reagent rotates to form thione and thiol, resulting in two chromophores. Chelation to a metal ion induces rigidity throughout the molecule, changing both absorption bands. For lead, the chelated chromophore lies between the absorption bands for the free chelate, as shown in Figure 31.

related to the thione and thiol structures of the reagent. These two absorption bands remove long (red) and short (blue) light, leaving behind intermediate visible light (green). After complexation to the metal, the crystal structure of dithizone metal chelate shows planarity and the linking expected through the compound as well as the bond lengths, etc. It is evident from the measured bond lengths that pi-electrons in the N-N-C-N-N chain are delocalized in all cases and that there are no localized single or double bonds. A single absorption band results, which occurs between the original two (Figure 31). The resulting color varies from red through purple and black, with the color tuned by the perturbation of the organic molecular orbitals by the chelated central metal atom as shown in Table 16.

The reagent is organic soluble only, as shown in Table 17. In order to use the dithizone chemistry as an analytical method, the metal ion must be removed from solution into the organic phase. This extraction process involves stripping the reagent of its protons to move it into the aqueous phase, which requires buffering of the analyte solution to a high pH. The aquated complex binds to the metal, and moving back to the organic phase. Both equilibrium effects (constants for the extraction equilibrium) and kinetics need to be considered in successfully applying the method.

$$M^{2+}_{aqueous\ phase} + (nH_2L)_{organic\ phase} \leftrightarrows (M(HL)_{2n})_{organic\ phase} + nH^+ \quad Kex$$
$$(61)$$
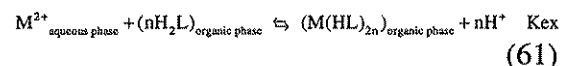
Extraction constants are shown in Table 18.

Kinetics are taken into account by performing the extraction for exactly the same amount of time for each analyte. Extraction of lead by lead to carbon tetrachloride from a citrate buffer was less than 5 s at pH 7.

The extraction process can potentially remove other metals as well. Several strategies may be considered for introducing
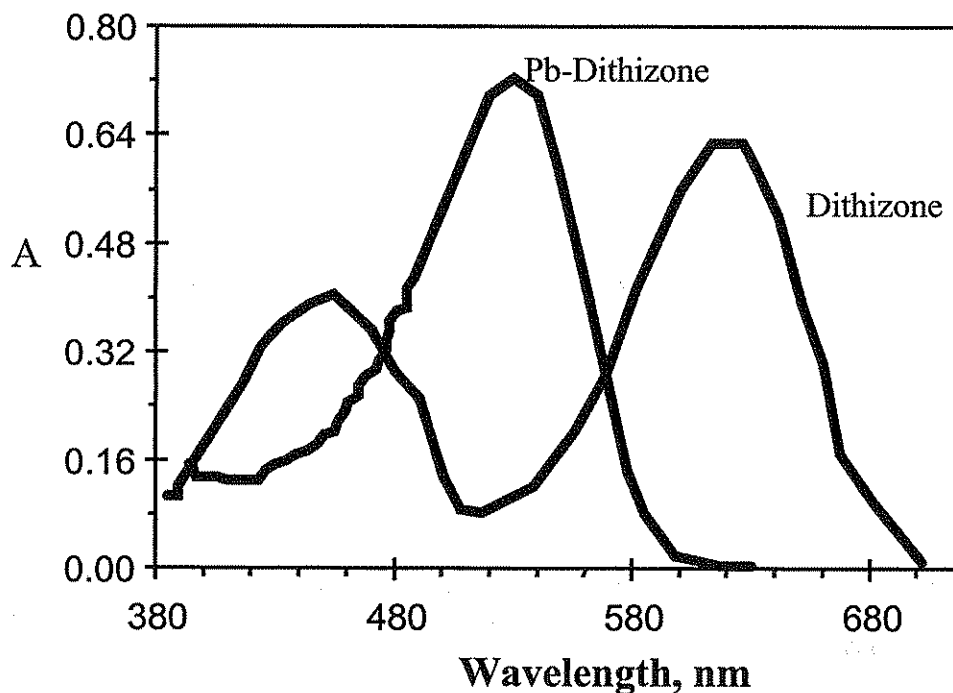
FIGURE 31. Absorption spectra of free dithizone with bands at 450 and 620 nm in carbon tetrachloride. Also shown is the absorption spectra of lead-chelated dithizone at 518 nm.

TABLE 16
Absorption Bands and Colors of Dithizone Chelates

Primary	Color	Visible bands/nm	:NH Stret.	:NH Bend	IR bands (nm) N-phenyl	NCS
Ag(HDz), H$_2$O	Orange-red	470, 465	3200	1520	1357,1265	1202–1128
Tl(HDz)	Dark red	515,605sh,518	3200	1517	1357	1130
Mn(HDz)$_2$	Dark red	525–618 sh	3350,3200	1525	1350	1210,1150
Co(HDz)$_2$	Black	410sh, 545, 555	3230	1530	1335	1190,1167,w
Ni(HDz)$_2$	Dark purple	484,670,480, 565,665	3250	1535	1340	1237
Cu(HDz)$_2$	Black	545,	3220	1530	1340	1212
	Brown	445	3200	1515	1310	1133
Zn(HDz)$_2$	Gray-green	532	3220	1527	1342, 1275	1205,1140
Cd(HDz)$_2$	Orange-brown	518,608,520	3220	1530	1346,1275	1208,1155
Hg(HDz)$_2$	Dark red	490	3250	1527	1355	1200,1170,1152
Pb(HDz)$_2$	Red	518,608sh	3220	1530	1346,1275	1208,1155
Pd(HDz)$_2$	Purple	450,570,640	3230	1534	1340	1230
	Black	470,510		1530	1285,1257	1215
	Black	500		1535	1330	1210
Pt(HDz)$_2$	Black	430sh,488,710	3260	1528	1335	1217
Bi(HDz)$_3$	Green	498,490		1525	1357	1195,1150
Bi(Hdz)$_2$Cl,2HCl	Dark red	500,620	3200	1530	1325	1200,1135

TABLE 17
Solubility of Dithizone

Solvent	Solubility (g/l), 20°C
Chloroform	16.9
Carbon disulfide	2.83
Chlorobenzene	1.43
Acetonitrile	1.0
Carbon tetrachloride	0.512
Pentanol	0.054
Water	2×10^{-5}

selectivity as can be deduced by consideration of the equilibrium constants shown in Table 19.

Inspection of this table suggests that raising the pH should precipitate certain metals such as Al^{3+}, Fe^{3+}, Hg^{2+}, and Cr^{3+} before much Pb^{2+} is lost. This strategy would be flawed, however, because of occlusion of lead in the precipitate.[92] Further inspection of this table reveals that lead does not form a complex with CN$^-$, which can be used to scavenge other metal ions (Cd^{2+}, Cu^{2+}, Fe^{2+}, Fe^{3+}, Hg^{2+}, Ni^{2+}, Ag^{2+}, and Zn^{2+}) and prevent their reaction with dithizone.

The formation of ferricyanide presents another problem because this compound is a facile electron transfer reagent.

$$Fe^{3+} + 6CN^- \leftrightharpoons Fe(CN)_6^{3-} \qquad (62)$$
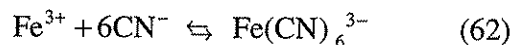
Fe(CN)$_6^{3-}$ reacts with dithizone that can be easily oxidized it (Figure 32):

$$2Fe(CN)_6^{3-} + 2e \to 2Fe(CN)_6^{4-} \quad E^\circ_{red,Fe} \quad -2F(E^\circ_{red,Fe}) \qquad (63)$$

$$2DS^- \to 2e + 2DS^\beta \quad -E^\circ_{red,DS\beta} \quad -2F(-E^\circ_{red,DS\beta}) \qquad (64)$$

$$\underline{2DS^\beta \to DSSD} \quad K_{dimerization} \quad -RTln(K_{dimerization}) \qquad (65)$$

$$2Fe(CN)_6^{3-} + 2DS^- \to DSSD \quad E^\circ_{reaction} \quad -2F(E^\circ_{red,Fe} - E^\circ_{red,DS\beta})$$
$$RTln(K_{dimerization}) \,(66)$$
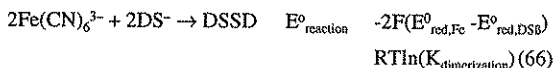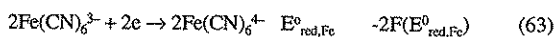
The ferricyanide formed reacts with the deprotonated dithizone reagent in the aqueous phase (reactions 63 and 64) to form an unstable radical species of the dithizone. The reaction is favorable because the formal potential for the reduction of the ferricyanide is more positive than the formal potential for the reduction of the dithizone

TABLE 18
Extraction Coefficients for Dithizone Complexes from Water

Metal ion	log Kex	
	CCl_4	$CHCl_4$
Ag^+	6.5, 7.18, 7.9, 8.94	5.8
Bi^{3+}	9.54 (KCN), 9.75 10.91,	5.36
Cd(II)	1.58, 3.14	0.53
Co(II)	1.5–1.59	
Cu(II)	10.53, 9.56	6.50, 8.5
Fe(II)	–3.4	–5.0
Ga(III)		–1.3,
Hg(II)	26.86	
In(III)	4.84	0.6
Ni(II)	–1.19, –0.63, –0.7	–2.92, 2.46
Pb(II)	0.38, –2.86 (citrate), –3.53(citrate + cyanide)	–0.89
Pd(II)	42.5	
Sn(II)	–2	
Tl(I)	–3.5	
Zn(II0	1.7, 2.3, 1.8–2.0	–0.52, –1.52

TABLE 19
Equilibrium Constants (Log) for Masking Reagents in Dithizone Method

Metal	Citrate $K_1K_2K_3K_4$	CN^- $K_1K_2K_3K_4$	K_{sp}	OH^- $K_1K_2K_3K_4$	K_{sp}
Al^{3+}					–33.5
Cd^{2+}	4.2	17.9		7.7	–14.4
Ca^{2+}	3.2			1.3	–5.2
Ce^{3+}					–19.8
Cr^{3+}					–30
Cu^{2+}	14.2	10.3		6.3	–20.4
Fe^{2+}	3.1	35.4		4.5	–15.1
Fe^{3+}	11.8	43.6		22.3	–38.8
Pb^{2+}	5.7			13.9	–15.2
Mg^{2+}	3.2			2.6	–11.2
Hg^{2+}		17		20.9	–25.5
Ni^{2+}		30.2		8.0	–15.2
Ag^{+3}		21.4	–15.7	4.0	–7.7
Zn^{2+}		19.6	–15.5	15	–15.5

radical (or oxidation of dithizone). The bracketed term on the left-hand side of the overall reaction (reaction 66) is consequently positive, leading to a negative free energy for the reaction. The reaction is also boosted by the dimerization of the dithizone radical (reaction 65). The end result is a consumption of the reagent that can decrease the absorption signal, resulting in false low readings for the lead dithizone present. To solve this problem, citrate is added to prevent the formation of the ferricyanide.

Green   Reddish Brown
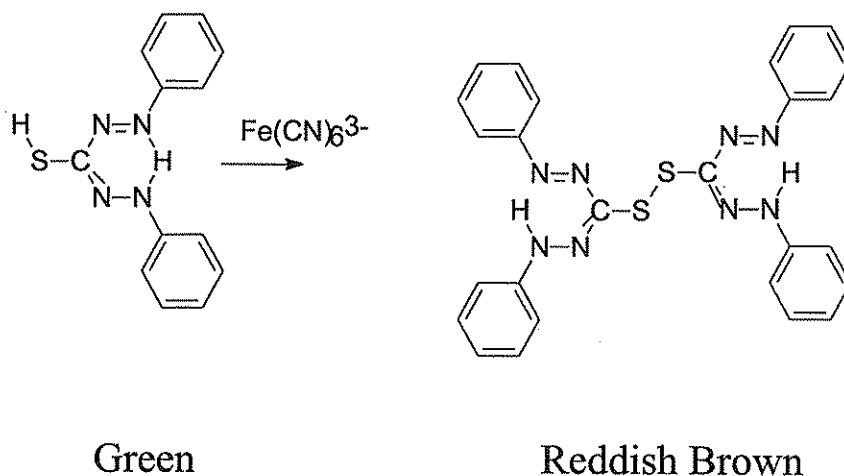
FIGURE 32. Decomposition of the reagent in the presence of $Fe(CN)_6^{3-}$ involves oxidation to the dimer to form a reddish brown product.

Just as the complex is sensitive to interferents capable of oxidizing it, it is also unstable to light. Light apparently stimulates decomposition of chloroform that produces $COCl_2$, which reacts to form a ring closed product.[93] The possible oxidation products of dithizone,[94] involve ring closure[95] and tautomerization reactions.[96]

Several species are not removed by scavenging with citrate and CN^-: Ca^{2+}, Ba^{2+}, Al^{3+}. These latter species may precipitate with PO_4^{2-} in the solution, carrying lead down with them. The only remaining species found to interfere are Bi^{2+}, Tl, and Sn^{2+}.

The dithizone lead complex formed is now ready to be extracted into an organic phase. The original methodology calls for CCl_4 or chloroform, but because these species are carcinogenic the method has been updated with extraction into methylene chloride.[97] In methylene chloride, free dithizone absorbs at 444 and 612 nm due to the thione and thiol tautomers with molar absorptivities of 15,000 M^{-1} cm^{-1} and 34,800 M^{-1} cm^{-1}, respectively. The lead complex has a maxima 518 nm, which lies in a deep valley between 444 and 612 nm absorption of the free dithizone.

a. Other UV-Vis Lead Reagents

One interesting way of achieving UV-Vis sensitivity for lead is elegant coupled chemistry shown in Figure 33. A neutral ionophore (see Section III.B) for lead brings lead into a non-aqueous phase requiring expulsion of charge from the phase. Charge compensation is accomplished by the loss of protons from a chromophoric group

$$Pb^{2+}_{aqueous} + L_{nonaqueous} + 2HC_{nonaqueous} \rightleftharpoons PbL^{2+}_{nonaqueous} + 2H^+_{aqueous} \quad (67)$$
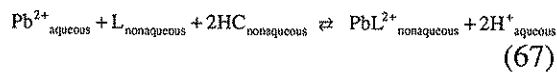
The change in UV-Vis absorption is monitored and is directly related to the lead concentration within the organic phase. Of the ionophores studied the most selective for lead was one containg an S/O/N functional group (ETH 5435). This method has been adapted to a fiber optic probe tip.[98,99] A linear range for the method spanned 5×10^{-9} to 5×10^{-3} M. The nanomolar detection limit converts to 0.2 ppt.

2. Molecular Fluorescence

A molecular reagent that absorbs in the UV-Vis region can potentially fluoresce.
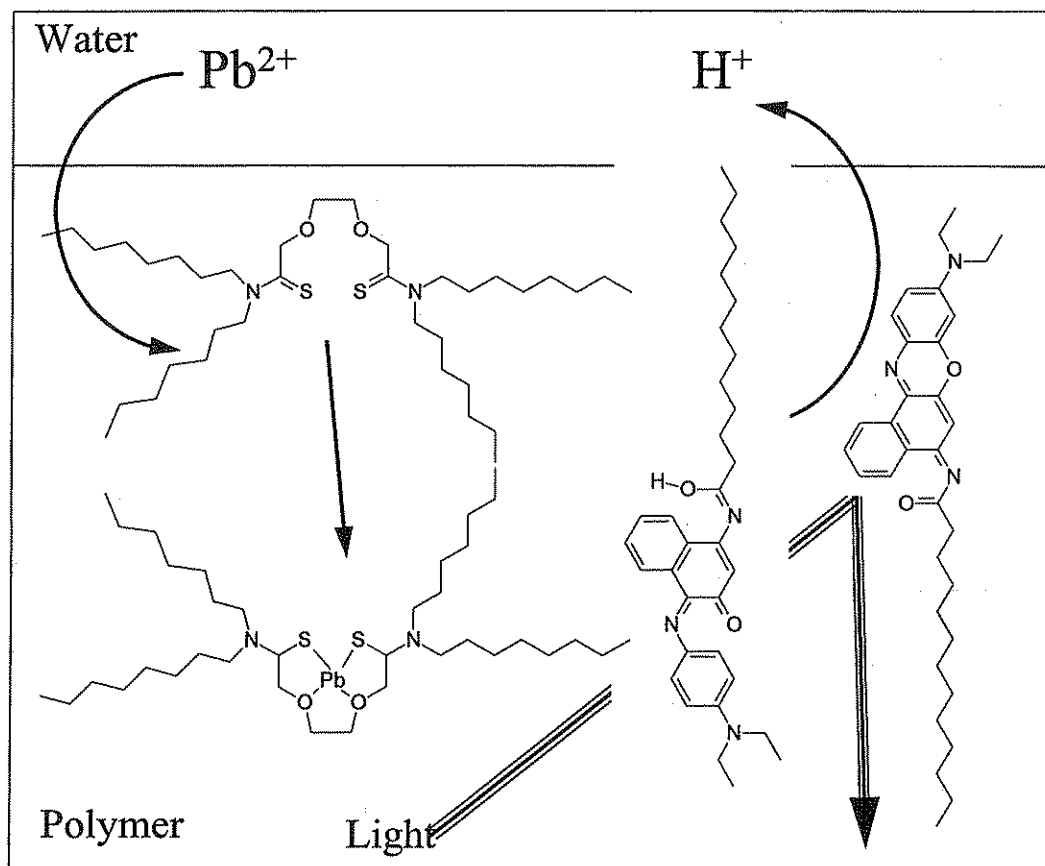
FIGURE 33. Schematic of the mechanism of a fiber optic sensor for lead. A membrane containing a metal binding ionophore brings lead from the aqueous phase into a polymeric coating on a fiber tip. Charge neutrality requirements cause the deprotonation of the chromophore, changing its absorption spectra, which is probed from the backside of the membrane by light carried by the optical fiber.

The fluorescence is very easily quenched by lead atoms through a heavy atom effect. The fluorescing species emits light when the excited electron relaxes to a ground state. The orbiting electrons on lead create a magnetic moment that can couple to the magnetic moment associated with the spin of the fluorescing electron that allows those electrons to dissipate energy without relaxation to the ground state with the emission of light. The quenching has been thought to be nonselective, as no molecular recognition of lead is required, simply some proximity in order to promote an intersystem electronic transfer. Non-specific quenching of a chelating reagent by lead can be used

to monitor the binding of lead to that compound.[100,101] An example is the determination of lead binding to humic materials (soil organic matter) by fluorescence quenching.[102,103,104]

More specific fluorescence-based methods are based on combining a lead-selective chelating reagent with the fluorophore. One method is based on ion pair formation between the fluorescing reagent eosinate and an 18-crown-6 lead complex. The detection limit for this method was 3 to 500 ppb, and no interferences were found.[105] A step beyond this is to combine the chelating arm and the fluorophore onto a single reagent. An example is the coupling of the

ionophore group (crown ether type) to a fluorescent active aromatic ring. In this scheme the reagent is non-active until the nitrogen lone pair is deactivated to prevent quenching. Fluorescence increases. Figure 34 shows the reagent mechanism involved. In this mechanism absorption of light by the aromatic ring leaves an empty spot in the HOMO that is filled by electron transfer from the nitrogen lone pair, effectively preventing fluorescence.[106]

3. Erythrocyte Protoporphyrin Fluorescence: Indirect Blood Lead Level Measurement

Lead binds to enzymes by attacking the S^{2-} functionalities. This leads to denatured and less active enzymes. Lead, in particular, interferes with the enzyme activity of ALA dehydratase, ferrochelatase, and coproporphyrinogen oxidase. These enzymes are involved in the final step of inserting iron into
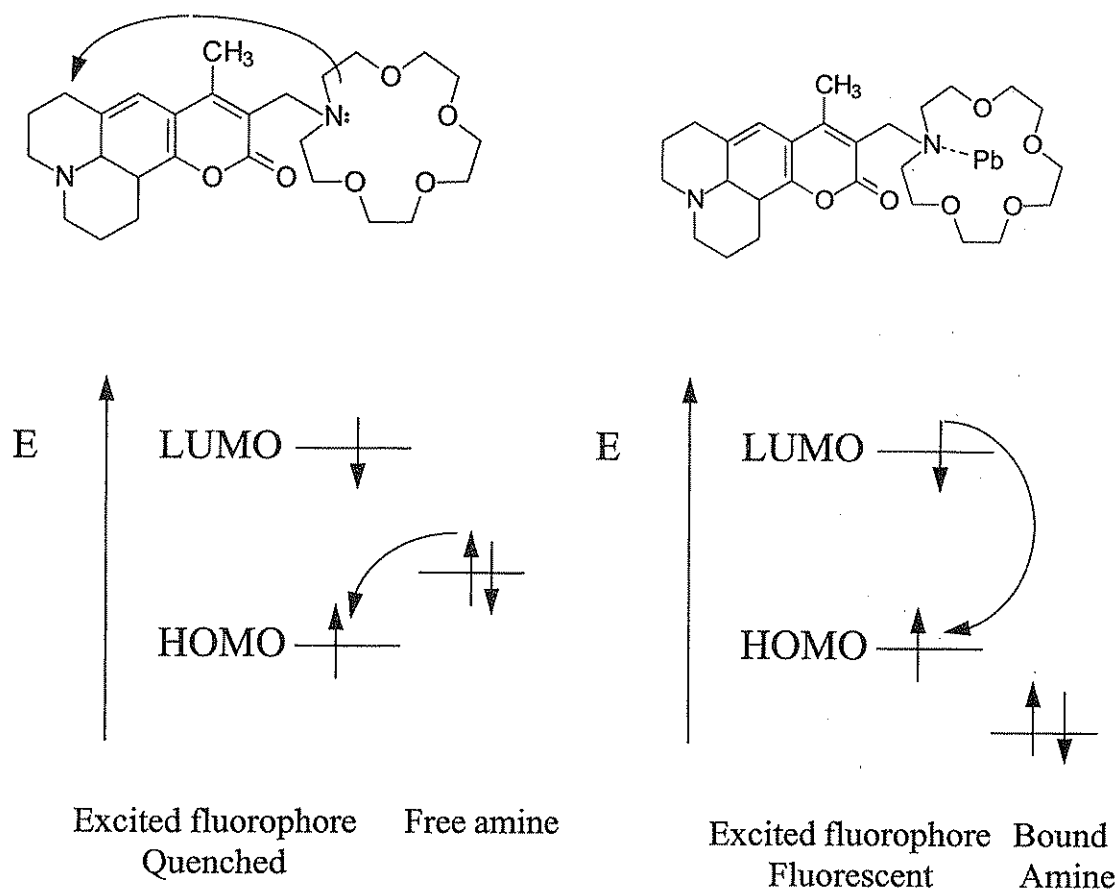
FIGURE 34. A lead-sensitive fluorescencing reagent. The chromophore and active site is the coumarin. After excitation of the chromophore, a vacancy in the HOMO of the coumarin is formed. The HOMO vacancy is filled by the nitrogen, thus preventing the excited state electron from falling back to ground state with concomitant release of light. In contrast, when the amine is bound no electron transfer from the amine to the fluorophore HOMO is possible, and fluorescence is activated.

the protoporphyrin to create heme. The free heme pool is depressed. Because the heme pool controls the activity of ALA synthase via a feedback loop, ALA synthase initiates an increased activity. The result of this activity is the synthesis of more protoporphyrin IX (PPIX), primarily as Zn protoporphyrin IX (ZPP).[107] The elevated levels of ZPP correlate directly with the amount of blood lead (g Pb/dl blood) (Figures 35 and 36).

Because of this correlation, early on it was determined that blood lead screening could be accomplished cheaply via monitoring ZPP. Early methods for protoporphyrin analysis extracted protoporphyrins and heme from the erythrocyte (blood cell) to get a PP unbound to the erythrocyte (free erythrocyte protoporphyrin [FEP]). The extract was treated with acid to demetallate the porphyrins and reextracted to get a sample that discriminated against the heme co-extracted in the first step. This protoporphyrin sample, FEP, can be monitored via fluorescence at 606 nm when excited at 405 nm. Contamination of the sample with Fe, Cu, or Mn depresses the signal, as these metals form nonfluorescing metal porphyrin complexes.

Elevated levels of FEP are associated with three clinical diseases: Fe deficiency (5 to 10 × normal FEP levels), protoporphyria
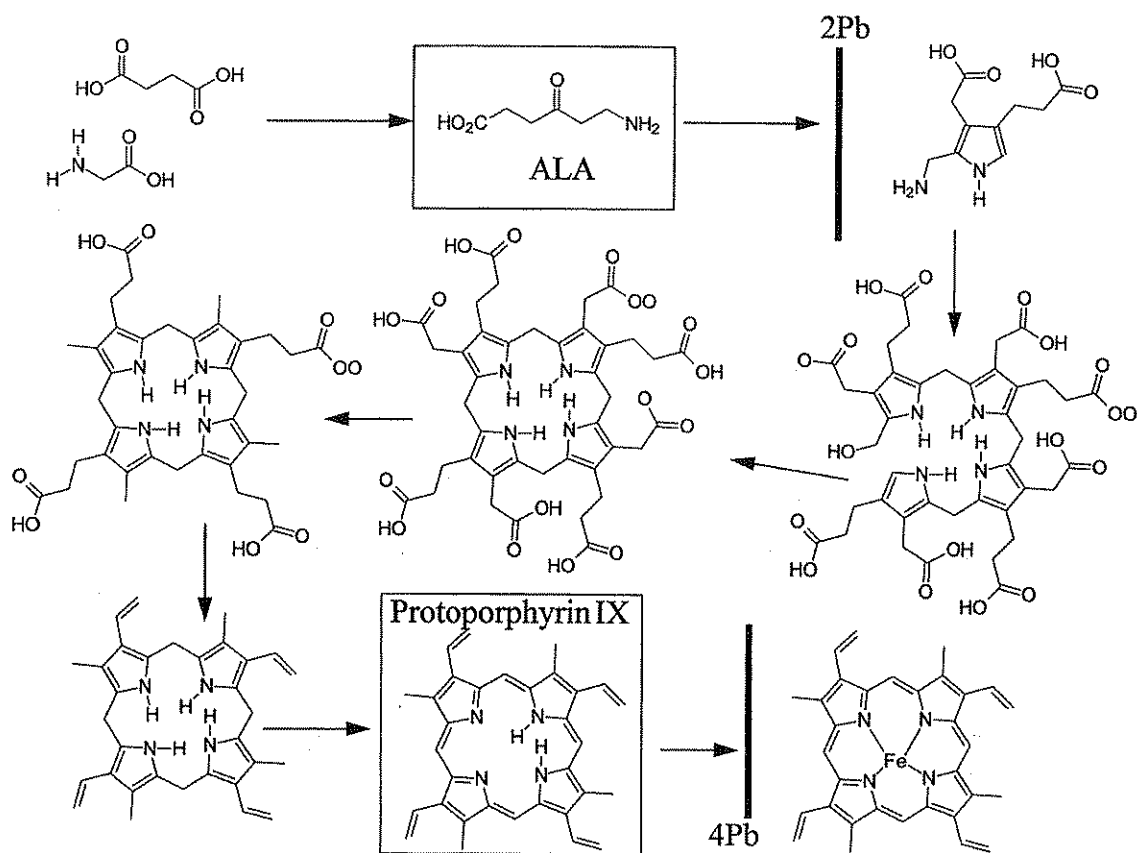
FIGURE 35. (A) The synthesis of haem involves seven different steps. Lead terminates synthesis in a number of steps. One of the steps is in the conversion of 5-aminolaevulinic acid (ALA) to porphobilinogen, resulting in elevated ALA levels. A second point of action on the cycle is on the enzyme ferro-chelatase. The result is overproduction of protophorphyrin IX. This protoporphyrin, in its Zn form, can be monitored by UV-Vis fluorescence (see Figure 36).

FIGURE 36. The lead dose, zinc protoporphyrin response curve. (From P. B. Hammond, R. L. Bornschein, and P. Sucop, *Environmental Research,* 1985, **38,** 187–196.)

(a rare inherited metabolic disease), and (10 to 250 × normal FEP levels for clinical lead poisoning).[108] Normal FEP levels are 20 μg FEP/dl blood and a blood lead level of about 20 g Pb/dL blood is necessary to show elevated FEP levels.[109]

The measurement method described above is cumbersome, requiring as it does the extraction method. Furthermore, it does not discriminate against the genetic disease protoporphyria. As it turns out, the elevated FEP associated with lead poisoning comes primarily in the zinc protoporphyrin, ZnPP, not PPIX, form.[110] ZnPP can be monitored via its fluorescence at 594 nm. FEP associated with unmetallated PPIX fluoresces at 625 nm. Fluorescence can be measured in diluted whole blood, thus simplifying the whole procedure,[111] although it has been suggested that the heme itself is a potent quencher of ZnPP fluorescence.[112]

One last comment is appropriate here. The lowest level of blood lead that causes an elevated ZnPP is 20 μg Pb/dl, which is a

value well above currently acceptable levels. However, the cost of this measurement is $1 to $5 per sample and is amenable to decentralized testing.[48] Furthermore, if one tracks both blood lead and PP it is possible to determine the date of lead exposure.[113]

E. Inner Shell Electron-Based Determinations

Inner shell electrons can be probed both for qualitative (bonding information) and for quantitative information. When a photon of angstrom wavelength strikes an atom it penetrates to the inner shell electrons (Figure 37). There the beam can be diffracted (X-ray diffraction) or it can cause the ejection of a photoelectron whose energy is less than that of the original photon by the binding energy of the shell. The absorption of the high-energy beam is measured as absorbance. The loss of the photoelectron leaves behind a vacancy that can be filled by an electron

FIGURE 36. The lead dose, zinc protoporphyrin response curve. (From P. B. Hammond, R. L. Bornschein, and P. Sucop, *Environmental Research*, 1985, **38**, 187–196.)

(a rare inherited metabolic disease), and (10 to 250 × normal FEP levels for clinical lead poisoning).[108] Normal FEP levels are 20 μg FEP/dl blood and a blood lead level of about 20 g Pb/dL blood is necessary to show elevated FEP levels.[109]
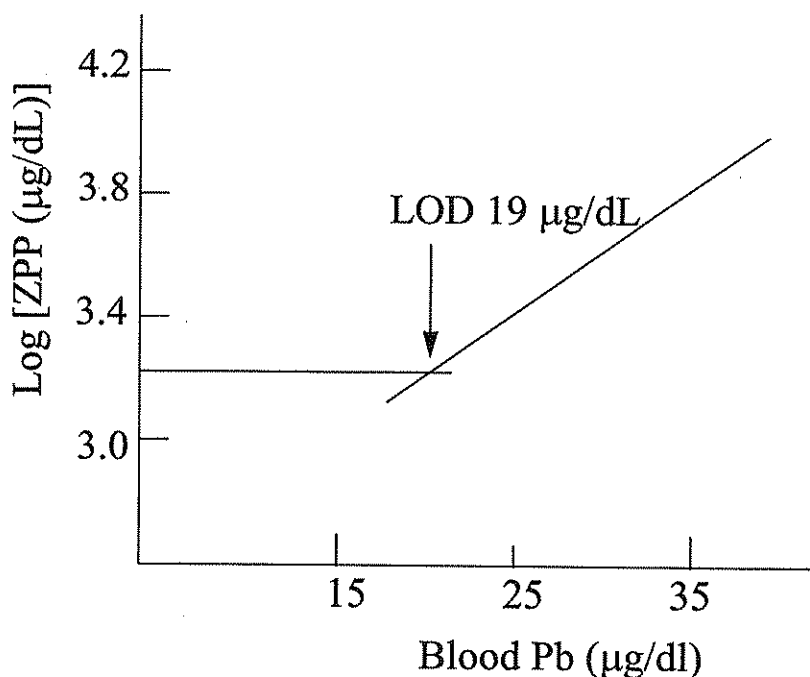
The measurement method described above is cumbersome, requiring as it does the extraction method. Furthermore, it does not discriminate against the genetic disease protoporphyria. As it turns out, the elevated FEP associated with lead poisoning comes primarily in the zinc protoporphyrin, ZnPP, not PPIX, form.[110] ZnPP can be monitored via its fluorescence at 594 nm. FEP associated with unmetallated PPIX fluoresces at 625 nm. Fluorescence can be measured in diluted whole blood, thus simplifying the whole procedure,[111] although it has been suggested that the heme itself is a potent quencher of ZnPP fluorescence.[112]

One last comment is appropriate here. The lowest level of blood lead that causes an elevated ZnPP is 20 μg Pb/dl, which is a value well above currently acceptable levels. However, the cost of this measurement is $1 to $5 per sample and is amenable to decentralized testing.[48] Furthermore, if one tracks both blood lead and PP it is possible to determine the date of lead exposure.[113]

E. Inner Shell Electron-Based Determinations

Inner shell electrons can be probed both for qualitative (bonding information) and for quantitative information. When a photon of angstrom wavelength strikes an atom it penetrates to the inner shell electrons (Figure 37). There the beam can be diffracted (X-ray diffraction) or it can cause the ejection of a photoelectron whose energy is less than that of the original photon by the binding energy of the shell. The absorption of the high-energy beam is measured as absorbance. The loss of the photoelectron leaves behind a vacancy that can be filled by an electron

FIGURE 37. Schematic of absorption and fluorescence of X-ray radiation. An incoming X-ray is absorbed with the ejection of a photoelectron, an event corresponding to the ionization of the atom. Ionization events are quantized, resulting in one absorption edge from K (inner most) three absorption edges from L orbits. The vacancy in the inner shell can be filled by an electron from a more outlying shell (L, M, N, O), resulting in emission of photons. (See Figure 38 for an emission spectra of lead.)

from an outershell with the release of an X-ray photon giving rise to X-ray fluorescence.

1. X-Ray Absorbance

In X-ray absorbance an inner shell electron is ionized, a process requiring very energetic radiation (0.014 nm, or 0.14 Å). The absorption spectrum for lead is shown in Figure 38. The first "peak" observed involves transitions from the first shell (n = 1) called K band. The second and third "peaks" involve transitions from the three sublevels in the L band. The probability of lead interact-

ing with high-energy radiation is high (large cross section) due to the large number of electrons present. Table 20 shows the main wavelengths (and energies) of the absorption bands.

a. X-Ray Absorbance Fine Structure (XAFS)

When X-ray absorption is probed with a high-energy source (synchontron radiation) perturbations in the energies of the inner shell valence electrons by binding of the outershell electrons can be observed. These
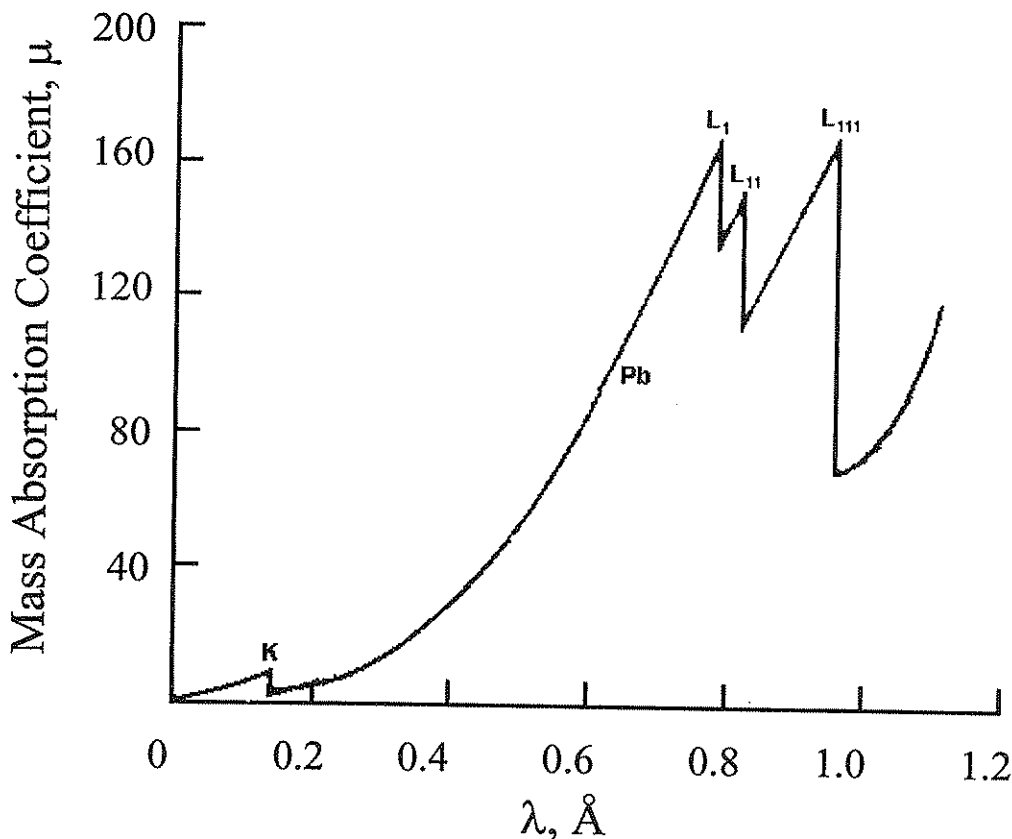
FIGURE 38. Absorption edges for lead showing the K, and three L transitions resulting in the removal of an electron from the inner shell.

TABLE 20
X-Ray Absorption Bands for Lead

Absorption Band	Wavelength Å	keV
K	0.141	88.037
L_I	0.782	15.858
L_{II}	0.815	15.202
L_{III}	0.950	13.041
M_{IV}	4.757	2.606
M_V	4.955	2.502

perturbations are fingerprinted for the valence of the atom (Pb^{2+} vs Pb^{4+}) and by the strength of binding. An example are the slight differences observed between αPbO, βPbO, and βPbO_2 shown in Figure 39.[114] The difficulty in these measurements is that lead due to its multiple valency and its midpoint between ionic and covalent bonding in the

oxides will have multiple binding sites within a given compound, leading to difficulty in interpreting the fine structure. This method is used to determine the types of compounds of lead present in soils, with the hope of either determining the source of lead, or evaluating the potential toxicology from the different forms of lead present.

2. X-Ray Fluorescence

The hole left behind by the inner shell electron can be occupied by the relaxation of an outer shell electron (Figure 37). This relaxation is accompanied by emission of light, X-ray fluorescence. Lead has three major X-ray fluorescence bands at 75 (K), 10.5 (L), and 2.3 (M) KeV[115] (Tables 21, 22, 23,

315
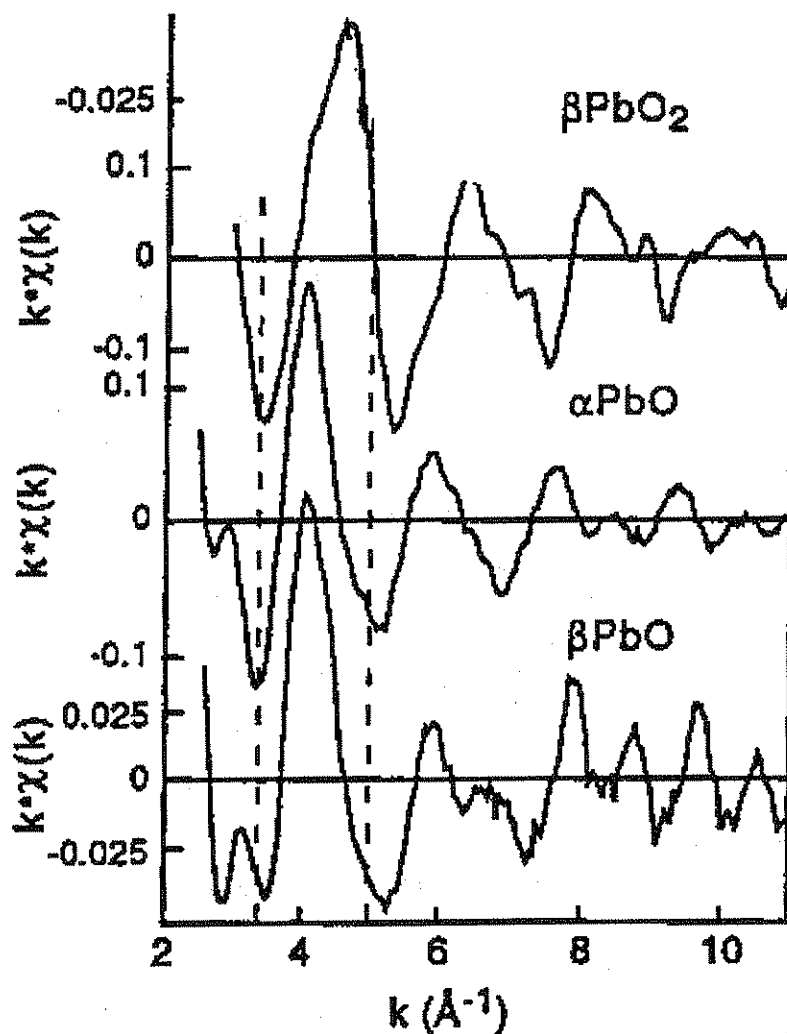
FIGURE 39. When an highly intense radiation source is used (synchotron), the absorption edge transitions can be resolved into fine structure, which is the result of valence shell electron bonding. This figure illustrates the difference observed between α and β PbO. (From A. Manceau, M.-C. Boisset, G. Sarret, J-L. Hazemann, M. Mench, P. Cambier, and R. Prost *Environ. Sci. Tech.* 1996, **30**, 1540–1552.)

TABLE 21
Main K X-Ray Emission Lines for Lead

Intensity	Type	Å	keV
150	α1,2(K–L₃)	0.167	74.25
100	α1 (K–L₃)	0.165	75.15
50	α2 (K–L₂)	0.170	72.94
15	β1 (K–M₃)	0.146	84.93
15	β3 (K–M₃)	0.147	84.35
5	β2 (K–N₃,₂)	0.147	84.35
<0.1	β4 (K–N₄,₅)	0.141	87.94

and Figure 40). These bands are selective for lead. An X-ray fluorescence spectrum is shown for lead in Figure 41.

X-ray machines contain several parts: a source of energy (often a Co[57] source), a detector (Si(Li) semiconductor), shields to protect the user from the source of energy, and electronics to count and sort the X-ray beam. For in lab use, the instrument also contains a sample holder. The sample is prepared as a thin film or as a gas. X-ray

TABLE 22
Main L X-Ray Emission Lines for Lead

Intensity	Generic	Type	Å	KeV
100	Lα	$\alpha2$ (L$_3$–M$_5$)	1.175	10.55
10	Lα	$\alpha2$ (L$_3$–M$_4$)	1.186	10.45
50	Lβ	$\beta1$ (L$_2$–M$_4$)	0.982	13.9
20	Lβ	$\beta2$ (L$_3$–N$_5$)	0.983	12.6
6	Lβ	$\beta3$ (L$_1$–M$_3$)	0.969	12.79
5	Lβ	$\beta4$ (L$_1$–M$_2$)	1.007	12.31
1	Lβ	$\beta5$ (L$_3$–O$_{4,5}$)	0.953	13.01
10	Lγ	$\gamma1$ (L$_2$–N$_4$)	0.840	14.76
1	Lγ	$\gamma2$ (L$_1$–N$_2$)	0.822	15.08
2	Lγ	$\gamma3$ (L$_1$–N$_3$)	0.815	15.2
3	L,	,(L$_3$–M$_1$)	1.350	9.18

TABLE 23
M X-Ray Emission Lines for Lead

Type	Å	keV1
$\alpha1$(M$_5$–N$_7$)	5.285	2.346
$\alpha2$(M$_5$–N$_6$)	5.299	2.34
β(M$_4$–N$_6$)	4.674	2.44

spectrometry has been used to determine the amount of lead in gasoline in the ASTM method 5059. Leaded gasoline is diluted with Bi-2-ethylhexoate as an internal standard. Lead is monitored at the L-α_1 line (1.175 Å) and Bi at the L-α_1 line (1.144 Å). The method is valid from 0.0026 to1.32 g Pb/l.

X-ray fluorescence can also be used on-site. Listed in Table 24 are the costs (1995) of several commercial instruments. Despite the cost, XRF has been popular because it is nondestructive and portable. X-ray fluorescence has been used as on-site monitoring of polluted soils at army firing ranges (lead azide is used as a initiator for propellants).[116,117] The method has been applied extensively to monitoring of homes for leaded paints.

How well does the X-ray fluorescence machine work? The energy source beam must penetrate the paint and the emitted beam come back out again. Typically, the K line is used as it is the most energetic and capable

of penetrating overlayers of non-leaded paint. The effect of layering is important. A typical paint chip 33.2 mil (845.8 m) thick. Often the leaded paint lies under 3 to 5 layers. Consequently, the X-ray beam may not penetrate to the toxic coat. Cianflone reports the depth of penetration as 2 mils.

Even if the beam penetrates all layers, the data are acquired as the amount of lead per area illuminated. Thus, one does not know if the instrument is recording a very large amount of lead in the surface layer or small amounts of lead in several underlying layers. For example, the "detection limit" of an instrument may be reported as 0.9 mg/cm². This could mean that the instrument could measure 0.9 mg in one layer of paint or 0.9 mg in all layers of paint combined. (A typical 50-year-old house may have 10 to 20 layers of paint.) Conversion of this number to a weight/weight number for interpretation for ingestion is based on the assumption that one layer of paint containing 1% lead by weight has 0.08 mg Pb/cm².[115] Using these values and assumptions, an XRF instrument has a detection limit of 11.25wt%.[118]

Another problem with X-ray fluorescence machine is high background signals associated with light scattering. The National Institute of Standards and Technology (NIST) in 1989 reported readings of 2.0 mg/cm² on

n=4, N
n=3, M

β_3L at 0.969 A

β_1L at 0.9829 A

90

80

n=2, L

70

α_1L at 1.175A

60

50

α_2K at 0.1703A

α_1K at 0.165A

40

30

20

10

n=1,K   0

I   II   III   IV   V
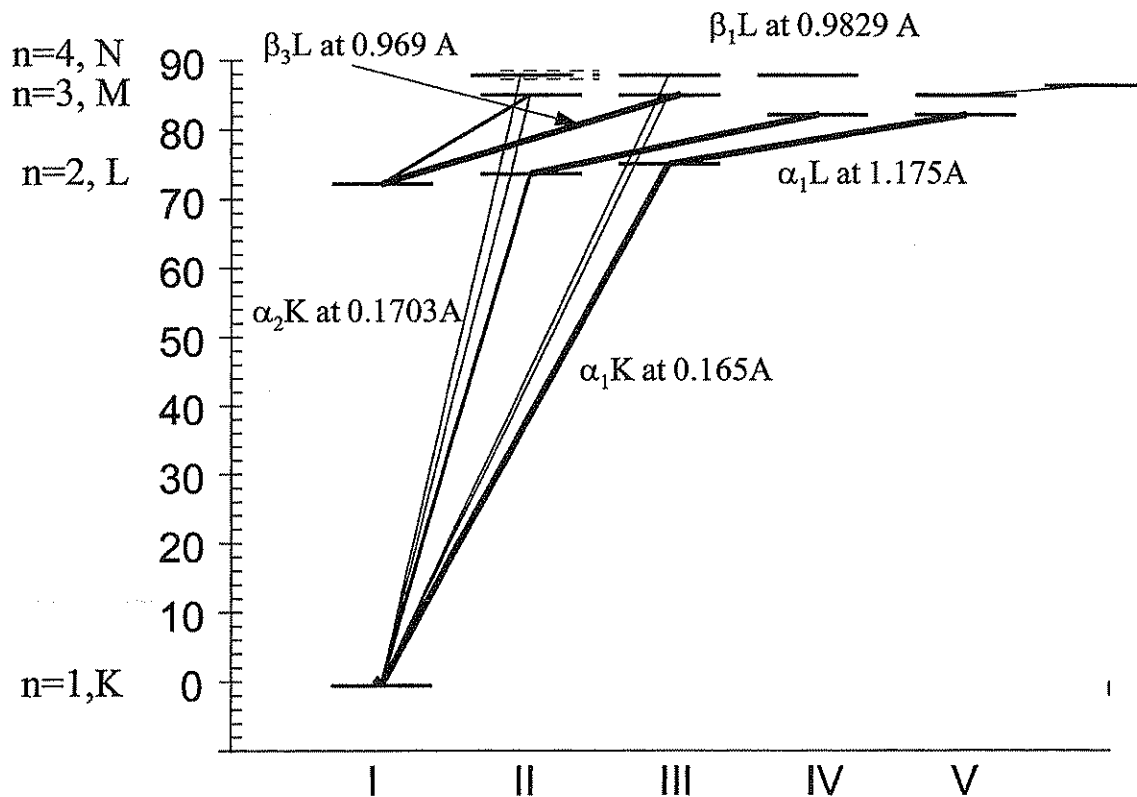
FIGURE 40. A diagram of some of the more important inner shell transitions for lead.

lead-free surfaces. Thus, one gets a false-positive reading. Readings are accurate only if the reading is 3 to 4 mg/cm². A comparison of measurements of lead by XRF, AAS, ICP-AES, and ASV indicated that the error associated with the XRF measurement was quite high.[119] The error is, in part, related to spatial the roughness of the sample, affecting the collection of the emitted beam.[120] This can be somewhat compensated by the technique of total reflection X-ray fluorescence.[121,122,123,124,125] Total reflection XRF uses a grazing angle source coupled to the sample holder that minimizes the source beam contribution to the background, thus lowering the limit of detection.

In the late 1990s X-ray fluorescence has been studied aggressively to monitor *in vivo* bone lead concentrations as a marker of short- and long-term exposure and of post-expo-sure metabolism in retired occupationally exposed workers.[126,127,128,129,130,131,132,133,134,135] The number of lead fluorescent photons is compared with the number of photons from calcium hydroxyapatite, generally using a Cd γ-ray source. The normalization method accounts for variations in bone shape, size, density, overlying tissue thickness, and movement.[136]

3. X-Ray Diffraction

In X-ray Diffraction (XRD) the pattern by which the X-ray beam is scattered from the subvalence shell electrons in the compound is distinctive for the position of the atoms in the compound. XRD is used primarily to identify pure compounds. Constituent minerals must be present in
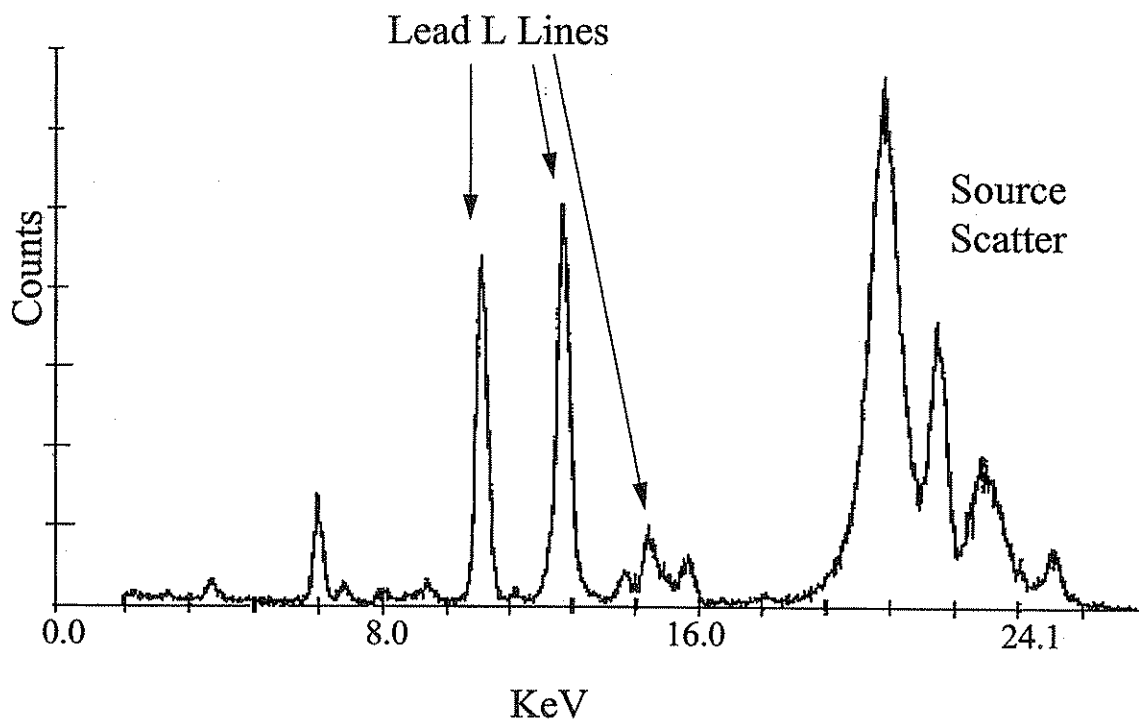
FIGURE 41. X-ray fluorescence spectrum of a munitions contaminated soil showing both the source background and the lead L lines. (From J. F. Schneider, J. Lee, J. Dolph, C. W. Dickhut, A. Bohm, 4th Int. Conf. On-Site Analysis, Orlando, Florida.)

TABLE 24
Commercial XRF

Manufacturer	Cost (1995)
Cianflone Scientific Instruments	$21,000
NHV systems	$20,000
Spectrace	$60,000
Seiko	$60,000–80,000

amounts greater than 5% to be recognizable. In addition, the crystal particle size should be no larger than 10 μm to avoid stacking effects (loss of randomness). Particles should also be larger than 0.1 m to avoid broadened reflected lines. Table 25 shows some of the reflection lines observed for common lead compounds, particularly those of interest in lead acid battery technology.[137]

VI. OTHER SPECTROSCOPIES

A. ibrational Spectroscopies

1. Infrared Spectroscopy

In IR spectroscopy a beam of micrometer wavelength light is impinged on the sample and its absorption is measured. The energy of the micrometer wavelength is not energetic enough to cause electrons to change energy states, but it is strong enough to cause bonds between C-O, O-Pb or Pb-N to wiggle, wag, bend, and vibrate (covalent single, double, and triple bonds, or ionic) and to the weight of each of the atoms. Therefore, the method is sensitive to the chemical environment of the compound and is useful in identification of lead species. Table 26 shows vibrational bands associated with a variety of simple lead com-

TABLE 25
Diffraction Lines for Common Lead Compounds

Material	Strongest reflections of lattice plane distances				Intensity ratio d in Å
Pb (metal)		2.86	2.48	1.49	100:50:32
PbO (tetragonal)	3.12	2.81	1.87		62:37
PbO (rhombic)	3.07	2.95	2.74		31:28
Pb$_3$O$_4$		3.38	2.90	2.79	50:45
α–PbO$_2$	3.12	2.74	2.63		70:70
		3.13	1.84	2.73	30:20
β–PbO$_2$	2.80	3.51	1.85		90:70
		3.50	2.80	1.86	100:100
Pb(OH)$_2$		3.23	3.05	2.70	100:80
PbSO$_4$		3.25	8.10	2.87	30:30
4PbO·PbSO$_4$		1.98	1.95	2.70	100:70
		3.23	2.65	1.94	80:80
3PbO·H$_2$·PbSO$_4$	3.25	3.13	3.07		80:80
		3.26	9.79	3.13	60:45
2PbCO$_3$·Pb(OH)$_2$	2.67	3.61	3.29		90:90
PbCO$_3$		3.59	3.50	2.49	40:32

TABLE 26
Vibrational Bands of Simple Lead Compounds

Harmonic Frequences, cm^{-1}

Diatomic

(PbX) Compound	vcm^{-1}	Compound	vcm^{-1}
PbO	721.8 (754.74)	PbF	507.2 (697.23)
PbS	428.1 (552.48)	PbCl	303.8 (533.59)
PbSe	277.6 (384.69)	PbBr	207.5 (383)
PbTe	211.8 (327.32)	PbI	160.5 (327.8)

Triatomic

PbX$_2$ Compound	v_1 cm^{-1}	v_2 cm^{-1}	v_3 cm^{-1}	v_4 cm^{-1}
PbF$_2$ bent	531.2	165	507.2	
PbCl$_2$ bent	297		321	
PbI$_{2(g)}$ bent	200	64		

Pyramidal

PbX$_3$ Compound	v_1			
[PbCl$_3$]$^-$ soln	249	—	—	—
[PbBr$_3$]$^-$ soln	176	—	164	58
[PbI$_3$]$^-$ soln	137	—	127	30~45

Tetrahedral

v_5 cm^{-1} Compound	v_1 cm^{-1}	v_2 cm^{-1}	v_3 cm^{-1}	v_4 cm^{-1}	v_5 cm^{-1}
PbCl$_4$	331	90	352	103	

Octahedral

[PbCl$_6$]$^{2-}$	281	209	262	142	139

From Kazuo Nakamoto Infrared and Raman Spectra of Inorganic and Coordination Compounds, 4th ed., *Wiley, 1986.*

Note: Values in parenthesis are calculated assuming a single bond with k = 500 N/m.

pounds. It can be noted that the frequency of the vibration shifts lower as the anion gets larger, consistent with heavier mass. The larger the mass, the slower the frequency of the vibration ($v \propto \sqrt{(1/\mu)}$). Second, the measured frequencies are larger for Group VIb as opposed to the halogens even though the reduced masses are similar, such as occurs for Te (amu = 127.61) and I (amu = 126.91). For these two the calculated frequencies are close to identical, but the measured frequencies differ by 51 cm^{-1}. This might reflect a partially covalent nature of the Pb bonds with Group VIb atoms. It is known that lead has a partially covalent bond with these atoms, which would imply a stronger force constant when compared with a purely ionic bond, as would occur for the halogens.

A good example of the use of IR measurements is in the binding of lead to EDTA.[138,139,140,141,142] The intensity and frequency changes the accompany the binding of Pb^{2+} can be monitored. Table 27 indicates the bands observed for EDTA in solution at pH 11. A key observation from Table 27 is that there is a plethora of bands, as would be predicted from the 3N-6 rule (192-6 = 186 possible). The authors of this investigation state that due to the complexity they do not attempt to assign all of the bands. The bands of interest will be at higher wavenumbers than the lead halogens. Carbon containing (covalent) bonds (C-C, C-H, C-O) have stronger force constants than those observed for the ionic lead-halogens. In addition, they have lower atomic weights.

TABLE 27
EDTA Vibrational Bands

Vibrational Bands (Raman) Observed for EDTA

Wavenumber, cm^{-1}	Strength, Breadth	Assignment
350	m,b	vM-O(A$_1$) MN
400	m,b	M-N≡C stretches K
450	w,sh	
595	w,b	
710	w,b	
800	w,b	
845	w,b	
918	vs	C-C acetate stretch MN
975	w,b	
1020	w	
1085	w	C-N stretch K
1140	m,b	
1200	w	CH$_2$ wag in-CH2COOH (K
1265	m	
1280	vw,sh	
1335	s	
1406	vs	Carbonyl K
1435	m,sh	Carbonyl K
1450	m,sh	Carbonyl K
1600	m,b	Carbonyl K
2841		C-H in HCOO-MB
2936	s	C-H in CH$_3$COO-MB

From K = K. Krishna and R. A Plane, *J. Am. Chem. Soc.*, 1968, 90, 12, 3195. Alternative assignments by **MB** = M. L. Morris and D. H. Bush, *J. Am. Chem. Soc.*, 1954, 78, 5178 or **MN** = A. A. McConnell and R.H. Nuttal, *Spectrochim. Acta.*, 1977, 33A, 459–462.

In EDTA there are potentially six binding sites, two of which are nitrogen (electron donors) and four of which are carboxylic acid sites. Lead has a very high affinity for oxygen, so it may reasonably be presumed that lead will bind strongly to oxygen. Binding to EDTA will perturb the bond strength of the C-O bonds and may impact on the C-C bond in CH_2-COO- (Table 27).

The binding of the metal lead to the EDTA can be monitored, then, either at characteristic carbonyl lines (decrease in their intensity), changes in the C-C stretch at 900 cm^{-1}, or by the development of covalent metal nitrogen bonds. These nitrogen bands are interesting because their frequency tracks very nicely with the covalency of the bond. The larger the ion, the less the charge density and the less the covalent nature of the bond with the nitrogen lone pairs. This is deduced from the clustering of frequency with radius and charge, as shown in Table 28.

This same type of trend is observed at the carbonyl band.[143] When the charge/radius (q/r) is greater than 3.6 covalent binding predominates and the frequency of the C-O band (1750 cm^{-1}) shifts to 1625 or 1650 cm^{-1}. When q/r is less than 3.6, the C-O band shifts to 1590 to 1615 cm^{-1} indicative of ionic bonding. The Pb^{2+} carbonyl band occurs at 1600 cm^{-1}. The explanation for this shift and its dependence on the type of bonding is related to the impact of the metal oxygen bond on the resonance structure of the carboxyl acid group. The greater the ionic character of the metal-oxygen bond, the greater the single bond character of the C-O bond, which shifts it from a high force constant (1000 N/m) to a lower force constant (500 N/m), resulting in a shift to a lower frequency.[144]

IR spectroscopy has been used to elucidate the type of binding experienced by lead in the solid EDTA complex. Many divalent complexes are expected to have a sixfold coordination with the six donor sites on EDTA, octahedral structure is expected. However,

TABLE 28
N–M Bond Vibrations of EDTA Complexes in Neutral Aqueous Solution

Metal Ion	Radius Å	Wavenumber/cm⁻¹
Cu2+	0.71	470 s
Mg2+	0.78	450 m, b
Zn^{2+}	0.83	460 s
Mn^{2+}	0.91	445 s
Cd^{2+}	1.03	435, s
Ca^{2+}	1.06	445 m
Hg^{2+}	1.12	425 vs
Pb^{2+}	1.32	424 vs

From Trend in M-N Raman band with radius of metal ion. K. Krishnan and R. A. Plane, *J. Am. Chem. Soc.*, 1968, **90**, 12, 3195.

the s^2 lone electron pair on divalent lead may distort the octahedral configuration may distort the octahedral configuration. The investigators concluded (by monitoring the M-O and M-N bands at <400 cm^{-1}) that PbY^{2-} adopts a distorted octahedral symmetry to give a pentagonal bi-pyramid.[145]

Because of changes in the C-O intensity in the uncomplexed sample on addition of Pb^{2+} and the formation of a new frequency identified with PbY^{2-} (Y = EDTA), the extent of binding of lead to EDTA can be monitored (Figure 42). Samples could conceivably be dissolved in water; however, water is highly IR active (O-H stretches) and creates too large of a background for the experiment. Other possible solvents are CS_2, CH_3Cl, and CCl_4. All are reasonable solvents for IR spectroscopy. Because $Pb(EDTA)^{2-}$, however, is an ionic salt, solubility will be a problem. Samples are therefore prepared as a finely ground solid (<2 μm particle size) in a heavy oil support on KBr window. The oil, Nujol, is a paraffin mixture.

2. Raman Spectroscopy of Lead-Tin Oxides

Raman spectroscopy samples the same phenomena as IR, vibrational information that leads to bond information and somewhat
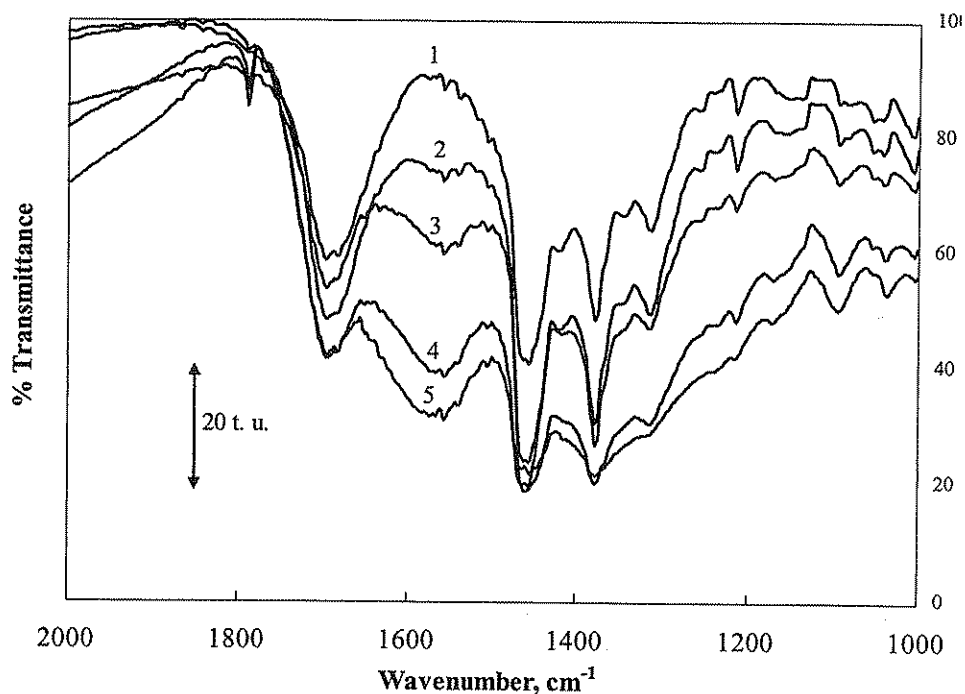
FIGURE 42. The binding of lead to the carboxyl groups on EDTA (see Figure 12) changes the single/double bond character of the carbonyl bond of the COO functional group. Deprotonation and stabilization of the carboxylate group with a metal ion maximizes resonance enhancing the single bond character of the carbonyl group, lowering the frequency of the vibration. Infrared spectra of PbEDTA and EDTA mixtures, the molar ratio of PbEDTA being (a) 0; (b) 0.25; (c) 0.5; (d) 0.75, and (e) 1.0. Each of the mixtures has a total of 10 μmol of ligand. (From S. Dragan and A. Fitch, *J. Chem. Ed.,* 1998, **75,** 1018–1021.)

similar selectivity. Raman spectroscopy has the advantage of being silent to water. In Raman spectroscopy a molecule is excited to a "virtual" state. The process is shown in Figure 43. Most of the time the molecule relaxes to ground state reemitting the same energy of light, resulting in Rayleigh scattering of light. When the excited electron begins to be vibrationally excited, the relaxation can emit light that is the sum of the energy of the excitation beam and the vibration energy (anti-Stokes line). When the excited electron falls to a vibrationally excited state, a Stokes line is observed. With this method, vibrational information is obtained in the UV-Vis region by using laser beams. The advantage this brings is the ability to easily manipulate and monitor the light, even with the weak energy of the vibrational

transition. The size and cost of lasers have decreased rapidly in the last 20 years, bringing Raman spectroscopy into the fieldable stage. Raman spectroscopy has been used to examine previously inaccessible materials such as fragile paper illuminated manuscripts. The darkening of $PbCO_3$ to PbS in tenth century Buddhist manuscripts has been detected by the bond vibrations of the lead pigments.[146, 147] Different lead yellows have been used at different time periods in history and their appearance in paintings can be used to detect forgeries (Table 29). In particular, a nondestructive analysis can be performed to distinguish between Lead Tin yellow II and lead tin yellow I, as shown by the band assignments in Table 30.

Raman spectroscopy has been suggested as a fieldable **quantitative** technique.[148] The

$\lambda_{out} < \lambda_{in}$
Raman
anti-Stokes Line

$\lambda_{out} = \lambda_{in}$
Rayleigh
Scattering

$\lambda_{out} > \lambda_{in}$
Raman
Stokes Line
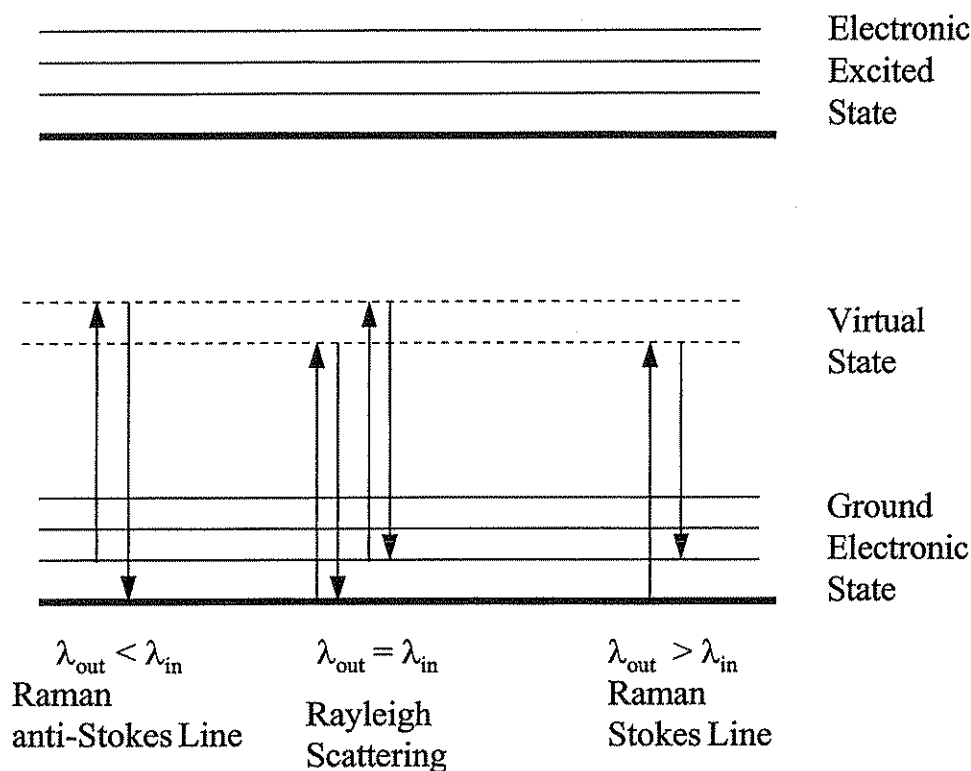
FIGURE 43. Schematic showing the origin of Raman scattering.

TABLE 29
Time Line for Lead-Based Yellow Pigments

Date	Location	Object	Pigment	
1500 B.C.	Tell al-Rimah	Glass	$Pb_2Sb_2O_7$	Lead Antimonate/Naples Yellow
1450–1350 B.C.	Nuzi	Glass		
1000–850 B.C.	Hasanlu	Glass		
600	Nimrud	Glass		
300–200	Rhodes	Glass		
140–260 A.D.	Caerleon	Glass		
200–300	Sardis	Glass		
300–500	Kenchreai	Glass	$PbSnO_3$	Lead Tin Yellow II
300–400	Shavei Zion	Glass	$PbSnO_3$	
<1300 A.D.	Europe	Paints		Orpiment
<1300	Europe	Paints	PbO	Massicot
1300–1650	Europe	Paints	$PbSn_{1-x}Si_xO_3$	Lead Tin YellowII/Venetian
Yellow				
1450–1750	Europe	Paints	Pb_2SnO_4	Lead Tin Yellow I/ Gial'lolino
1700–1850	Europe	Paints Glazes	$Pb_2Sb_2O_7$	Lead Antimonate/Naples Yellow
>1804	Europe	Paints	$PrCrO_4$	Chrome Yellow
			$PbCrO_4$–$PbSO_4$	Light fast chrome yellow

TABLE 30
Vibrational Bands Associated with Lead Yellow Pigments

Compound	Wavelength absorbed	Vibrational spectra
Pb_2SnO_4	514.5 nm	35wm, 58w, 80m, 129vs (lattice Pb-O stretch mode), 274w, 291wm, 379w, 454wm, 524w, 613w
$PbSn1_{-x}Si_xO_3$	514.5	40m, 66m, 85sh, 138vs (lattice Pb-O stretch mode) 324wm(br), 444w(br)
$Pb_2Sb_2O_7$	514.5	76s, 147vs (lattice Pb-O stretch mode), 343s, 464m, 513wm

proposed method starts with a gold surface modified through a S linkage with a tethered PAR chelate. An excitation into the UV-Vis absorption band at 514.5 nm results in resonance-enhanced Raman signals. Further enhancement is provided by the surface-enhanced effect of the underlying gold electrode. The 1023 cm^{-1} associated with the nitrogen shifts dramatically, indicating lead binding to the pyridyl group. The intensity of the band is quantitative with the extent of binding. Unfortunately, however, the band is also sensitive to chelation of other metal ions such as Cd^{2+} and Cu^{2+}. The binding of lead to the PAR group is 2 orders of magnitude less selective than for these other metal ions, resulting in a detection limit for lead of 522.3 ppb at pH 6.

B. Nuclear Probes (^{207}Pb)

1. Direct ^{207}Pb NMR

In the absence of a magnetic field, nuclear energy levels are identical (degenerate). When a magnetic field is imposed the energy level of the degenerate nuclear spins is split, corresponding to the possibility of two separate spin states (m_i) that interact differentially with the imposed magnetic field. If a molecule bathed in this magnetic field is irradiated with electromagnetic radiofrequency radiation ($\lambda = 30$ to 5 m; 10 to 500 MHz), a transition between energy levels can be observed for atoms that are NMR active.

The spin quantum number follows the rules:[149]

1. If the mass number, A, is odd, the nuclear spin, I, is 1/2.

2. If the mass number, A, and charge number, Z, are both even, the spin, I, is zero.

3. If the mass number, A, is even, but the charge number, Z, is odd, the spin, I, is integral.

Of these three possibilities, nuclei with spin number $I = 1/2$ are the most accessible for NMR studies (Table 31). Note that ^1H, ^{13}C, ^{19}F, ^{31}P, ^2D, ^{23}Na, ^{15}N, ^{29}Si, ^{199}Hg, and ^{113}Cd are active. Note that lead has a single isotope out of four that is directly NMR active.

The frequency, v_o, at which the transition occurs is governed by

$$v_o = \gamma(1 - \sigma)B_o/2\pi \qquad (68)$$

where γ is the gyromagnetic ratio, a constant of the isotope observed, B_o, is the magnitude of the applied magnetic field, and σ is the shielding constant that tends to diminish the effect of the magnetic field on the isotope nucleus. The shielding constant is determined by the electronic excited states and the charge of the atom.

Most spectra are plotted as a normalized frequency, δ, the chemical shift:

TABLE 31
Nuclear Spin Number, I

A atomic mass	Z atomic number	Example	I	NMR
Odd	Odd or Even	$^{1}_{1}H(^{1}/_{2}), ^{15}_{7}N(^{1}/_{2}), ^{13}_{6}C(^{1}/_{2}), ^{15}_{7}N, ^{207}_{82}Pb, ^{19}_{9}F$	1/2	Yes
Even	Odd	$^{2}_{1}H(1), ^{14}_{7}N(1)$	1	Fast relaxing
Even	Even	$^{12}_{6}C(0), ^{16}_{8}O(0), ^{208}_{82}Pb(0), ^{206}_{82}Pb, ^{204}_{82}Pb$	0	No

$$\delta_{ppm} = (v_o - v_{reference})10^6 / v_{ref} = (\sigma_{ref} - \sigma_{sample}) \times 10^6 \tag{69}$$

which is directly related to shielding.

Table 32 shows some the range of chemical shifts observed in proton NMR and in lead NMR, as well as the theoretical absolute shielding scale for the pure atom.[150] The shielding parameter grows directly with the number of electrons and accounts for the large observed chemical shift.[151,152,153,154,155,156,157] The variability in the shielding constant is a function of both the charge on the electron and the electronic states involved in bonding.[158] Because of the latter,[207] Pb NMR is sensitive to hybridization of the lead valence orbitals. As a result,[207]Pb NMR is sensitive to the activity of the lone pair of s electrons on lead.[159] ^{207}Pb NMR is also sensitive to the coordination number of the site in which lead finds itself. This holds equally true for solution phase as well as solid phase ^{207}Pb NMR. An example is the ability to resolve the two different valence states of lead in minium, Pb_3O_4.[160]

Solid state ^{207}Pb is fairly difficult to monitor because of the breadth of the bands to be observed.[161] Solid state NMR tracks the electron density on Pb from which information about the degree of covalency of a bond can be made. Figure 44 shows the 207-Pb chemical shift of PbM_xO_y compounds vs. the electronegativity difference of Pb/M. An electronegativity difference of 0 implies a 100% covalent bond, while that of 1.7 represents a bond that is 50% ionic in character and 3.5 represents a bond that is 100% ionic. In Figure 44 the chemical shift of lead is measured from lead in a covalent bond with C. All the compounds have an ionic bond character between Pb^{2+} and the M; however, lead is able to take more of the oxygen electrons in the chromate species, consistent with the mechanism for charge transfer pigmentation of the lead chromate compound.

2. Proton NMR Coupling

In addition to observing the chemical shift of ^{207}Pb directly, spin-spin coupling through bonds may be observed when other NMR active nuclei are present. Such spin-spin coupling can be felt, under optimum conditions, as far away as 6 to 7 bonds. Spin-spin coupling follows the

$$\text{bands observed} = 2*N*I + 1 \tag{70}$$

where N is the number of atoms involved, the I is the nuclear spin quantum number. Lead can be monitored indirectly through spin-spin coupling with the proton.

An indirect measurement of ^{207}Pb is given by the NMR structure of the lead EDTA complex (Figure 45). The acetate and ethylenic protons are close enough to the lead to have a chemical shift due to lead binding. The fraction of lead as ^{207}Pb will spin-spin couple with protons resulting in a doublet

TABLE 32
NMR Parameters

Species	δ(ppm)	γ(rad/(T-s)	Sensitivity	σ(pure atom)
^{1}H	0–13	2.68×10^8	1.00	17.73
^{6,7}Li		2.853×10^8		101.45
^{13}C	0–220	6.73×10^7	0.0159	
^{23}Na		7.07×10^7		628
^{35}Cl		2.62×10^7		1142
^{39}K		1.25×10^7		1329
^{67}Zn		1.67×10^7		2521
^{87}Rb		8.78×10^7		3366
^{111}Cd		-5.70×10^7		5780
^{199}Hg		4.84×10^7		9729
^{207}Pb	100–10,000	5.62×10^7	0.00916	10,060

NMR Chemical Shift for PbMxOy
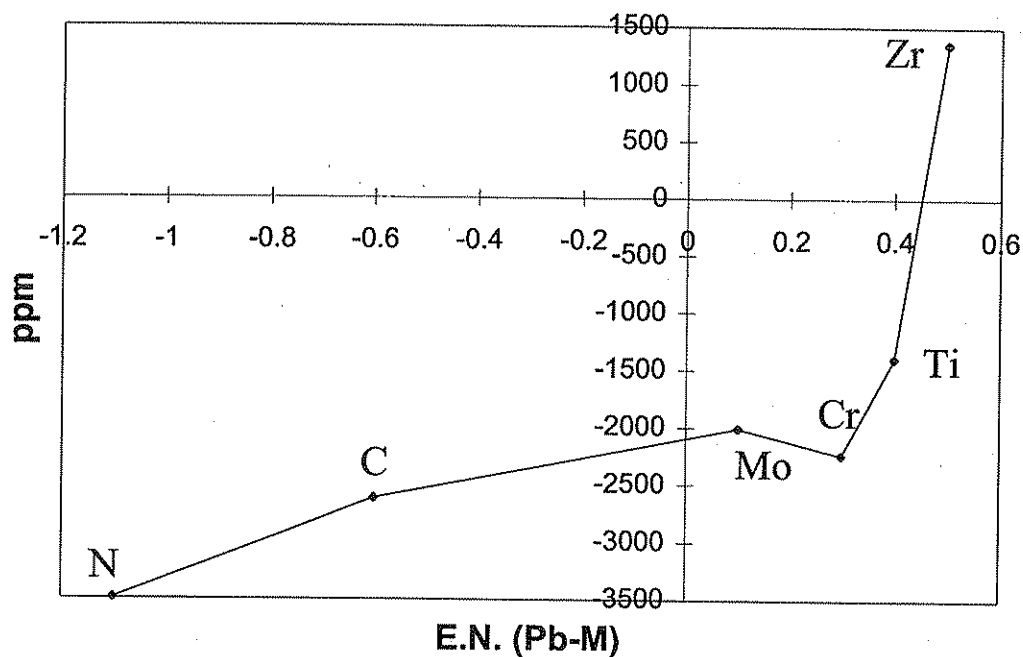
FIGURE 44. Chemical shifts associated with lead/metal/oxide compounds referenced to tetramethyllead. The shifts reflect changes in the covalent/ionic nature of the lead oxygen bond as tuned by the second metal. (Data abstracted from Neue, G., C. Dybowski, M. L. Smith, and D. H. Barich, *Solid State NMR*, 1994, **3**, 115.)
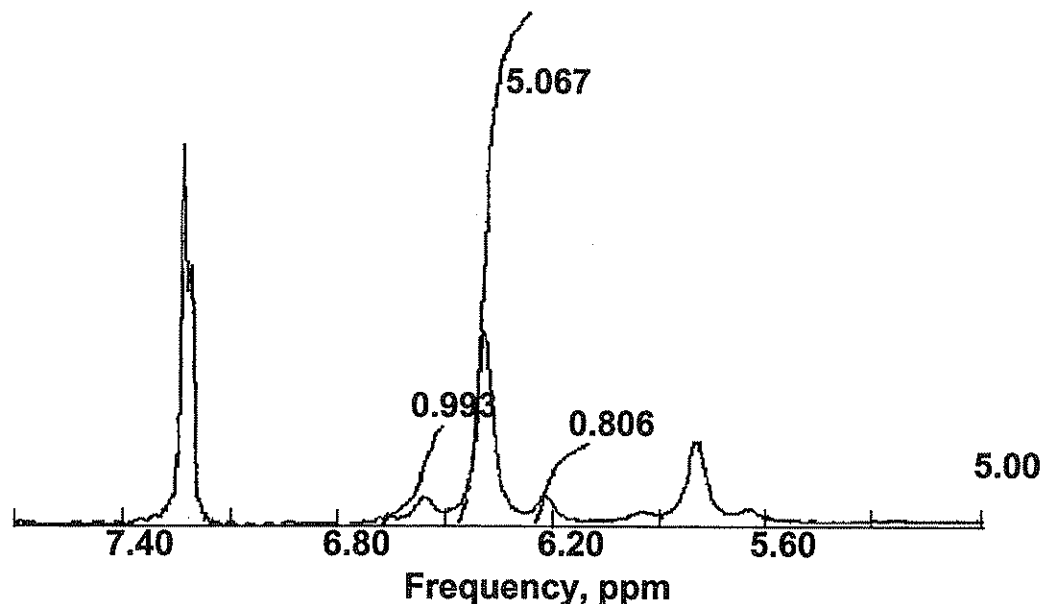
FIGURE 45. Spectra of Lead EDTA at pH 7 showing the ^{207}Pb-generated doublet at both the ethylenic and carboxylic protons. The integrated area of the doublet divided by the total area is a measure of the isotopic percent of ^{207}Pb.

$(2*N*I + 1 = 2*1*1/2 + 1 = 2)$.[162] If the absorption peak is Lorenzian, then the area under the peak should correspond to the number of species giving rise to the signal. Integration of the two satellites gives a measure of lead 207, which, when added to the center band area, gives the total lead content.

$$\%207 = \frac{(\text{area of both satellites})}{\text{total area (side + center)}} \times 100$$

(71)

The relative abundance of ^{207}Pb is of interest due to the differences observed for this isotope across various mines, Table 33.

The resolution of the doublet from the center band for ^{204}Pb, ^{206}Pb, and ^{208}Pb chemically shifted EDTA depends on the lifetime of the complex, making the experiment not totally trivial. The lifetime of the complex τ must be greater than $1/J$, where J is the coupling constant or distance between the doublet peaks. The coupling constant for ^{207}Pb to the proton can be determined by

$J = (\text{difference in ppm between } ^{207}Pb \text{ peaks}) * \text{Instrument frequency}$

(72)

where the instrumental frequency is 300 MHz, 400 MHz, etc. The coupling constant $J_{(Pb-H)}$ can vary[163] with the compound used, as shown in Table 34.[164] The coupling constant is related to the electronegativity of the other atom, X, in the complex, increasing with the electronegativity of X. When trimethyllead is chelated, the chelation does not perturb the orbital structure of lead and therefore apparently does not change the coupling constant.[165] For the EDTA complex of lead, the doublets associated with ^{207}Pb were observed up to a mole ratio of 0.15, at which point precipitation of the complex (1 M $Pb(NO_3)_2$).[166] The lifetime data suggest that the complex is not rigidly coordinated into an octahedral complex but exchanges ligand edges rapidly.

The coupling constant $J_{(Pb-H)}$ for the complex NTA (nitrilotriacetic acid: $N(CH_2COOH)_3$) has been reported to be 18.9 Hz. This suggests that the lifetime of

TABLE 33
Pb–H couplings, J

Me₃PbXMe₃ compound	J, Hz	X, electronegativity	
Me₃PbSe Ph₃	−61.9; 41	Se	2.76
Me₃PbPbMe₃	−42.1; +22.9	Pb	1.61
Me₃PbSnMe₃	−40.1; +31.9	Sn	1.58
Me₃PbNMePh	−65.3; 44.5	N	
Me₃PbPPh₂	−52.0	P	

TABLE 34
% Relative Abundance 207Pb

Mine	%207	RSD
Mo, Joplin	20.01 ± 0.035	0.175
Idaho, Bunker Hill	22.496 ± 0.056	0.256
Mexico, San Antonio	21.196 ± 0.026	0.123
Australia, Broken Hill	22.66 ± 0.047	0.207
Northwest, Conmir	23.53 ± 0.022	0.094
B.C., Bluebill	21.56 ± 0.068	0.315
average	21.90 ± 1.24	5.69%

the Pb-H proton interaction (complex lifetime) has to be greater than 52.9 ms. The lifetime of the complex has been studied in detail.[167] The reactions that can possibly affect the lifetime are:

$$^{207}PbNTA^- +^{204,206,207*,208} Pb \rightleftarrows {}^{204,206,207*208} PbNTA^- +^{207} Pb \qquad (73)$$

$$^{207}PbNTA^{*-} + NTA_{Total} \rightleftarrows {}^{207} PbNTA^- + NTA^*_{Total} \qquad (74)$$
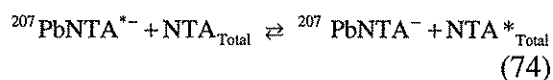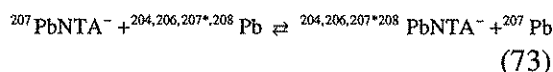
where NTA_{total} refers to the exchanged species distributed through all of the various pH forms of NTA:

$$NTA_{Total} = [H_3NTA] + [H_2NTA^-] + [HNTA^{2-}] + [NTA^{3-}] \qquad (75)$$

Lower pH values tend to increase the number of possible noncomplexed species and hence the total molar concentration of NTA_{total}. This means that the reaction is driven to the right and exchange takes place more rapidly. As a result, the lifetime of the complex at low pH is less than the lifetime of the complex at high pH and peak broadening is expected, which would diminish the resolution of the ^{207}Pb doublet.

In addition, increasing the concentration of the NTA complex in solution with respect to lead gives a similar result, decrease in lifetime, decrease in the doublet resolution. The decrease in the doublet, and the increasing width of the doublet, can be used to get kinetic rate constants.

$$\tau_2 = t/(\Delta peak \ width \ in \ Herz) \qquad (76)$$

The averaged rate constant (accounting for the NTA species prevalent fom pH 4.8 to 9.0) was found to be $4.41 \times 10^3 \ M^{-1} \ s^{-1}$. For NTA it was found that the $[NTA_{total}]/[Pb]$ had to be less than 1.0082 in order to observe the double peaks.

C. ICP-MS Determination of Pb

Mass spectral analysis of lead was investigated very early on with the pioneering works of Nier[168,169] and others.[170,171] With these methods, lead is converted to tetramethyl lead and injected as the gas into a mass spectral analyzer.

Since the mid-1980s, the ICP has also been coupled to a mass spectrometer detector.[172, 173, 174] With this method the ICP is used to create a gas phase of ionized atoms, using a 27-MHz RF field. The temperatures range from 6000 to 8000°K. At these temperatures all molecules are desolvated, broken to atoms, and ionized. Some species (first row elements) can be doubly ionized. Very few molecular species are left. Those molecular species that are found can be dimers, oxides, and (for a nitric acid digestion) nitrides. The background ions are argon cations, which are present in very high proportion due to the role of the argon as the shaping gas for the plasma.

The ions are pulled into the vacuum chamber by a sampling cone that has been set to some small potential. Between the ICP (1 atm pressure) and the mass spectrometer (10^{-6} millibar) there is a 9-order magnitude drop in pressure that is handled by several pumping stages, including diffusion pumps in which a mist of hot oil is sprayed into the chamber, where it impacts with the gas phase ions, collecting them and dropping them into a cooled collection chamber. Only a portion of the gas phase atoms remain. The diffusion pump is often "backed" by backing pumps that are two-stage rotary pumps.

The very low pressure of the mass spectral analysis chamber is designed to create a mean free path for the ions such that there is no gas phase interaction between ions. In a quadrupole mass spec analyzer the direction and velocity of the ion is controlled by a quadrupole consisting of four separate poles (Figure 46). The trajectory down the pathway is the "Z" plane and leads to the detec-

tor with a distance 10 to 15 cm long. Two poles define the X plane and are "tied" together (have the same voltage), while the remaining two poles define the Y plane and are also tied to each other, having an opposite polarity as the X plane poles. An AC field is applied to the poles so that an ion traveling in the center of the poles experiences a fluctuating electric field that alternately drives the cation in the X and then in the Y plane. Small ions will oscillate between the poles. If the frequency with which the AC field changes is too fast, the ions will not immediately respond and will crash into the pole. Large ions do not respond to the AC field, their trajectory is controlled by an offset or DC voltage.

The ion that arrives at the detector is counted individually from all other ions, because of the very low background (10^{-6} mbar pressure!). Combined with the large amplification of each individual ion (10^8), very low limits of detection can be achieved (pp trillion). Typical counts for a 1-ppm solution are 256,000 cps. and the background count is low. A complete scan of masses can be obtained with 100 ms, allowing for co-spectra addition and S/N enhancements.

Resolution between isotopes (Figure 47) is limited by the fact that the background noise (from the plasma flicker and the high argon ion concentration) is changing during the scan. In order to achieve the type of resolution necessary for isotope ratio work for archeological or source provencing of lead, the ICP-MS must be operated in the peak hopping mode. Better yet is the use of multichannel detectors that simultaneously monitor several peaks to be used for the isotope ratio measurements.[175]

Thermal ionization mass spectrometry historically preceeds ICP-MS. The method is more accurate at lower levels of lead and is used extensively within the geological community for the measurement of lead isotope ratios. The continued use of the thermal ionization method is related to the fact that it

Heavy Atoms
Respond Less to
the AC perturbation
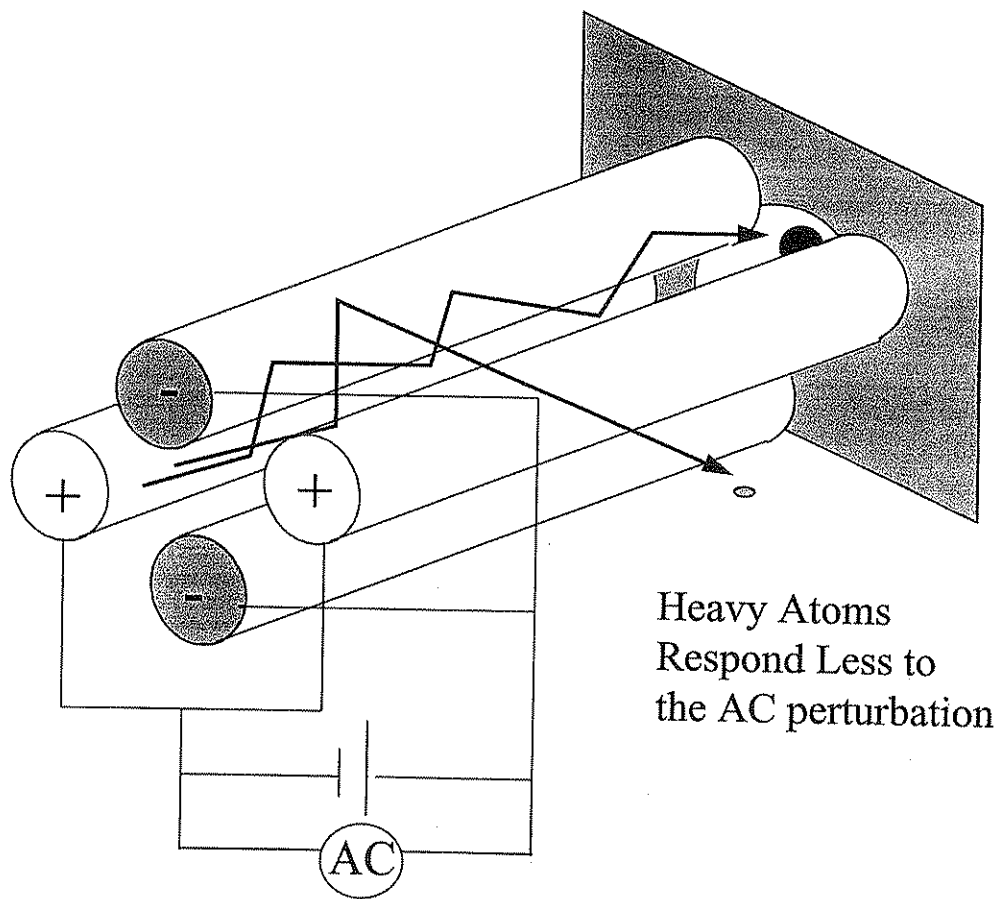
FIGURE 46. Schematic of the quadrupole mass analyzer used in an ICP-MS. Opposing rods are tied together. An oscillating AC bias over a set DC voltage tunes the trajectory of an ion moving in the quadrupole. Light ions responding to the AC voltage will not complete the trajectory of the quadrupole.

is highly selective for metal over hydrocarbons and light gases. It produces the purest ion beams and can be optimally tuned for intense and stable ion beams. Gas phase production occurs within the vacuum chamber. Because ion- and atom-containing vapor is not pulled through an orifice into the mass analyzer, effusion, based on mass, is not as significant a problem. Effusion can result in mass fractionation due to the variable velocity of the atoms through the orifice.[176]

VII. THERMAL ANALYSIS

Given the large number of highly reliable alternative spectroscopic measurements,

thermal analysis of lead is not well developed. One report for leaded gasolines relies on reaction 60 in which a dialkyl dihalogenated lead salt is formed. The heat of this reaction is measured enthalpically with a measurement range of 0 to 2500 ppm.[177]

VIII. CHROMATOGRAPHIC METHODS OF ANALYSIS

A. GC Determination of Tetraethyllead in a Homologous Alkane Series

Tetraethyllead is a component in leaded gasolines. It was introduced in the 1920s.

331
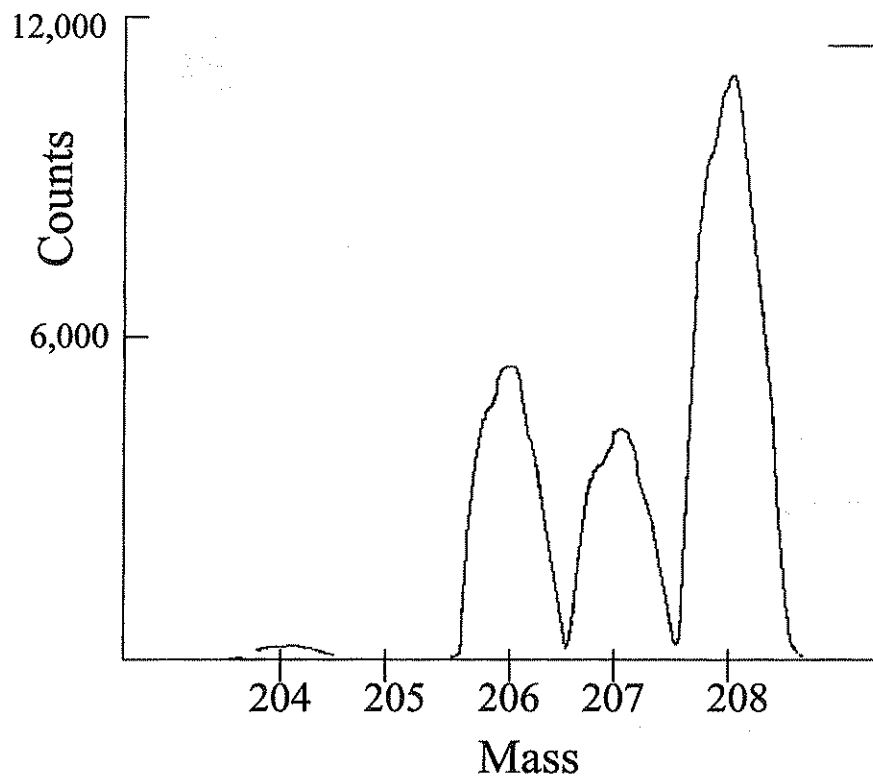
FIGURE 47. A mass spectrum of lead obtained on an ICP-MS showing the four isotope peaks associated with lead.

The role of the tetraethyllead is to scavenge radical species in the gas phase mixture to prevent spontaneous combustion prior to ignition with the spark plug. Spontaneous ignition causes slamming of the pistons in the combustion engine, which results in knocking and in a decreased lifetime of the engine.

$$PbR_4 \rightarrow PbO_2 + RCH_2 \cdot \rightarrow PbO + RCH_2O \cdot \tag{77}$$

$$RCH_2O \cdot + O_2 \rightarrow RCHO \tag{78}$$

$$PbO \rightarrow PbCl_2 \tag{79}$$
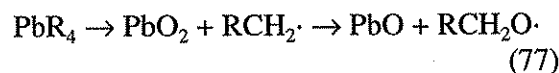
The volatile tetraethyllead mixes well with the gas, but is also unstable. It can convert to lead oxide and scavenge radicals. To prevent deposition of PbO within the engine, a chloride source is added so that lead can be exhausted as a gas. Octane ratings for lead content can be found in the ASTM handbook of 1983, method D2699, which indicates that when no tetraethyllead was added to gasoline the octane rating was 100. The octane rating increased to 120 with the addition of 6 ml tetraethyllead/gallon of gasoline. Typical values of lead with gasoline range from 2.5 to 25 mg/l.

Tetraethyllead has a formula weight of 323.44 amu and a density of 1.653 g/cm³. The boiling point for this low-molecular-weight species is 84 to 85°C at a pressure of 15 mm. Its volatility makes it suitable for use as an amendment in gasolines and contributes to its toxicity via inhalation. As of

1983 a standard method of analysis for tetraethyllead involved a distillation to separate it from other similar species (triethyllead) (ASTM method D1949). The distillate below 133°C contained the more volatile lead alkyls such as tetra*methyl*lead, whereas the distillate above 133°C contained the tetra*ethyl*lead-containing fraction. The lead in these fractions was subsequently measured by dilution with methyl isobutyl ketone, stabilization of alkyl lead with iodine, and quaternary ammonium salts followed by atomic absorption monitored at 283.3 nm (ASTM method D3237).

Current methods utilize the *same chemistry* and sometimes even the same detection.[178] However, distillation for separation is accompanied on a heated column, that is, by gas chromatography. In gas phase chromatography the sample is heated to volatilize the components into the gas phase. The gas phase species join a carrier gas (He or N_2) to travel across a solid phase. The solid phase is usually some silaceous material whose surface has been modified to a desired polarity. The polarity of the surface is given by standard designation such as OV-1, OV-3, OV-17. The designator indicates the decrease of polarity, the larger the number the more polar groups are contained on the surface (Table 35).

As "like dissolves like," a non-polar surface will dissolve non-polar species in the gas phase, retarding their passage. Different species with variable polarity will be differentially retained on the column and will exit the column at different times. (The choice of the stationary phase modifying the solid support depends on solubility considerations and on stability of the stationary phase. The more polar the column (Carbowax) the more unstable the phase.

Gasoline is formed by boiling crude oil and selectively condensing the vapors for prechosen ranges of temperatures. Gasoline is a fraction boiling roughly between 40 and 200°C, while jet fuel is the fraction that boils between 175 and 325°C. The alkanes in gasoline generally have from 5 to 10 carbon atoms. Because it boils between 40 and 200°C, it is suitable for injection into a heated port and transport in the heated column. The retention of its various alkanes should follow the homologous series and can be varied by varying the flow rate, the injection port temperature, and the temperature of the column. Tetraethyl lead should also be separable from the alkanes due to both the boiling point and the polarity of the compound (Table 36). Typical analysis for leaded gasoline is shown in Table 37. Figure 48 shows a GC-AES measurement of organolead compounds, with retention time governed by the chain length on the organo constituent and by the ion present.

B. Preparative Ion Chromatography

Lead has been sensitively separated since the initiation of the nuclear weapons era due

TABLE 35
Common Stationary Supports for GC

Column trade name	Composition	Maximum temp °C
OV-1	Polydimethyl siloxane	350
OV-101	Dimethylsiloxane fluid	
OV-7	Phenylmethyl dimethylsiloxane (20% phenyl; 80% methyl)	350
OV-17	Poly(phenymethyl) siloxane (50% phenyl, 50% methyl)	250
Carbowax	Polyethylene glycol	250

TABLE 36
Boiling Points of Simple Carbon Chains

Compound	Carbons	Boiling point °C
Pentane	5	35–36
Hexane	6	68–70
Heptane	7	98
Octane	8	125–127
Nonane	9	151
Tetraethyllead	8	84–85

to the interest in ^{210}Pb during nuclear testing. In addition, because lead isotope ratios are used in geochronology and because early mass spectral measurements required high purity lead samples, preparative lead separations have been based on anion exchange.[179]

One method first used was that of the lead chloride system (Section II.E). The formation of either a dianionic ($PbCl_4^{2-}$) or anionic ($PbCl_3^-$) species can be achieved when the molarity of the chloride ion is > 1.[180,181] Problems with this method are that the metal complex must remain well intact and be strongly attracted to the column (distribution coefficient, K_D, large) to be retained quantitatively on the column for preparative methods. The K_D value for distribution of chloride lead species onto a Dowex 1X8 column is 30.[182] In 0.5 M HBr, the K_D value

is 821.[183] The change in the distribution coefficient onto a Dowex 1X8 resin is shown in Figure 49.[184] The larger distribution coefficient of the ion complex to the anion exchange column is, in part, related to the larger binding of the lead ion to the bromide ion, consistent with the large size of the bromide ion.

Another example of ion chromatography is the determination of EDTA-Pb using the reaction scheme shown in Figure 50.[185,186] The system relies on the formation of a dianion $Pb(EDTA)^{2-}$ species that is exchanged with the ion exchange column. Detection of the eluting chelate can be made directly to the EDTA, although with low sensitivity or by post-column derivitization using a highly fluorescent cation species that ion pairs with the lead complex.

C. Ion Pair Chromatography (HPLC)

EDTA-Pb measurements can be made by an ion pairing mechanism similar to that of the post-column derivitization reaction. The chelated species ion paired to a quaternary ammonium species with alkyl chain can be retarded on an organic phase column. The general scheme is shown in Figure 50.

TABLE 37
GC Analysis for Tetraethylleaded Gasoline

Source	Patterson	Brunetto	Lobinski
Column	6 ft × 2 mm i.d. glass column	1 m × 0.08 in i.d. glass column	25 m × 320 μm i.d.
Stationary Phase	4% SP2100 (Supelco)	3% OV-101 on Chromosorb W (60–80 mesh)	Liner: Deactivated silica, 20-mm Tenax coated with 3% OV-101
Carrier Gas	N_2 at 20 ml/min	N_2 at 30 ml/min	He, 300 cm³/min
Temperature injection		180°C	5°C
Temperature column	60–180°C programmed	50–200°C programmed at 8°C/min	2°C/s to 25, hold 2 min increase 12°C/s to 230°C hold for 1 min
Detector	Flame ionization	Atomic absorption	Atomic emission
t_m for tetraethyllead		4 min	8.5 min
Detection limit (ng)		0.25 ng	0.1 ng/dm3 = 0.1 ng/l = 0.1 pg/ml

FIGURE 48. Chromatogram obtained using GC-AES of a mixture of propylated organolead standards (3 to 4 pg each) obtained with a Tenxax-packed liner after 60 s solvent venting: (1) Me_3Pb^+; (2) Me_2Pb^{2+}; (3) Et_3Pb^+; (4) Et_2Pb^{2+}; and (5) Pb^{2+}. Emission intensity measured in arbitrary units. (From R. Lobinski, F. C. Adams, *J. Anal. Atomic Spectrometry*, 1992, **7**, 1987.)
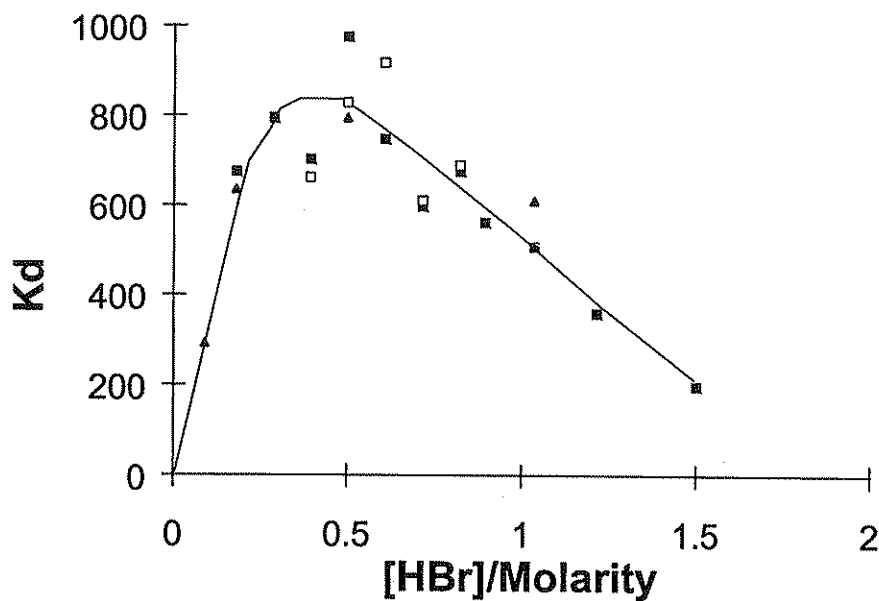
FIGURE 49. Distribution coefficient, K_D, of Pb between anion-exchange resin and HBr as a function of HBr molarity [open circles = Dowex 1 × 8, 200-400 mesh; closed circles = Amberlite) RA 900, 16 to 20 mesh]. Kraus, K. A. In: Proc. 1st Int. Conf. Peaceful Uses Atomic Energy, Geneva, 1955, **7**: 113–125.

FIGURE 48. Chromatogram obtained using GC-AES of a mixture of propylated organolead standards (3 to 4 pg each) obtained with a Tenxax-packed liner after 60 s solvent venting: (1) Me_3Pb^+; (2) Me_2Pb^{2+}; (3) Et_3Pb^+; (4) Et_2Pb^{2+}; and (5) Pb^{2+}. Emission intensity measured in arbitrary units. (From R. Lobinski, F. C. Adams, *J. Anal. Atomic Spectrometry*, 1992, **7**, 1987.)
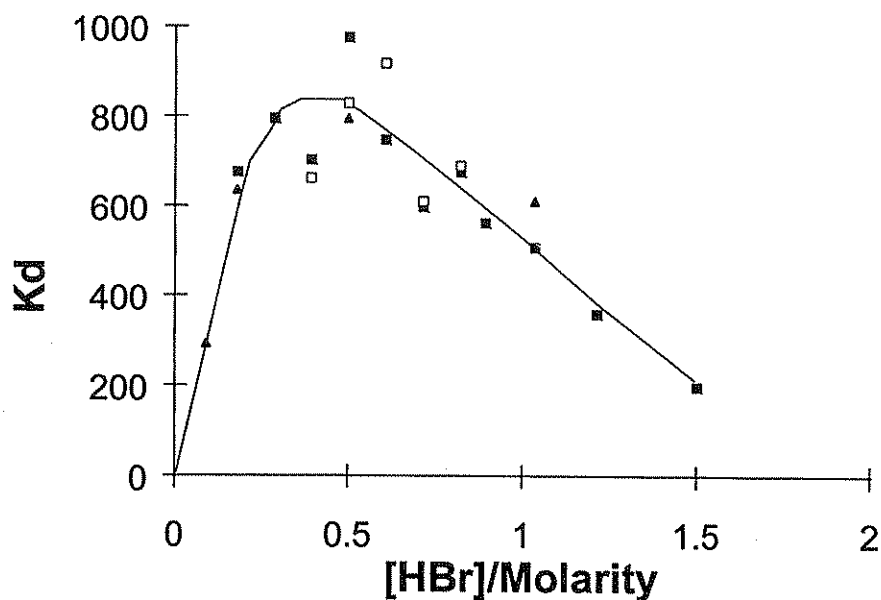
FIGURE 49. Distribution coefficient, K_D, of Pb between anion-exchange resin and HBr as a function of HBr molarity [open circles = Dowex 1 × 8, 200-400 mesh; closed circles = Amberlite) RA 900, 16 to 20 mesh]. Kraus, K. A. In: Proc. 1st Int. Conf. Peaceful Uses Atomic Energy, Geneva, 1955, **7**: 113–125.

FIGURE 50. (A) Schematic of Ion chromatography. (B) Schematic of Ion pair chromatography.

EDTA and other complexes have absorption maximum in UV. The peak depends on the metal ion.[187,188,189,190,191,192,193] For example, Pb is observed at 240 nm and that of Bi at 270 nm.[194] The absorbance of the complex maximizes at a 1:1 molar ratio even in the presence of excess chelate.[195] Lead-chelate was monitored at 242 nm. The shift in the absorption band of the free EDTA from the lead EDTA from <220 to 240 nm is most likely due to a perturbation of the nonbonding electrons on the nitrogens in the EDTA complex by the lead cation. Using 254 nm as a detection wavelength (Pb-EDTA has a tail that extends to 260 nm) EDTA complexes are monitored for Cr(III), Fe(III), Ni(II), Cu(II), Mn(II), and Pb(II).

The separation of these species is accomplished by ion pairing mechanism.[196] The reactions are (where EDTA chelate is denoted H_4Y)

$$H_4Y \rightleftarrows H_2Y^{2-} + 2H^+ \tag{80}$$

$$H_2Y^{2-} + 2Na^+ \rightleftarrows Na_2H_2Y \tag{81}$$

$$Pb^{2+} + Na_2H_2Y \rightleftarrows PbNa_2Y \tag{82}$$

$$PbNa_2Y + 2TMA^+ \rightleftarrows Pb(TMA)_2Y \tag{83}$$
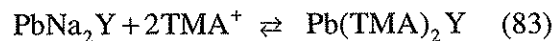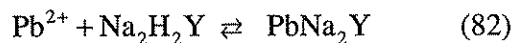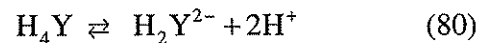
Reactions [80] and [81] are simply the pH equilibria of the chelate in a sodium salt matrix. At pH 7 all of the protons should be lost to give Y^{4-}. When lead chelates with the complexes (reaction [82]) a dianion is then formed, shown compensated with two sodium ions. Finally, in reaction [83] the compensating ions become the organic cation tetramethylammonium. It is this reaction that provides solubility of the complex in the C-18 chain stationary phase on the ODS column.

Depending on the kinetics of the reactions and the distribution onto the stationary phase (Figure 51), the polarity of the overall ion pair complex, the various metal ion chelates exit the column at different times, thus providing separation of the chelates (Figure 52).

Lead can be separated on a liquid chromatographic column based on the same type

of chemistry as explored for EDTA and dithizone extractions. At least two methods have been proposed. In one method the sample is reacted with a chelate (diethyldithiocarbamate) DEDTC, which is separated onto a octadecylsilica gel and monitored via UV-Vis spectroscopy.[197,198] The chemistry exactly parallels that of the dithizone chemistry.

Columns can also be made that directly chelate the lead, relying on the rather precarious selectivity of the chelate. One such method is the immobilization of the chelate PAR to a solid phase that should give the desired selectivity.[199]

IX. SAMPLE PREPARATION

In all of the above methods the sample has to be prepared. This generally consists
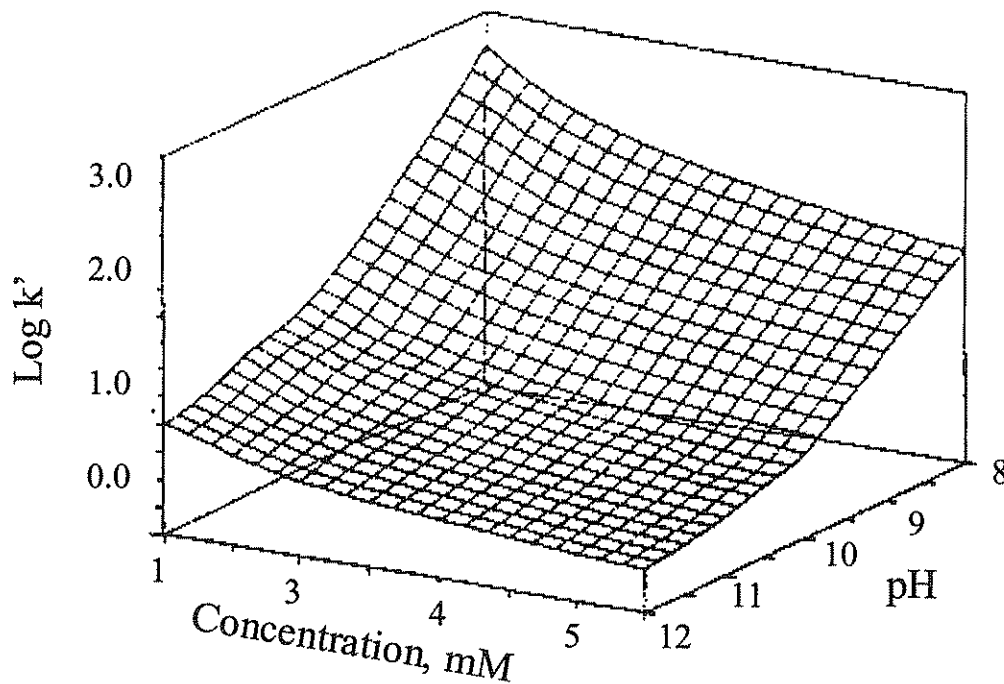
FIGURE 51. Calculated retention surface for the anionic PbEDTA complex eluted with HCO_3^-- CO_3^{2-} buffer (conc. - $[HCO_3^-] + \{CO_3^{2-}\}$). (From P. Hajos, G. Revesz, O.Horvath, J. Peear, C. Sarzanin, J. Chrom. Sci. 1996, **34**, 291.)

Cl⁻

NO₃⁻

PbEDTA²⁻

ZnEDTA²⁻

CuEDTA²⁻

AcO

Retention Time, Min
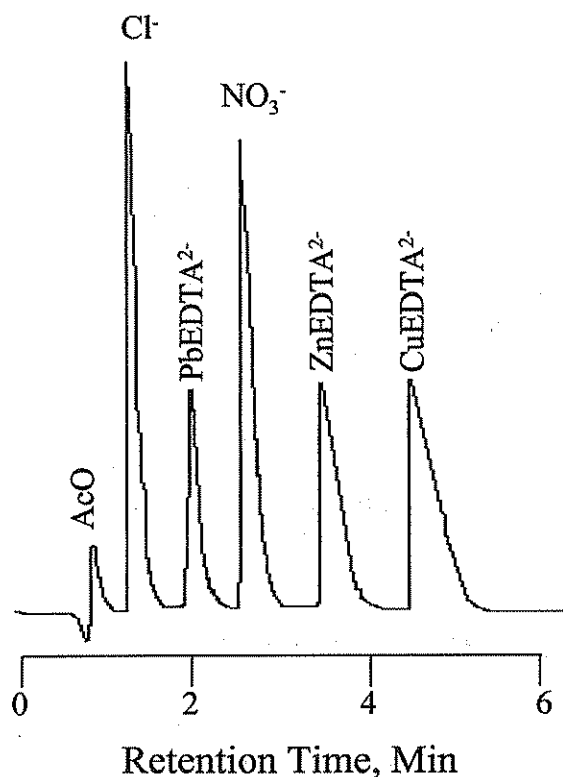
FIGURE 52. Chromatogram of anionic metal-EDTA complexes and simple anions obtained by using carbonate eluent ((conc. $[HCO_3^-] + [CO_3^{2+}] = 3.5$ mM, CO_3^{2-}-$HCO_3 = 2.0/1.5$). The pH was 10.4, the sample volume was 50 μl, and a conductivity detector was used. (From P. Hajos, G. Revesz, O. Horvath, J. Peear, C. Sarzanin, *J. Chrom. Sci.* 1996, **34**, 291.)

of a digestion of the sample, particularly because most of the systems of interest consist of insoluble matrices containing lead. Sample preparation involves breaking apart the compound into its constituent parts to soluble or gas phase species. In some cases the sample can be oblated directly into the instrument, such as laser desorption for gases into GFAA or the ICP-MS. Many matrices have a large organic component (soil humic materials, blood, bones, plant materials, etc.). In these samples it is tempting to first ash the sample prior to digestion; however, care should be exercised for cross-contamination by vapor and/or loss of lead-containing vapor. For digestion two methods are prevalent,

the hot plate digestion and the microwave digestion.

A. Dry Ashing

Dry ashing was used extensively in the early literature for removal of organic materials from inorganic matrices. Thus, the determination of lead in bone may have begun with a dry ashing to remove organics, followed by a digestion. There has been some concern about loss of the lead from more volatile species (lead chlorides) on ashing. The amount of lead lost depends on the temperature at which ashing occurs. Typical ashing is at 500°C where organics can be burned and driven off. Lead as lead chloride melts at 500°C and can have a significant vapor pressure that could cross-contaminate multiple samples within an oven. A second problem with dry ashing is the deposition of lead chlorides and/or oxides into the furnace and re-volatilization from batch to batch.[200,201] An example of the expected vapor pressures for the chlorides is given in Section III.A.

B. Hot Plate Acid Digestion

Table 38 gives the oxidation states of Cl and N and is used to demonstrate that HNO_3 when compared with HCl is useful in digestions because it acts not only as an acid source but to oxidize the sample. An examination of the structure of nitrate leads to the prediction that the product of the reduction of nitrate would be NO_2, and from this the potential of the conversion of nitrate to NO could be computed to be +0.96.

In addition to being a more reactive acid, there was the advantage of the remaining sample matrix. The nitric acid digestion leaves a nitrate matrix that can be decomposed at relatively low temperatures to stable metal oxides (see graphite furnace dis-

TABLE 38
Oxidation states of Cl and N

Oxidation state	Nitrogen	Chlorine
−3	NH_3	
−2	N_2H_4	
−1	NH_2OH	HCl
0	N_2	Cl_2
+1	N_2O	$HOCl$
+2	NO	
+3	N_2O_3	$HOClO$
+4	NO_2	
+5	HNO_3	$HOClO_2$
+6		
+7		$HOCl_3$

cussion), while the chlorides sublimate easily. Lead will easily remain in solution with the chlorides due to complexation chemistry. Thus, depending on whether the subsequent method of analysis contains a heating component in which the lead chlorides are lost, it may be analytically superior to perform a nitric acid digestion.

HF digestions are even more vigorous and are used when the absolute total amount of lead locked into crystalline material is required.

C. Microwave Digestions

Microwave digestion[202] has been approved recently by the EPA. The advantages of microwave digestion is the rapid time (30 min) for digestion similar to the hot-plate method. Hot-plate digestion requires conduction of heat and energy through the walls of the vessel, and heat is distributed throughout the solution through convection or thermal gradients, providing poor homogeneity to the process. Microwave energy heats the entire sample uniformly, allowing a full boiling throughout the sample.

Closed vessel microwave digesters generate higher temperatures and pressures than in open vessel digesters. The SPEX CDS 7000 system allows for pressures up to 220 psi and temperatures of 200°C. For the purposes of control, the pressure sensors are designed into the lid of the vessel. Further precautions involved the use of a disposable PFA rupture disc, which will break when pressure ratings are exceeded.

Acids can reach a much higher temperature in the closed vessel than in open air vessel. Thus, nitric acid alone (as opposed to HF) can be used to achieve a more efficient digestion. Sulfuric acid, however, should be avoided because the polymeric materials of the vessel may melt at the boiling point of sulfuric acid.

Sample size should be small in order to avoid gas evolution of organic-containing materials. Two gram samples are used for inorganics (low organic matter soils), 1 g for organics, and 50 ml for liquids.

In the SPEX 7000 closed digestion system (CDS), recommended digestions are shown in Table 39.

TABLE 39
Settings for Microwave Digestion of Lead in Various Materials

Material	Amount	Reagent	Time
Glass air filter	1.09 g	HF HCl HNO_3	30 min
Kaolin clay	0.49 g	HF HCl HNO_3	22 min
Latex paint	0.23 g	HNO_3	30 min
Soil (EPA 3051)	0.5 g	HNO3	10 min
Water (EPA 3015)	45 ml	HNO_3	20 min

D. Direct Vapor Production

For methods that rely on a gas phase measurement (atomic absorption, atomic emission, atomic fluorescence, mass spectrometry, gas chromatography), it is possible to bypass the ash (digestion), step. A good example is laser induced breakdown spectroscopy (LIBS) in which a focused laser beam produces a plasma that is swept into the atomic emission unit. A similar method has been used to couple the ICP-MS to fiber optic imaging of samples.

REFERENCES

1. Gilbert, T. W. In: Treatise on Analytical Chemistry. Part II: Analytical Chemistry of the Elements, Vol. 6, Ed. I. M. Kolthoff, P. J. Elving, John Wiley and Sons, 1964, p. 153

2. Hoffman, W. A. and W. W. Brandt, Anal. Chem. 1956, 28, 9, 1487-1489.

3. Accum, F. C., A Treatease on the Adulteration of Food and Culinary Poisons Exhibiting Fraudulent Sophistications of Bread, Beer, and Wine, London, 1820.

4. Askin, D., Alvarez, B., Occuptaional Health and Safety, Feb. 1993, 34.

5. Hancock, R. D., Shaikjee, M. S. Dobson, S. M. Boeyens, J C A, Inorg. Chim. Acta., 1988, 154, 229.

6. Hegetschwecler, K., M. Ghisletta, and V. Gramlich, Inorg. Chem. 1993, 32, 2699-2704.

7. Caruso, F., M. L. Chan, M. Rossi, Inorg. Chem. 1997, 36, 3609-3615.

8. Abu-Dari, Kamal, T. B. Karpishin, and K. N. Raymond, Inorg. Chem. 1993, 32, 3052-3055.

9. Rogers, R. D. And A. H. Bond, Inorg. Chim. Acta, 1992, 163-171.

10. Drew, M. G., B.,; D. G. Nicholson, I. Sylte, A. K. Vasudevan, Acta Chem. Scan. 1992, 46, 396-398.

11. Nicholson, D. G., I Sylte, H. K. Vasudvan, L. J. Saethal, Acta Chem. Scan. 1992, 358-362.

12. Hayashita, T., K. Yamasaki, Z. Huang, and R. A. Bartsch, Chem. Lett. 1993, 1487-1490.

13. Hiratani, K., T. Takahashi, H. Sugihara, K. Kasuga, K. Fujiwara, T. Hayashita, and R.A. Bartsch, Anal. Chem. 1997, 69, 3002-3007.

14. Fabri, G. and N. Castellino in Inorganic Lead Exposure, Ed., Castellino, N., P. Castellino, N. Sannolo, Lewis Publishers, 1995, p. 257-278.

15. Rivera, M., Zheng, W. Aposhian, H. V., and Fernando, Q. Toxicol. Appl. Pharmacol, 1989, 100, 96-106.

16. Fang, X. And Q. Fernando, Chem. Res. Toxicol. 1994, 7, 770-778.

17. Fang, X. And Q. Fernando, Chem. Res. Toxicol., 1994, 7, 148-156.

18. Welcher, F. J., The Analytical Uses of Ethylenediamine Tetraacetic Acid, D. Van Nostrand Co., Inc., Princeton, N. J., 1958,, xv.

19. Flaschka, H. A., EDTA Titrations, An Introduction to Theory and Practice, Pergamon Press, Oxford, 1964., 16 and 64.

20. McConnell, A. A. Nuttall R. H., Spectrochim. Acta, 1977, 33A, 459-462.

21. Sawyer, D. T., Paulsen, P. J. J. Am. Chem. Soc., 1959, 81, 816-820

22. Langer, H. G., J. Inorg. Nucl. Chem. 1964, 26, 767-772.

23. Khosraviani, M., A. R. Pavlov, G. C. Flowers, and D. A. Blake, Env. Sci. Tech., 1998, 32, 137-142.

24. Goncalves, M. De L. S.,L. Sigg, L. Stumm, Env. Sci. Tech. 1985, 19,141-146.

25. Feldman, B. J., J. D. Osterloh, B. H., Hates, and A. D'Aessandr., anal. Chem. 1994, 66, 1983-1987.

26. Aldstadt, J. H., and H. D. Dewalt, Anal. Chem., 1992, 64, 3176-3179.

27. Liu, T. Z., D. Lai, and J. D. Osterlosh, Anal. Chem., 1997, 69, 3539.

28. Desimoni, E., Palmisano, F., L. Saboatini, 1980, Anal. Chem., 52, 1889.

29. Neeb R., and I. Kiehnast, 1967, Anal. Chem., 241, 1142-145.

30. Pretty, J. R. And J. A. Caruso, J. Anal. Atom. Spectros. 1993, 545.

31. Bott, A. W. Current Separations, 1995, 14:1.

32. Feinberg, J. S. And W. J. Bowyr, Microchemical J. 1993, 47, 72-78.

33. Pawlak, M. K., Czech. Chem. Comm. 1993, 58, 291.

34. Opperman, J. H., J. F. Van Staden, R. G. Bohma, S. Afr. Tydskr Chem. 1988, 41, 1.

35. Peter, Ray, and N. Andersen, Anal. Chim. Acta, 1998, 368, 3, 191.

36. Jayaratna, H. G., C. S. Brintlett, P. T. Kissinger, Anal. Chem. Acta., 1996, 332, 165-171.

37. Jayaratna, H. G., Anal. Chem. 1994, 66, 18, 2985.

38. Limson, J. T. Nyokou, Anal. Chim. Acta, 1997, 344, 87-95.

39. Adebju, S. B., A. M. Bond, and M. N. Briggs, Anal. Chem. 1985, 57, 1386.

40. Olsen, K. B., J. Wang, R. Setladji, and J. Lu, Env. Sci. Tech., 1994, 28, 2074-2078.

41. Zen, J. M. and S. Y. Huang, Anal. Chim. Acta, 1994, 294, 77.

42. Hu, Z., C. J. Seliskar, W. R. Heineman, Anal. Chim. Acta. 1998, 369, 93-101.

43. Prabbu, S. V., R. P. Baldwin, L. Kryger, Electroanlaysis, 1989, 1, 13.

44. Arden, J. W. And N. H. Gale, Anal. Chem. 1974, 46, 1, 2-9.

45. Fleischmann, M. And M. Liler, Trans. Faraday Soc., 1958, 54, 1370.

46. Hertelendi, L., Z. Anal. Chem., 1941, 122, 30.

47. Linsey, A. J., Analyst, 1935, 60, 598.

48. Noble, D., Anal. Chem. 1993, 65, 267A.

49. Wang,J., B. Tian, Anal. Chem., 1992, 64, 1706-1709.

50. Wang, J., B. Tian, Anal. Chem., 1993, 65, 1529-1532.

51. L. K. Shpigun, O. V. Basanova, and Y.A. Zolotov, Sensors and Actuators,B, 10, 1992, 15-20.

52. Kamata, S. And K. Onoyama, Anal. Chem. 1991, 63, 1295-1297.

53. Deval, A. And J. Sneddon, Microchemical Journal, 1995, 52, 96-100.

54. Bass, D. A. and J. A. Holcombe, Anal. Chem., 1988, 60, 578-582.

55. Bass, D. A. and J. A. Holcombe, Anal. Chem., 1987, 59, 974-980.

56. Deval, A. And J. Sneddon, Microchemical Journal, 1995, 52, 96-100.

57. Eloi, C., C., J. D. Robertson, V. Majidi, Anal. Chem., 1995, 67, 335-340.

58. McLaren, J. W., Wheeler, R. C., Analyst, 1977, 102, 542.

59. Imai, S., Y. Hayashi, Anal. Chem., 1991, 63, 772-775.

60. Dabeka, R. W. Anal. Chem., 1992, 64, 2419-2424.

61. Dedena, J. and D. L. Tsalver, Hydride Generation Atomic Absorption Spectroscopy, Wiley and Sons, 1995, 130, 288-307.

62. Fleming, D. E.and G. A. Taylor, Analyst, 1978, 103, 101-104.

63. Li, J., Y. Liu, and T Lim, Anal. Chem. Acta., 1990, 231, 151-155.

64. Madrid, Y., M. Bonilla, and C. Camara, Analyst, 1990, 115, 563-565.

65. Madrid, Y., J. Meseguer, M. Bonilla, C. Camara, Anal. Chim. Acta, 1990, 237, 181-187.

66. Sanz, J., P. Basterra, J. Galban, J. R. Catillo, Microchem. J., 1989, 40, 115-124.

67. P. N. Vijan, and G. R. Wood, Analyst, 1976, 966-974.

68. Lead Chemicals, International Lead Zinc Research Organization, Inc.,N.Y., 1973

69. Willard, H. H., L. L. Merritt, Jr., J. A. Dean, F. A. Settle, Jr., Instrumental Methods of Analysis, 7th Ed., Wadsworth Publishing Co., Belmont, Ca.

70. Azeredo, L. C., R. E. Sturgeon, A. J. Curtiss, Spectrochim. Acta., 1993, 46B, 1, 91-98.

71. Beinrohr, E., Cakrt, M. Rapta, M. Tarapic, P., 1989, Fres. Z. Anal. Chem., 335, 1005-1007.

72. Creed, J., Martin, T. Lobring, and J. O'Dell, Env. Sci. Tech., 1992, 26, 102-106.

73. Fang, Z., Sperling, M. Welz, B., 1990, J. Anal. At. Spectrom. 5: 639.

74. Holak, W., Anal. Chim. Acta., 1975, 74, 216.

75. Lau, O. W., and K. L. Li, Analyst, June, 1975, 100, 430.

76. Porta, V., Abollino, O., Meritasti, E., Szrzanim, C., 1991, J. Anal. At. Spectr. 6, 119-122.

77. Sperling, M., X. Yin, B. Wetz., Fres. Z. Anal. Chem., 1992, 343, 6754.

78. Doidge, P. S., Spectrochim. Acta, 1991, 46B, 1776-1787.

79. Zong, Vam Y., Parsons, P.J., and Slavin, W., Spectrochim. Acta, 1994, 49B, 1667-1680.

80. Wibetoe, G. Langmyhr, Anal. Chim. Acta., 1986, 186, 155-162.

81. Ohta, K., H. Taniguti, S.I. Itoh, T. Mizuno, Mikrochim. Acta., 127, 51-54. 1997.

82. Moenke-Blankenberg, L. in Lasers in Anal. Atom. Spectroscopy, Ed. J. Sneddon, T. L. Thiem, Yill Lee, VCH Publishers, 1997, p. 125, N.Y. N.Y.

83. Varma, Asha, CRC Handbook of ICP-AES, 1991, CRC Press, p. 68, Boca Raton, Fla.

84. Wisbrun, R., R. Niessner, H. Schroder, Anal. Methods and Instrumentation, 1993, 1,1, 17-22.

85. Marquardt, B. J., S. R. Goode, S. M. Angel, Anal. Chem., 1996, 68, 977-981.

86. Cremers, D. A., Applied Spectroscopy, 1987, 41, 4, 572-579.

87. M. A. Bolshov, C. F. Boutron, and A. V. Zybin, Anal. Chem., 1989, 61, 1758-1762.

88. Cheam, V.; J. Lechner, I. Sekerka, R. Desrosiers, J. Nriagu, and G. Lawon, Anal. Chim. Acta., 1992, 269, 129-136.

89. Neuhauser, R.E., Panne, U., R. Niessner, G. A. Petrucci, P. Cavalli, and N. Omenetto, Anal. Chim. Acta., 1997, 347, 37-48.

90. Ueno, K., and T. Imamura, "Chelating Reagents with Sulfur Functions, CRC Handbook of Organic Analytical Reagents, 2nd Ed.

91. Irving ,H. M. N. H., "Dithizone" 1977, The Chemical Society.

92. Sandell, E. B. Colorimetric Determination of Traces of Metals, Interscience Publishers, N.Y., 1950

93. Rupainwas, D. C., Anal. Chem. Acta., 1969, 48, 187-188.

94. Kassim, A. Y., Inorg. Chim. Acta, 1978, 27, 243-248 and 1978, 29, 237-241.

95. Irwing, H. M. N. H., D. C. Rupainwas, S. S. Salota, Anal. Chem., 1969, 45, 249-254.

96. Irwing, H. M. N. H., A. M. Kiwan, D. C. Rupainwas, S. S. Sahota, Anal. Chim. Act., 1971, 56, 205-220.

97. Murcia, N. S., E. G. Lundquist, S. O. Russo, D. G. Peters, J. Chem. Ed., 1990, 67, 7, 608.

98. Lerchi, Markus, E. Bakker, B. Rusterholz, and W. Simon, Anal. Chem. 1992, 64, 1534-1540.

99. Bakker, E., M. Willer, and Erno Pretsch, Anal. Chim. Acta., 1993, 282, 265-271.

100. Blatt, E., W. H. F. Sasse, A. W. H. Mu, J. Phys. Chem., 1988, 92, 4151.

101. Dederer, J.C., M. Van der Auweraer and F. C. De Schryve, J. Phys. Chem., 1981, 85, 1198.

102. Cabaniss, S. E., Env. Sci. Tech., 1996, 26, 1133.

103. Susetyo, W., L. A. Carreira, L. V. Azarraga, D. M. Grimm, F. J. Anal. Chem., 1991, 339, 624.

104. Saar, R. A. And J. A. Weber, Anal. Chem., 1980, 52, 2059.

105. Sanz-Medel, A., D. Blanco Gomis, E. Fuente, and S. Arribis Jimeno, Talanta, 1984, 31, 7, 515-519.

106. Bourson, J., F. Badcioni, B. Valeur, J. Fluorescence, 1994, 4, 4, 275-277.

107. Moore, M. R., A. Goldberg, A. A. C. Yeung-Laiwah, Annals of New York Academy of Sciences, p. 191.

108. Chisholm, J. J., and J. H. Brown, Clin. Chem., 1971, 21, 1669.

109. Piomelli, S., C. Seaman, D. Zullow, A. Curran, B. Davidow, Proc. Nat'l Acad. Sci., USA, 1982, 79, 3335.

110. Chisholm, J. J. and D. H. Brown, Biochem. Med., 1979, 22, 214-237.

111. Lamola, A. A., M. Joselow, T. Yamane, Clin. Chem. 1975, 21/1, 93-97.

112. Hanna, T. L., Dietzler, D. N., Smith, C. H., Gupta, S., Zarkowsky, H. S., Clin. Chem., 1976, 22, 161.

113. Sassaroli, M., R. da Costa, H. Vaananen, J. Eisinger, Cytometry, 1992, 13, 339-345.

114. Manceau, A., M. C. Boisset, G. Sarret, J.L. Haxemann, M. Mench, P. Cambier, and R. Prost, Env. Sci. Tech., 1996, 30, 1540-1552.

115. Raspberry, S. D., Appl. Spec. 1973, 27, 2, 102.

116. Schneider, J. F., J. Lee, Jayne Dolph, C. W. Dickhut, A. Bohm, Characterization of Heavy Metal Contamination in Soil Using Portable X-Ray Fluorescence and Hyperspectral Remote Sensing, 4th International Conference On-Site analysis, Orlando.

117. Zellmer, S. D. And J. F. Schneider, Argonne National Lab, ESD/TM-59, 1993.

118. M. Sperling, X. Yin, B. Wetz., Frenz. J. Anal. Chem. 1992, 343, 754.

119. Pyle, S. M., J. M. Nocerino, S. N. Deming, J. A. Palasota, J. M. Palasota, E. L. Miller, D. C. Hillman, C. A. Kuharic, W. H. Cole, P. M. Fitzpatrick, M. A. Watson, and K. D. Nichols, Env. Sci. Tech. 1996, 30, 204-213.

120. Argyraki, A., M. H. Ramsey, P. J. Potts, Analyst., 1997, 122, 743-749.

121. Freimann, P. and D. Schmidt, 1989, Spectrochim. Acta, 44B, 5, 505.

122. Michaelis, W., Fres. Z. Anal. Chem., 1986, 324, 662-671.

123. Muia, L. and R. Van Grieke, Anal. Chim. Acta., 1991, 251, 177.

124. Prange, A., A. Knochel, and N. Michaelis, Anal. Chim. Acta, 1985, 172, 79.

125. Tolg, G. and R. Klockenkamper, Spectrochim. Acta., 48B, 2, 111, 1993.

126. Nilsson, U., R. Attewell, J. O. Christofferson, A. Schutz, L. Ahlgren, S. Skerfving, S. Maltson, Pharm. And Toxic., 1991, 69, 477-484.

127. Schutz, A. , S. Skerfving, S. Mattson, J.-O. Christofferson, L. Ahlgren, Arch. Env. Health, 1987, 42, 6, 340.

128. Bellinger, D., H. Hu, L. Titlebaum, and H. L. Needlleman, Arch. Of Env. Health, 1994, 49, 2, 98.

129. Hu, Howard, S. Korrick, J. Am. Med. Ass. 1994, 272, 19, 1512.

130. Watanabe, H., Hu, H., A. Rotnitzky, Am. J. Ind. Med., 1994, 26: 255-264.

131. Hu, H., Aro, A., Payton, M., Korrick, S., Sparrow, D., Weiss, S.T., A. Rotnitzky, JAMA, 1996, 275, 15, 1171.

132. Goldman, R. H., R. White, S. N. Kales, and H. Hu, Am. J. Ind. Med., 1994, 25, 417-424.

133. Erkkila, J., R. Armstrong, V. Riihimaki, D. R. Chettle, A. Paakkari, M. Scott, L. Somervaille, J. Starck, B. Kock, A. Aitio, Brit. J. Ind. Med., 1992, 49, 631-644.

134. Schutz, A., S. Skerfving, J. Ranstam, J-O. Christoffersson, Scan. J. Work Environ. Health, 1987, 13, 221-231.

135. Schutz, A., S. Skerfving, J. O. Christoffersson, I. Tell, Sci. Of the Total Env. 1987, 61, 201-209.

136. Somervaille, L., Chettle, D., Scott, M. 1985, 30, 929-43.

137. Bode, Hans, R. J. Brodd and K. V. Kordesh, Lead Acid Batteries, The Electrochemical Society, Wiley and Sons, N. Y., 1977., p. 196.

138. Nakamoto, K. Infrared and RamanSpectra of Inorganic and Coordination Compounds, 4th Ed., 1986, Wiley, N. Y.

139. Krishan, K. And R. A. Plane, J. Am. Chem. Soc., 1968, 90, 12, 3195

140. Morris, M. L. And D. H. Busch, J. Am. Chem. Soc., 1954, 78, 5178.

141. McConnell, A. A. And R. H. Nuttal, Spectrochim. Acta., 1977, 33A, 459-462

142. Sievers, R. E. And J. C. Bailar, J. Inorg. Chem., 1962, 1, 174.

143. R. E. Sievers and J. C. Bailar, J. Inorg. Chem., 1962, 1, 174

144. M. L. Morris and D. H. Busch, J. Am. Chem. Soc., 1956, 78, 5178

145. A. A.McConnell and R. H. Nuttal, Spectrochim. Acta., 1977, 459-462

146. Clark and Gibbs, Chem. Comm. 1997, 1003.

147. Gibbs, Seddon, Brovenbo, Petrosym, R. J. H. Clark, J. Raman Spectrosc. 1997, 28, 91

148. Crane, L. G., D. Wang, L. M. Sears, B. Heyns, and K. Carron, Anal. Chem., 1995, 67, 360-364.

149. Hanna, M. W., Quantum Mechanics in Chemistry, 2nd Ed., W. A. Benjamin Inc., 1969.

150. Jameson, C. J. And J. Mason, in Multinuclear NMR, Ed. J. Mason, Plenum Press, N. Y., 1987, p. 51- 88.

151. Wrackmeyer, B., C. Stader, and K. Horchler, J. Of Mag. Res. 1989, 83, 601-607.

152. Cox, R. H., J. Mag. Res. 1979, 33, 61-70.

153. Wrackmeyer, B. J. Mag. Res. 1981, 42, 287-297.

154. Wrackmeyer, B. J., J. Mag. Res. 1985, 61, 536-539.

155. Wrackmeyer, B., C. Stader, K. Horchler, H. Zhou, D. Schlosser, Inorg. Chim. Acta, 1990, 176, 205- 21

156. Dean, P. A. W., Can. J. Chem. 1983, 61, 1795.

157. Pannell, K. H., J. M. Rozell, S. Cortez, and R. Kapoor, Organometallics, 1990,9, 1322-1324.

158. Kennedy, J. D. And W. McFarlane, in Multinuclear NMR, Ed. J. Mason, Plenum Press, N.Y., 1987, p. 305-333.

159. Kennedy, J. D., W. McFarlane, and G. S. Pyne, J.C.S. Dalton, 1977, 2332.

160. Kim, K. S. And P. J. Bray, J. Mag. Res. 1974, 16, 334-338.

161. Neue, G., C. Dybowski, M. L. Smith, and D. H. Barich, Solid State NMR, 1994, 3, 115.

162. Fujiwara, S., Y. Ogimura, and K. Nagashima, 1968, Chemical Instrumentation, 1(1), 21-32.

163. Barbieri, G. And f. Taddei, J. C. S. Perkin II, 1972, 262.

164. Kennedy, J. D., W. McFarlane, B. Wrackmeyer, 1976, 15, 6,1299.

165. Sayer, T. L., S. Backs, C. A. Evans, E. K. Millar, D. L. Rabenstein, Can. J. Chem, 1977, 55, 3255.

166. Harrison, P. G., M. A. Healy, and A. T. Steel, Inorganic Chimica Acta, 1982, 67, L15-16.

167. Rabenstein, D. L. JACS, 1971, 93:12, 2869.

168. Nier A. O., Phys Rev. 1939, 55, 153.

169. Nier, A. O., R. W. Thompson, and B. F. Murphey, Phys. Rev. 1941, 160, 112.

170. Gilman, H. And R. G. Jones, J. Am. Chem. Soc., 1951, 72, 1760.

171. Richards, J. R. Microchim. Acta. 1962, 620.

172. Miller, P. E. And M. Bonner Denton, J. Chem. Ed., 63, 617, 1986.

173. Gray, A. L. And J. G. Williams, J. Anal. Atomic Spectrometry, 1987, 2, 599.

174. Hutton, R. C. And A. N. Eaton, J. Anal. Atomic Spectrometry, 1987, 2, 595.

175. Beary, E. S. And P. J. Paulsen, Anal. Chem., 1995, 67, 3193-3201.

176. Habfast, K. In Modern Isotope Ratio Mass Spectrometry, Wiley, 1997, 11-82.

177. Bark, L. S. And A. Garba, J. Of Thermal Analysis, 1997, 48, 925-935.

178. Huitink, G. M., D. P. Poe, and H. Diehl, 1979, Talanta, 21, 1221.

179. Bolsho, M.A; C. F. Boutron, A. V. Zybin, Anal. Chem., 1989, 61,1758.

180. Chen, J. H., and G. J. Wasserbury, Anal. Chem., 1981, 53, 2060-2067.

181. Roddick, J. C., W. D. Loveridge, and R. R. Parrish, Chemical Geol. 1987, 66, 111-121.

182. Kraus, K. A. And Nelson, IN: Proc. 1st Int. Conf. Peaceful Uses At. Energy, Geneva, 1955, 7: 113- 125.

183. Strelow, F. W. E., 1978, Anal. Chem. 54, 827A-832A.

184. Manton, W. I., Chem. Geol., 1988, 73, 147-152.

185. Ye, L. And C. A. Lucy, Anal. Chem. 1995, 67, 2534-2538.

186. Buckberge, W. Haddad P. R. And P. W. Alexander, J. Chromatography 1991, 558, 181.

187. West, T. S. And A. S. Sykes, Analytical Applications of Diamino-ethane-tetra-acetic Acid, 2nd Edition by The Bristish Drug Houses Ltd, Poole, England, 1960.

188. Sweetser, P.B. and C. E. Bricker, Anal. Chem. 1954, 26, 195.

189. Wilhite, R. N. and A. L. Underwood, Anal. Chem., 1955, 27, 1334

190. Kornev, V. I. And Semakin, V.P. Koord. Khim, 3(10) 1486-1489 1977.

191. Nozaki, T. And Ohno, Y. Nippon Kagaku Kaishi, 8, 1455-1460 , 1973.

192. Bermejo-Barrera, A. And Bermejo-Martinzes, F. Acta Quim. Compostelano 3(3) 107-114 (1979)

193. Bermejo-Barrera, A., and Bermejo-Martinez, F., Acta Quim. Compostelana 3(4) 125-133. 1979.

194. Underwood, A. L. J. Chemical Education, p. 394, 1954, 31.)

195. Bermejo-Barrera, A., M. Angela Gomez-Doval, and F. Bermejo-Martinez, Micro-chemical Journal, 33, 162-167 1986

196. Marina, M. L., P. Andres, J.C. Diez-Masa, Chromotographia, Vol. 35, 9-12, 621.

197. Svoboda, L. and P. Prokes, Collect. Czech. Chem. Commun. 1992, 57, 1843.

198. P. Richter, J. M. Fernandlez-Romero, M. D. Luque de Castro, and M. Valcarcel, Chromatographia, 1992, 34, 445.

199. Hayashita, T., K. Yamasaki, X Huang, R. A. Bartsch, Chem. Lett. 1993, 1487-1490.

200. Middleton, G. And R. E. Stuckey, The Preparation of Biological Material for the Determination of Trace Metals, 1953.

201. Gorsuch, T. T., Loses of Trace Elements during Oxidation of Organic Materials, 1962.

202. Onuska, F I, K. A. Terry, Chromatographia, 1993, 36, 191-194.